

# **Role of dendritic cells on Ebola virus immunity and dissemination**

## **Dissertation**

submitted with the aim of achieving the degree of  
Doctor of Natural Sciences (Dr. rer. Nat.)  
at the Faculty of Mathematics, Informatics and Natural Sciences

Department of Chemistry  
University of Hamburg

by

**Anja Lüdtke**

Hamburg, 2016



Supervisor: Dr. César Muñoz-Fontela  
Emerging Viruses, Heinrich Pette Institute, Leibniz Institute for Experimental Virology

Co-Supervisor: Prof. Dr. Chris Meier  
Department of Chemistry, University of Hamburg

Additional supervision by Prof. Dr. Stephan Günther  
Department of Virology, Bernhard Nocht Institute for Tropical Medicine

Date of the oral defense: 03.06.2016

This doctoral thesis was funded by a fellowship from the Leibniz Center of Infection and supervised by Dr. César Muñoz-Fontela at the Heinrich Pette Institute and Prof. Dr. Stephan Günther at the Bernhard Nocht Institute between August 2012 and March 2016. Co-supervisor at the University of Hamburg was Prof. Dr. Chris Meier.

## I. Table of contents

1	Abstract .....	1
2	Zusammenfassung .....	3
3	Introduction .....	5
3.1	Concepts of antiviral immunity .....	5
3.1.1	Innate antiviral immune mechanisms .....	6
3.1.2	Dendritic cells bridge innate and adaptive immunity .....	7
3.1.3	Adaptive antiviral immunity .....	9
3.1.4	Dendritic cells in antiviral immunity .....	11
3.2	Ebola virus .....	16
3.2.1	Molecular characterization .....	16
3.2.2	History of EBOV outbreaks .....	17
3.2.3	Ecology .....	19
3.2.4	Clinical symptoms .....	19
3.3	Pathogenesis and host immune response to EVD .....	20
3.3.1	Inhibition of the IFN-I response .....	21
3.3.2	Infection of macrophages and DCs .....	21
3.3.3	Role of B and T lymphocytes .....	23
3.4	Animal models for EBOV .....	23
3.4.1	Non-human primates .....	24
3.4.2	Mouse models .....	24
4	Aims of this thesis .....	27
5	Results .....	29
5.1	Natural routes of EBOV infection in IFNAR <sup>-/-</sup> knockout mice .....	29
5.1.1	IFNAR <sup>-/-</sup> mice are susceptible to natural routes of EBOV infection .....	29
5.1.2	Mucosal infection leads to local and systemic EBOV replication .....	31
5.2	Establishment of immunocompetent mouse models susceptible to EBOV ...	33
5.2.1	EBOV infection in bone marrow chimeric mice .....	33
5.2.2	EBOV infection in humanized NSG-A2 mice .....	35
5.3	Investigation of EBOV immunity <i>in vivo</i> .....	46
5.3.1	EBOV immunity in bone marrow chimeric mice .....	46
5.3.2	EBOV immunity in humanized NSG-A2 mice .....	60

5.4	Analysis of APCs during human EVD .....	62
6	Discussion .....	67
6.1	Natural routes of EBOV infection .....	67
6.2	Establishment of immunocompetent mouse models .....	69
6.2.1	EBOV in bone marrow chimeric mice .....	69
6.2.2	EBOV in humanized mice .....	71
6.3	EBOV Immunity .....	73
6.3.1	Inflammatory response during EBOV infection .....	73
6.3.2	EBOV infection of lung DCs .....	74
6.3.3	Role of IFN-I signaling in hematopoietic immunity to EBOV .....	78
6.3.4	Protective role of T cells during EBOV infection .....	79
6.4	APCs in peripheral blood of EVD patients .....	80
6.5	Proposed model.....	81
6.6	Outlook .....	84
7	Material.....	85
7.1	General consumables .....	85
7.2	Viruses .....	85
7.3	Cell lines .....	85
7.4	Mouse colonies .....	85
7.5	Reagents, buffers and kits .....	86
7.6	Media and solutions .....	86
7.7	Antibodies .....	87
7.8	Laboratory equipment.....	88
7.9	Software.....	88
8	Methods.....	89
8.1	BSL-4 experiments .....	89
8.2	Virus amplification.....	89
8.3	Focus formation assay.....	89
8.4	Isolation of murine bone marrow cells .....	90
8.5	Purification of human CD34 <sup>+</sup> HSCs from cord blood .....	90
8.6	Generation of chimeras .....	91
8.6.1	Generation of bone marrow chimeras .....	91
8.6.2	Generation of humanized NSG-A2 mice .....	92

8.7	Animal experiments in BSL-4 .....	92
8.7.1	Infection.....	92
8.7.2	Blood draw .....	93
8.7.3	T cell depletion .....	93
8.7.4	Monocyte and neutrophil depletion .....	93
8.8	Organ preparation.....	94
8.9	Clinical parameters .....	94
8.10	Sample preparation for flow cytometry .....	94
8.11	Antibody panels and gating strategies for mouse experiments .....	95
8.12	Sample preparation of PBMCs from human EVD patients .....	99
8.13	Antibody panel and gating strategy for human EVD samples .....	100
8.14	Statistical analysis .....	101
9	References .....	103
10	Appendix .....	117
10.1	Publication list.....	117
10.2	Toxicity of chemicals.....	118
10.3	Acknowledgments.....	119
10.4	Eidesstattliche Versicherung .....	121





## II. List of abbreviations

APC	antigen-presenting cell
AST	aspartate aminotransferase
Batf3	Basic leucine zipper transcription factor ATF-like 3
Bcl-2	B-cell lymphoma 2
BM	bone marrow
BSL-4	Biosafety Level 4
CCR2	C-C chemokine receptor type 2
CCR7	C-C chemokine receptor type 7
CD	cluster of differentiation
CDC	Centers for Disease Control and Prevention
cDC	conventional dendritic cell
CLR	C-type lectin receptor
CTL	cytotoxic T lymphocyte
CTLA-4	cytotoxic T-lymphocyte-associated protein 4
CSF1	colony stimulating factor 1
CSF1R	colony stimulating factor 1 receptor
DC	dendritic cell
DC-SIGN	dendritic cell-specific intercellular adhesion molecule-3 grabbing non-integrin
DENV	Dengue virus
DMEM	Dulbecco's modified eagle medium
DRC	Democratic Republic of Congo
dsRNA	double-stranded RNA
DTR	diphtheria toxin receptor
EBOV	Ebola virus
EBV	Epstein-Barr virus
EDTA	ethylenediaminetetraacetic acid
EHF	Ebola hemorrhagic fever
EML	European Mobile Laboratory
EVD	Ebola virus disease
FBS	fetal bovine serum
FFU	focus forming units
GP	glycoprotein
HBSS	Hank's Balanced Salt Solution
HIV	Human immunodeficiency virus
HLA	human leukocyte antigen
hMGL	human macrophage galactose- and N-acetylgalactosamine-specific C-type lectin
HSC	hematopoietic stem cell
HRP	horseradish peroxidase
Id2	inhibitor of DNA binding 2
i.d.	intradermal

IFN-I	type I interferon
IFN-II	type II interferon
IFNAR (IFN $\alpha/\beta$ R)	interferon- $\alpha$ and $\beta$ receptor
IHC	immunohistochemistry
IL	interleukin
i.m.	intramuscular
i.p.	intraperitoneal
IRF	IFN regulatory factor
ISG	interferon-stimulated gene
IVC	individually ventilated cage
LC	Langerhans cell
mAB	monoclonal antibody
maEBOV	mouse-adapted EBOV
MDA5	melanoma differentiation-associated gene 5
MHC	major histocompatibility complex
MOI	multiplicity of infection
mRNA	messenger ribonucleic acid
NHP	non-human primate
NK cell	natural killer cell
NLR	NOD-like receptor
NOD	nucleotide-binding oligomerization domain
NP	nucleoprotein
NPC1	Nieman-Pick C1
NSG	non-obese diabetic (NOD)/severe combined immunodeficiency (scid)-interleukin-2 (IL-2) receptor- $\gamma$ chain knockout
OAS	2',5'-oligoadenylate synthetase
PAMP	pathogen-associated molecular pattern
PBMC	peripheral blood mononuclear cell
PBS	phosphate-buffered saline
PD1	programmed cell death protein 1
pDC	plasmacytoid dendritic cell
PKR	RNA-dependent protein kinase
PML	promyelocytic leukemia protein
PRR	pattern recognition receptor
PT	prothrombin
PTT	partial thromboplastin time
qRT-PCR	quantitative real-time polymerase chain reaction
Rag-2	recombination-activating gene 2
RESV	Reston virus
RIG-I	retinoic acid-inducible gene I
RLR	RIG-like receptor
RNA	ribonucleic acid
RT	room temperature

s.c.	subcutaneous
SCID	severe combined immunodeficiency
SLAN	6-Sulpho N-Acetyl-D-lactosamine
STAT	signal transducer and activator of transcription
SUDV	Sudan virus
TAFV	Tai Forest virus
TCR	T-cell receptor
Tfh cell	T follicular helper cell
Th cell	T helper cell
TIM-1	T-cell immunoglobulin and mucin domain 1
TLR	Toll-like receptor
TMB	3,3',5,5' tetramethylbenzidine
TNF $\alpha$	tumor necrosis factor $\alpha$
Tregs	regulatory T cells
VHF	viral hemorrhagic fever
VP	virion protein
WHO	world health organization
WNV	West Nile virus
ZAP	zinc finger antiviral protein



## 1 Abstract

Ebola virus (EBOV) is the causative agent of hemorrhagic fever outbreaks including the recent epidemic of Ebola virus disease (EVD) in West Africa. Even though the first case of EVD was identified forty years ago, very little is known about the pathophysiology of EVD. In particular the mechanisms responsible for the initiation of antiviral immunity as well as those leading to viral dissemination are not known. One of the main hurdles to study EVD immunology has been the lack of small animal models. Immunocompetent mice are resistant to EBOV and previous studies have relied mostly on immunodeficient mice, which are not suitable to study immunology.

The goal of the present study was to improve the current understanding of EBOV immunology in particular the role of dendritic cells (DCs) during infection. DCs play a central role bridging innate and adaptive immunity, and in the context of EBOV infection, DCs have been proposed as viral targets contributing to EVD pathophysiology. Susceptible mouse models with functional hematopoietic immunity were established through transplantation of murine bone marrow or human hematopoietic stem cells into immunodeficient recipient mice. To validate findings in the mouse models, research was performed on human samples within the context of the European Mobile Laboratory (EML) response to the recent EVD outbreak in West Africa.

The findings of the present study indicate that not all DC subsets are equally infected by EBOV *in vivo*, rather, the virus infects DCs and macrophages expressing the C-type lectin dendritic cell-specific intercellular adhesion molecule-3 grabbing non-integrin (DC-SIGN) in the murine and human context. In particular, inflammatory DCs derived from monocytes were identified as important targets of EBOV *in vivo*, and infection of these cells as a possible mechanism for virus amplification and dissemination. Alterations of monocyte subsets were also identified in humans and associated with EVD severity. The data presented here strongly highlight the importance of monocytes and DC-SIGN<sup>+</sup> DCs on EBOV pathophysiology and point out to these cell subsets as putative targets for immunotherapy against EVD.



## 2 Zusammenfassung

Das Ebola Virus (EBOV) verursacht hämorrhagische Fiebererkrankungen einschließlich der jüngsten Ebolaepidemie in Westafrika. Obwohl der erste Fall von Ebolafieber vor 40 Jahren auftrat, ist immer noch sehr wenig über die Pathophysiologie bekannt. Insbesondere die Mechanismen, die für die Einleitung der antiviralen Immunantwort und für die Verbreitung der Viren verantwortlich sind, sind unbekannt. Eines der größten Hindernisse für die Untersuchung der EBOV-spezifischen Immunantwort ist das Fehlen von empfänglichen Kleintiermodellen. Immunkompetente Labormäuse sind resistent gegen EBOV und bisherige Studien wurden mit immundefizienten Mäusen durchgeführt, welche per Definition nicht für immunologische Studien geeignet sind.

Ziel dieser Arbeit war es, das gegenwärtige Verständnis der Immunantwort auf das EBOV und insbesondere die Rolle der Dendritischen Zellen (DCs) während der Infektion zu erweitern. DCs spielen eine zentrale Rolle bei der Immunantwort, da sie eine Verbindung zwischen angeborenem und adaptivem Immunsystem herstellen. Im Zusammenhang mit der EBOV-Infektion wird vermutet, dass DCs als Zielzellen des Virus zur EBOV-Pathophysiologie beitragen. In dieser Arbeit wurden Mausmodelle, die für EBOV empfänglich sind, etabliert. Die Transplantation von murinem Knochenmark oder humanen hämatopoetischen Stammzellen in immundefiziente Empfängermäuse generierte chimäre Mäuse mit funktionalem hematopoetischem Immunsystem. Die im Mausmodell gewonnenen Erkenntnisse wurden mit humanen Daten verglichen, die im Rahmen des Einsatzes des Europäischen Mobilen Labors (EML) während des jüngsten EBOV-Ausbruchs in Guinea gewonnen wurden.

Die Ergebnisse der hier präsentierten Studie zeigen, dass nicht alle DC-Subpopulationen mit EBOV *in vivo* infiziert werden, sondern vielmehr, dass DCs und Makrophagen infiziert werden, die das C-Typ Lektin DC-SIGN exprimieren. Dies konnte für murine als auch humane DCs und Makrophagen gezeigt werden. Insbesondere inflammatorische DCs, die von Monozyten abstammen, wurden als wichtige Zielzellen von EBOV *in vivo* identifiziert. Des Weiteren wurde herausgefunden, dass deren Infektion ein möglicher Mechanismus für

Virusvermehrung und Verbreitung ist. Zusätzlich wurden Veränderungen von Monozyten-Populationen in menschlichem Blut identifiziert, die mit schwerem Ebolafieber assoziiert waren.

Die hier präsentierten Daten betonen die Wichtigkeit von Monozyten und DC-SIGN<sup>+</sup> DCs für die EBOV Pathophysiologie und heben diese als potentielle Ziele für die Immuntherapie für das Ebolafieber hervor.



### **3 Introduction**

Infectious diseases are a major health concern worldwide since they account for approximately 12 million deaths in the world population per year (source: World Health Organization). Vaccination programs in the past have successfully eradicated smallpox and dramatically reduced incidences of poliomyelitis and measles. However, up to date licensed vaccines against many other infectious diseases including malaria, EVD or tuberculosis, do not exist.

Among the infectious diseases that pose major health threats to humans are those caused by emerging viruses, which can be defined as 'infections that have newly appeared in a population or have existed but are rapidly increasing in incidence or geographic range' (Morse, 1995). Emerging viral diseases are often of zoonotic origin caused by sporadic spillover from animals to humans. The fact that humans are in many cases immunologically naïve to these viruses accounts for their high lethality. Furthermore, viruses with an RNA genome, which represent the majority of emerging viruses, are able to adapt quickly to new hosts and have developed ways to escape the host immune response.

These factors have challenged vaccine development against emerging viruses, including pandemic Influenza virus or EBOV. Even though in the past successful vaccines have been developed empirically, a basic understanding of how a given pathogen interacts with its host immune response is of great importance for rational vaccine design.

#### **3.1 Concepts of antiviral immunity**

The function of the immune system is to protect an organism against disease. The basic mechanisms of the immune response apply for infectious diseases as well as for tumors. The immediate and nonspecific response of an organism against an antigen is called innate immune response that is followed by an adaptive immune response, which is acquired and antigen specific.

### **3.1.1 Innate antiviral immune mechanisms**

Upon viral infection the innate immune response forms the first line of defense. This response is based on germline-encoded receptors that recognize common pathogen-associated molecular patterns (PAMPs) and induce the expression of genes involved in the inflammatory response (Takeuchi and Akira, 2010). These so called pattern recognition receptors (PRRs) are expressed by local tissue cells, including epithelium and resident innate immune cells, in order to sense structures derived from invading pathogens, such as double-stranded RNA (dsRNA) from viruses.

The family of PRRs comprises Toll-like receptors (TLRs), NOD-like receptors (NLRs), RIG-like receptors (RLRs) and C-type lectin receptors (CLRs) among others (Takeuchi and Akira, 2010). Several virus-specific receptors have been described, such as TLR-2, 3, 7–9, retinoic acid-inducible gene I (RIG-I) and melanoma differentiation-associated gene 5 (MDA5), which mediate the expression of antiviral inflammatory cytokines including type I and type II interferons (IFN-I and IFN-II), tumor necrosis factor  $\alpha$  (TNF-  $\alpha$ ) and interleukin (IL)-1, 6, 12, 18 (Christensen and Thomsen, 2009).

Type I interferons (IFN-I) are crucial for the defense against viral infections because they induce an antiviral state in infected and surrounding cells in order to control viral replication. Moreover, they are important for antigen-presentation and activation of the adaptive immune system (Ivashkiv and Donlin, 2014; Fig. 1). Recognition of intermediate products of viral replication by PRRs induces the production of IFN-I, including IFN $\alpha$  and IFN $\beta$ . Auto- and paracrine activation of the IFN receptor by IFN-I results in the activation of signal transducer and activator of transcription (STAT) proteins and IFN regulatory factors (IRFs), which induce the expression of hundreds of IFN-regulated genes that will establish a state of resistance to viral infections. Classical proteins of the antiviral state are the RNA-dependent protein kinase (PKR), which inhibits proliferation of virus-infected cells, and the 2',5'-oligoadenylate synthetase (OAS), which activates RNase L for viral RNA degradation (Takeuchi and Akira, 2010). Other important IFN-stimulated genes that have been implicated in the defense against many viruses are promyelocytic leukemia protein (PML), interferon-stimulated gene 15 (ISG15) or zinc finger antiviral protein (ZAP) (Geoffroy and Chelbi, 2011; Skaug and Chen, 2010; Müller et al., 2007).

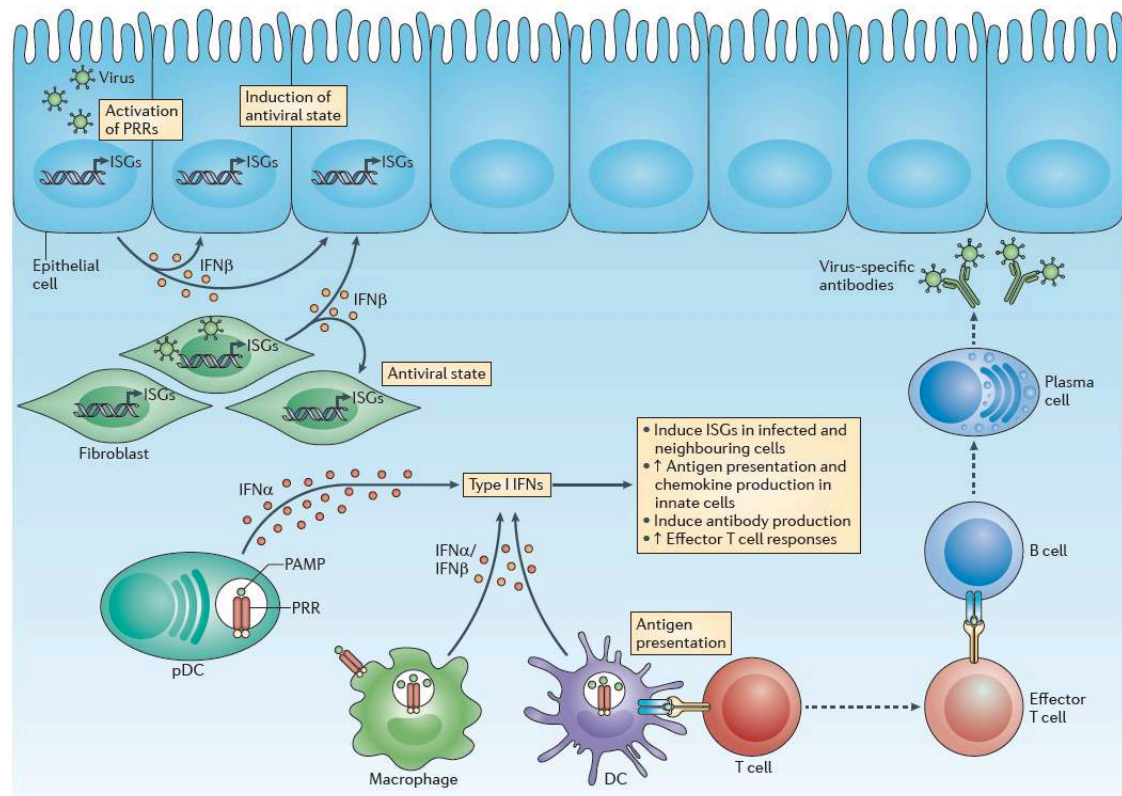


**Figure 1: Establishment of the antiviral state** Viral replication products are recognized via pattern recognition receptors (PRRs) expressed by epithelial cells, fibroblasts and immune cells such as macrophages and dendritic cells (DCs). PRR signaling induces the production of type I interferons, such as IFN $\alpha$  and IFN $\beta$ . IFN signaling on infected and neighboring cell activates the IFN receptor. This induces the expression of IFN-inducible genes, which establish an antiviral state (image from Ivashkiv and Donlin, 2014).

Among the first innate immune cells that are activated through PRR signaling are tissue-resident macrophages. They recognize, ingest and kill invading pathogens and secrete cytokines in order to recruit other innate effector cells such as neutrophils, monocytes and natural killer (NK) cells. While neutrophils and monocytes mediate proinflammatory responses, NK cells are especially important to induce programmed cell death of virus-infected cells.

### 3.1.2 Dendritic cells bridge innate and adaptive immunity

As a consequence of a successful innate response a virus-specific adaptive immune response is initiated. This step requires antigen presentation by professional antigen-presenting cells (APCs) to T lymphocytes. In this regard, the term antigen describes any substance that can be recognized by the adaptive immune system. Self-antigens that originate from the body can be distinguished from non-self-antigens that are derived from the environment, e.g. viruses.

Steady-state DCs, which are professional APCs, scan peripheral tissues in order to sense pathogens at their initial entry site. Encountering viral antigen activates PRR signaling (for example via TLR-3 and TLR-7), which induces activation of DCs. Upon activation, they downregulate proteins needed for phagocytosis and upregulate major histocompatibility complex (MHC) molecules and T cell co-stimulatory molecules for efficient antigen presentation. This process takes place during migration to the draining lymph nodes, where DCs present processed viral peptides on their MHC molecules to naïve T cells (Mellman and Steinman, 2001).

Key for T cell activation is the interaction of the peptide:MHC complex on the surface of the APCs with the T-cell receptor (TCR) on the surface of the T cell. Further requirement for proper activation is signaling via co-stimulatory molecules expressed by both cells. The MHC molecule is a glycoprotein that presents antigenic peptides on the surface of a cell. Two classes of MHC molecules exist. The MHC class I molecule is expressed by any nucleated cell and presents peptides from cytosolic pathogens, such as viruses, while MHC class II molecules are mainly expressed by APCs, namely DCs, macrophages and B cells, and present peptides derived from internalized pathogens. Peptide:MHC complex recognition by the T cell further depends on their co-receptors, CD4 and CD8. MHCI presented peptides will activate CD8 T cells, while MHCII presented peptides will activate CD4 T cells.

Important for the antiviral defense is a mechanism called cross-presentation achieved by DCs. This process is essential for DCs that have not acquired cytosolic antigen via direct infection in order to present internalized antigen via MHCI to cytotoxic CD8 T lymphocytes (CTLs), which in turn will kill virus-infected cells. For efficient cross-priming, this step also requires the help of activated CD4 T helper cells (Fig. 2).

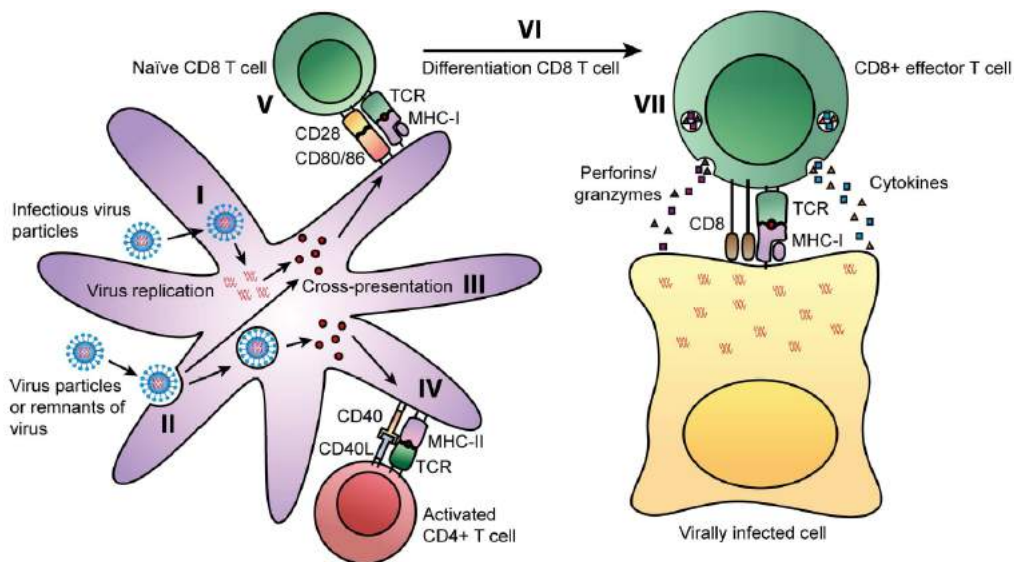


**Figure 2: Antigen presentation by dendritic cells (DCs)** In case of viruses that directly infect DCs cytosolic peptides are presented via MHC-I to CD8 T cells (I). Non-infected DCs prime CD4 T cells via MHC-II presentation of internalized virus particles or remnants of virus (II+IV). Furthermore, they also present exogenous antigen via MHC-I to CD8 T cells, which is called cross-presentation and especially important for antiviral immunity (II+III). CD40 – CD40L signaling of DC with CD4 T cells activates the DC to upregulate co-stimulatory molecules CD80/86 for efficient cross-priming of CD8 T cells. Activated CD8 T cells differentiate into effector T cells in order to kill virus-infected cells that present viral peptides via MHC-I (VI+VII) (image from Rosendahl Huber et al., 2014).

### 3.1.3 Adaptive antiviral immunity

B and T lymphocytes are key mediators of adaptive immunity. While B cells are responsible for humoral immunity producing antibodies against viral particles, T cells mediate cellular responses. Once naïve T cells have encountered an antigen presented by DCs, they start proliferating and migrating towards the inflamed tissue in order to perform effector functions.

Essential for the clearance of many viral infections are cytotoxic CD8 T lymphocytes (CTLs) (McMichael et al., 1983; Guidotti et al., 1996). CTLs induce apoptosis of virus-infected cells that present viral peptides via their MHC-I molecules through the release of cytotoxic granules, which contain perforin and granzymes (Peters et al., 1991). The other subset of T cells, called CD4 T helper cells (Th cells), fulfill important helper functions, such as activation of DCs through CD40 – CD40L interaction for efficient cross-priming of CTLs, promotion of CD8 T cell proliferation and differentiation via IL-2 production and sustainment of CTL responses during chronic viral infections (Ridge et al., 1998; Cox and Zajac, 2010; Matloubian et al., 1994). CD4 T cells comprise a heterogeneous population, which also perform different effector tasks. Important for the antiviral defense are T helper 1 (Th 1) cells, which suppress viral replication in target cells by IFN $\gamma$  production, as well as T

follicular helper (Tfh) cells, which mediate differentiation and formation of memory B cells (Franco et al., 1997; Hale et al., 2013). While regulatory T cells (Tregs) have been well characterized during tolerance induction, there is evidence that Tregs might be involved in mediating viral persistence by inhibiting antiviral effector T cell responses (Wing and Sakaguchi, 2010; Aandahl et al., 2004; Cabrera et al., 2004).

Signaling of the TCR with the peptide:MHC complex is crucial for T cell activation. However, positive and negative co-signaling between T cells and DCs determines the magnitude of the effector T cell response (Sharpe, 2009). While co-stimulatory signaling (e.g. CD28 – CD80/86 interaction) is required for T cell activation, co-inhibitory signaling (e.g. CTLA-4 and CD80/86 interaction) is important to control excessive T cell responses (Fig. 3). The fine balance of co-activation and co-inhibition results in a T cell response that can be divided into three phases, namely T cell expansion upon antigen recognition, T cell contraction after viral clearance and establishment of long-lived memory T cells, which are, upon reinfection, reactivated in order to perform antiviral effector functions mediating long-term protective immunity (Wherry and Ahmed, 2004).

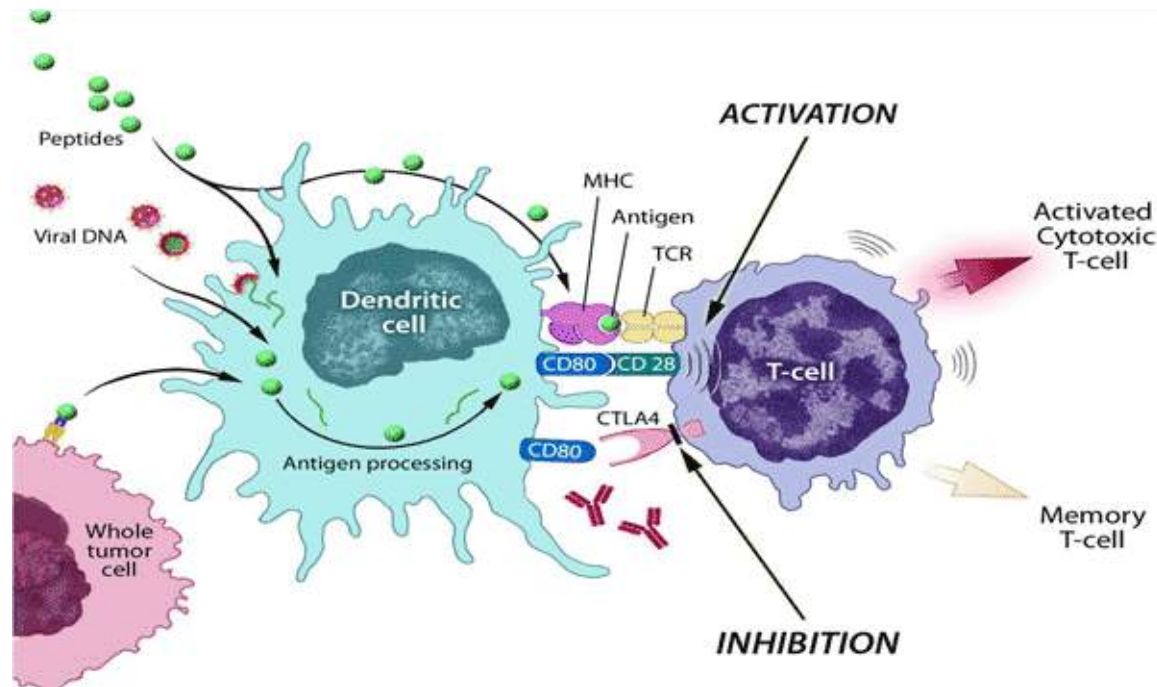


**Figure 3: Dendritic cell – T cell interaction** Co-stimulatory signaling between CD80 of the surface of the DC and CD28 on the surface of the T cells is important for T cell activation and allows T cells to perform effector functions (e.g. CTLs kill virus-infected cells). However, the interaction of CD80 with the co-inhibitory molecule cytotoxic T-lymphocyte-associated protein 4 (CTLA-4) leads to T cell inhibition and subsequently memory T cell formation (image from [www.cancer.gov/about-cancer/treatment/research/first-treatment-vaccine-approved](http://www.cancer.gov/about-cancer/treatment/research/first-treatment-vaccine-approved)).

During chronic viral infections a phenomenon called exhaustion is often observed describing the loss of effector functions and subsequently the failure to generate memory T cells (Zajac et al., 1998; Shin and Wherry, 2007). Exhausted T cells during chronic viral infections are characterized by the sustained expression of co-inhibitory molecules, such as programmed cell death protein 1 (PD-1) and cytotoxic T-lymphocyte-associated protein 4 (CTLA-4) (Barber et al., 2006; Day et al., 2006; Nakamoto et al., 2009).

### 3.1.4 Dendritic cells in antiviral immunity

In 1973, Ralph Steinman and Cohn reported the discovery of a “large stellate cell with distinct properties from mononuclear phagocytes, granulocytes, and lymphocytes” (Steinman and Cohn, 1973). They named this novel cell type “dendritic cell” due to the cytoplasm being “arranged in pseudopods of varying length, width, form and number” (Steinman and Cohn, 1973, Fig. 4). Later, Steinman and colleagues discovered high expression levels of MHCII molecules on the surface of DCs and found that they were “potent stimulators of the primary mixed leukocyte reaction” (Steinman et al., 1979, Steinman and Witmer, 1978). These findings together with following studies indicating that DCs were able to induce both cytotoxic T cell responses as well as T cell mediated antibody responses, made clear that DCs had a central role in the immune system bridging innate and adaptive immunity (Nussenzweig et al., 1980, Inaba et al., 1983).



**Figure 4: Morphology of dendritic cells** Phase-contrast micrograph of DCs isolated from mouse spleen and fixed in glutaraldehyde (image from Steinman and Cohn, 1973).

Since their discovery in 1973, researchers have made efforts to fully characterize development and function of the DC lineage. In general, DCs are divided into plasmacytoid DCs (pDCs), monocyte-derived DCs and conventional DCs (cDCs), the latter describing those discovered by Steinman. Conventional DCs are found in all non-lymphoid as well as in lymphoid tissues and represent a heterogeneous population of hematopoietic cells that can be divided into distinct subsets based on their development and function. Monocyte-derived DCs are derived from blood monocytes, which are recruited to extravascular compartments in the steady state and under inflammatory conditions (León and Ardavin, 2008). The recently identified pDCs are morphologically similar to plasma cells and produce large amounts of IFN $\alpha$  upon viral infection (Kadowaki et al., 2000; Asselin-Paturel et al., 2001). Nevertheless, still little is known about this novel cell type and its role during the immune response.

Due to the great importance of DCs to induce antiviral T cell responses, many viruses have evolved mechanisms to target DC functions. *In vitro* studies have demonstrated that many viruses can infect DCs leading to an impaired T cell response (Andrews et al., 2001; Engelmayer et al., 1999). However, *in vitro* studies do not reflect *in vivo* responses, therefore, the impact of DC infection on efficient T cell priming is not known for many viruses (Yewdell and Hill, 2002). Moreover, studies have suggested that some viruses utilize migrating DCs in order to reach other target cells, while other viruses might be able to induce apoptosis in DCs (Kwon et al., 2002; Bosnjak et al., 2005). Additional mechanisms have been described by which viruses evade the DC-mediated response, including interference with antigen processing and presentation and modulation of cytokine secretion (Yewdell and Hill, 2002).

### ***Murine DC subsets***

While the DC lineage has been intensely investigated in mice, the equivalents in humans are just starting to be identified. However, a major difference is that precursor DCs are found in human blood, while they do not exist in mouse blood. In both, mouse and human, DCs are characterized by their expression of the hematopoietic marker CD45, MHCII (in humans HLA-DR) and the lack of T, B and



NK cell markers (Merad et al., 2013, Collin et al., 2013). These markers, which help to phenotype different cell types, are called cluster of differentiation (CD) molecules that include surface and intracellular receptors and ligands.

In mice, two major subsets of cDCs are identified in non-lymphoid tissues: CD103<sup>+</sup> and CD11b<sup>+</sup> DCs, which account for 1-5 % of tissue cells (Merad et al., 2013). Both subsets have equivalents in lymphoid tissues, which are CD8α<sup>+</sup> and CD11b<sup>+</sup> (also referred to as CD4<sup>+</sup>) DC subsets, respectively (Fig. 5). Non-lymphoid tissue DCs, in lung, skin or intestine for example, are migratory populations that present tissue antigen acquired in the periphery, while lymphoid-resident DCs in spleen and lymph nodes present antigen from blood or the lymph.

CD103<sup>+</sup> and CD8α<sup>+</sup> DCs share common origin, transcriptome profiles and function (Hashimoto et al., 2011; Miller et al., 2012; Merad et al., 2013). They arise from cDC-restricted precursors and differentiate dependent on the transcription factors Basic leucine zipper transcription factor ATF-like 3 (Batf3), IFN regulatory factor 8 (IRF8) and the inhibitor of DNA binding 2 (Id2) (Hildner et al., 2008; Aliberti et al., 2003; Hacker et al., 2003). They both express the pattern recognition receptor TLR-3 and the C-type lectin langerin in several tissues, but lack the expression of the lectin-like receptor CD209, the mouse equivalent to human dendritic cell-specific intercellular adhesion molecule-3 grabbing non-integrin (DC-SIGN) (Edwards et al., 2003; Shortman et al., 2010; Hashimoto et al., 2011). CD103<sup>+</sup> DCs in non-lymphoid tissues and CD8α<sup>+</sup> DCs in lymphoid tissues efficiently sense invading pathogens and then migrate to the T cell zone of the draining lymph nodes to present tissue or blood antigen to naïve T cells. Both, CD103<sup>+</sup> and CD8α<sup>+</sup> DCs are very efficient at cross-presentation of antigen to CD8 T cells inducing a strong CTL response, which is especially important during viral infections (del Rio et al., 2007; Henri et al., 2010; Kim and Braciale, 2009).

CD11b<sup>+</sup> DCs in non-lymphoid and lymphoid tissues comprise a heterogeneous population that develops independently of Batf3, IRF8 and Id2. However, the transcriptome expression pattern and the relationship between CD11b<sup>+</sup> DCs in non-lymphoid and lymphoid tissues are still unclear (Hashimoto et al., 2011). In contrast to CD103<sup>+</sup>/CD8α<sup>+</sup> DCs, CD11b<sup>+</sup> DCs lack the expression of TLR3 and langerin, but do express CD209 (Edwards et al., 2003; Shortman et al., 2010; Hashimoto et al., 2011). It is generally accepted that CD11b<sup>+</sup> DCs develop from cDC-restricted

precursors or monocytes giving rise to conventional  $CD11b^+$  DCs or monocyte-derived  $CD11b^+$  DCs, respectively (Langlet et al., 2012). Due to the fact that there are no conditional depletion mouse models for conventional  $CD11b^+$  DCs, the role of this subset *in vivo* still needs to be defined. However, several studies have suggested a major role of conventional  $CD11b^+$  DCs in CD4 T cell priming (Kim et al., 2009; McLachlan et al., 2009).

Even though monocytes give rise to  $CD11b^+$  DCs in the steady state, the pool of monocyte-derived  $CD11b^+$  DCs is largely increased during inflammation. Circulating  $Ly6C^{hi}$  monocytes from the blood infiltrate inflamed tissue and give rise to monocyte-derived  $CD11b^+$  DCs (Auffray et al., 2009). Inflammatory DCs are characterized by their expression of Ly6C, CD11b, MHCII and CD11c (Serbina et al., 2003). Similar to conventional  $CD11b^+$  DCs, a role for monocyte-derived  $CD11b^+$  DCs inducing CD4 T cell responses has been reported (León et al., 2007).

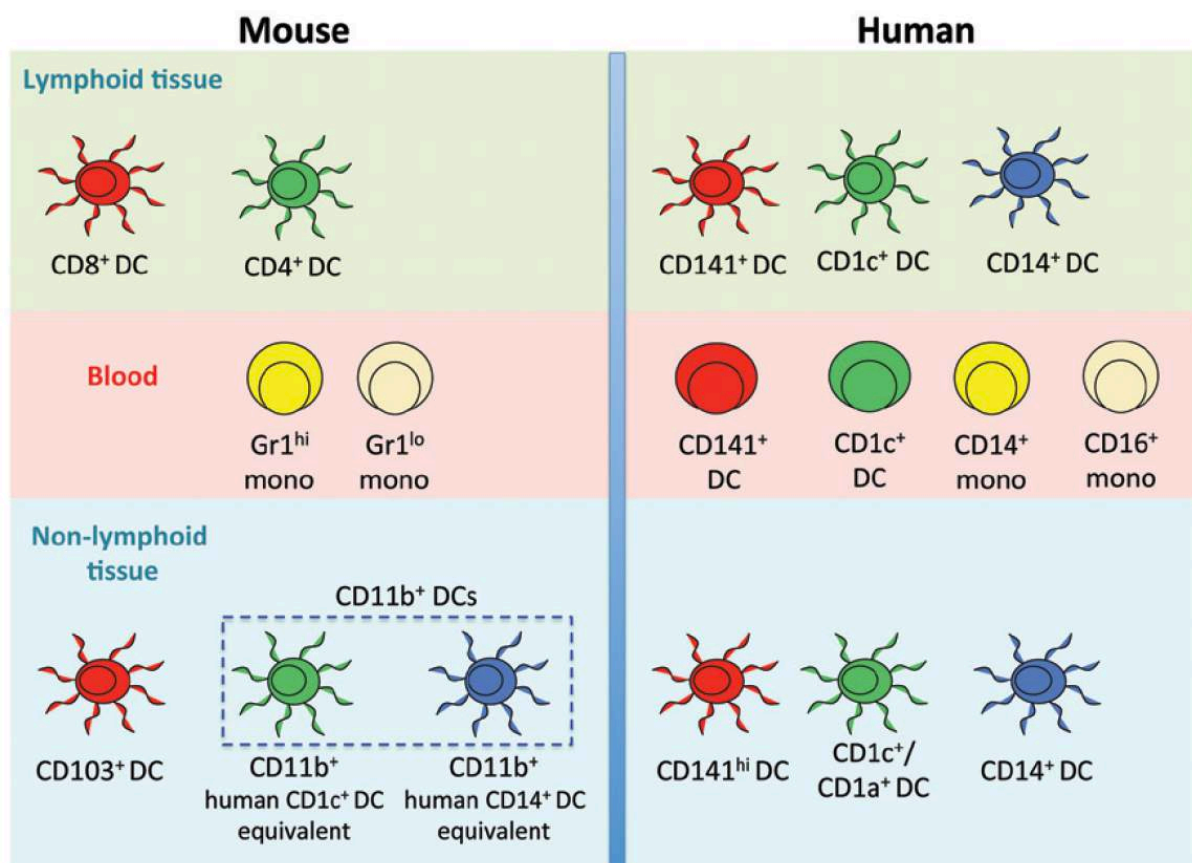


**Figure 5: Mouse and human DC subsets** Schematic represents the equivalents of dendritic cell and monocyte subsets in lymphoid tissues, blood and non-lymphoid tissues in mouse and human (schematic from Haniffa et al., 2013).

### ***Human DC subsets***

Human dendritic cell research has made enormous progress in the last years, nevertheless, due to limited access to human tissues, knowledge is still limited. Since both, monocytes and DCs, express CD11c in humans, further discrimination of both lineages is needed. Monocytes in human blood comprise of three subsets: classical CD14<sup>+</sup> monocytes, non-classical CD16<sup>+</sup> monocytes and double positive CD14<sup>+</sup> CD16<sup>+</sup> monocytes (Saha and Geissmann, 2011). Human blood dendritic cells lack both, CD14 and CD16, and can be subdivided into a major CD1c<sup>+</sup> subset and a minor CD141<sup>+</sup> DC subset (Collin et al., 2013). It is commonly accepted that CD1c<sup>+</sup> DCs are the equivalent to mouse CD11b<sup>+</sup> DCs, while CD141<sup>+</sup> DCs share homology with mouse CD103<sup>+</sup>/CD8<sup>+</sup> DCs (Fig. 5). CD1c<sup>+</sup> and CD141<sup>+</sup> DCs in human blood are the probable precursors of DCs found in non-lymphoid and lymphoid tissues (Dzionek et al., 2000). As seen for their murine counterparts, CD1c<sup>+</sup> DCs have been suggested as the major mediators of CD4 T cell immunity, while CD141<sup>+</sup> DCs have revealed a superior ability to cross-prime CD8 T cells (Haniffa et al., 2012; Bachem 2010). However, this is still controversial, since other studies have described similar cross-presenting abilities among the human DC subsets (Segura et al., 2013a).

In non-lymphoid tissues a third subset of human DCs has been identified: CD14<sup>+</sup> DCs, which are believed to be of monocytic origin (Haniffa et al., 2013). They express DC-SIGN and macrophage markers, which complicates the distinction between CD14<sup>+</sup> DCs and macrophages (Fehres et al., 2015). A recent study described human inflammatory DCs that were present during inflammatory conditions (Segura et al., 2013b). However, the origin of these cells remains to be elucidated. Non-classical CD16<sup>+</sup> monocytes are the equivalents of mouse Ly6C<sup>low</sup> patrolling monocytes. Moreover, researchers have reported a subset of CD16<sup>+</sup> monocytes, which expresses 6-Sulpho LacNAc (SLAN) and can respond to inflammatory stimuli, as another human blood DC subset present under inflammatory conditions (Hänsel et al., 2011).

Despite all the recent advances, there are still many gaps to be filled to understand development and function of human dendritic cells as well as the role of inflammatory DC subsets.

## 3.2 Ebola virus

Emerging infections of zoonotic origin are commonly caused by RNA viruses due to their capacity to adapt quickly to new hosts (Nichol et al., 2000). Among these zoonotic agents is a group of viruses causing viral hemorrhagic fevers (VHFs) that include members of the *Filoviridae*, *Arenaviridae*, *Bunyaviridae*, *Flaviviridae* and *Rhabdoviridae* families. They are highly pathogenic for humans and share common pathological features. The name refers to a more or less prominent feature that they cause hemorrhage in severe cases. More importantly however, is the fact that all causative agents of VHFs seem to cause a dysfunctional host immune response, which is likely to be critical for their high lethality (Geisbert and Jahrling, 2004).

The virus family *Filoviridae* consists of three genera, *Ebolavirus*, *Marburgvirus* and *Cuevavirus*, and belongs to the order *Mononegavirales*. *Filoviruses* are enveloped, non-segmented, negative-stranded RNA viruses. Their filamentous morphology gave the family its name (Fig. 6). The genus *Ebolavirus* includes five species of which at least three are pathogenic for humans: *Zaire ebolavirus*, *Sudan ebolavirus* and *Bundibugyo ebolavirus*. *Tai Forest ebolavirus* infection was reported as an isolated human case transmitted from an infected chimpanzee, while the fifth species, *Reston ebolavirus*, causes disease in non-human primates but is thought to be nonpathogenic for humans.

Ebola virus (EBOV) is the causative agent of EVD, previously referred to as Ebola hemorrhagic fever (EHF). There have been reported outbreaks in Central Africa and recently the biggest documented outbreak in West Africa. EVD is an acute and severe illness in humans with case fatality rates between 30 – 90 %, depending on the virus species. Currently, several vaccines and therapies are being evaluated in clinical trials. However, since EBOV is highly pathogenic for humans and still no vaccine or therapy exist, it has to be handled in Biosafety Level 4 (BSL-4) containment.

### 3.2.1 Molecular characterization

The EBOV genome has a length of around 19 kilobases and encodes 7 structural proteins in the following order: Nucleoprotein (NP), virion protein 35 (VP35), VP40, glycoprotein (GP), VP30, VP24 and RNA-dependent RNA polymerase (L) (Klenk and

Feldmann, 2004). The RNA genome together with NP, VP30 and VP35 and the RNA-dependent RNA polymerase (L) form the ribonucleoprotein complex for functional transcription and replication (Mühlberger et al., 1999). GP is a transmembrane protein expressed on the surface of the virion and VP24 and VP40 are membrane-associated proteins of which the latter is essential for particle formation (Noda et al., 2002). VP35 and VP24 have further roles as interferon antagonists (Basler et al., 2000, Reid et al., 2006). One non-structural protein, the soluble GP, is also encoded by the GP gene and is secreted by infected cells (Volchkov et al., 1995).

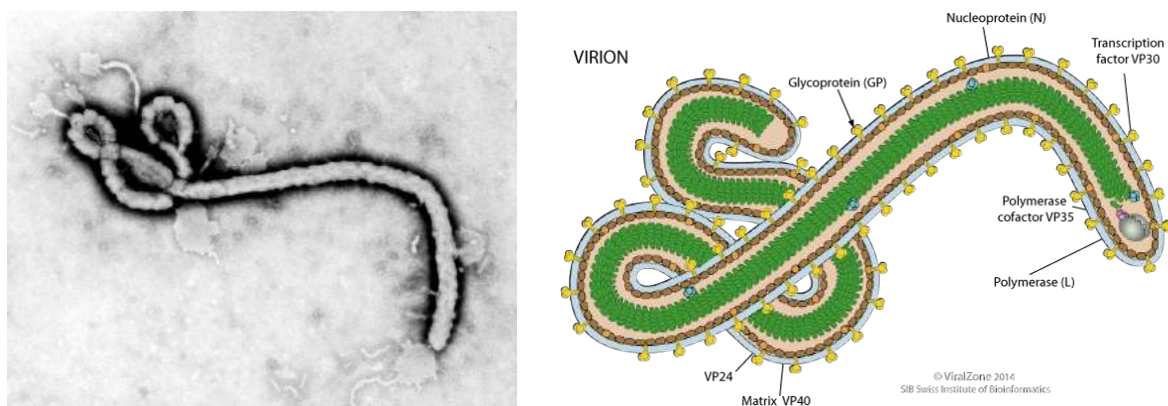


**Figure 6: Ebola virus (EBOV) morphology and molecular characterization** Left: Electron micrograph of ebolavirus (image from F.A Murphy, CDC), Right: Schematic representation of an ebola virion (image from [http://viralzone.expasy.org/all\\_by\\_species/207.html](http://viralzone.expasy.org/all_by_species/207.html))

### 3.2.2 History of EBOV outbreaks

*Filoviruses* were first discovered in 1967 in Marburg, Germany, when workers of a pharmaceutical company got infected through contact with imported African green monkeys (Siegert et al., 1967). The causative agent of this severe illness, which affected 31 people, was named Marburg virus. Since then, Marburg virus outbreaks occurred in the Democratic Republic of Congo (DRC), Angola and Uganda. The first case of EVD was reported in 1976 in DRC, formerly Zaire, where 318 people were infected with a high lethality of 88% (WHO, Ebola haemorrhagic fever in Zaire). In the same year a second epidemic occurred in Sudan with 284 reported cases and a case fatality rate of 53% (WHO, Ebola haemorrhagic fever in Sudan, Fig. 7). A research team, which included Karl Johnson and Peter Piot, identified the virus in 1976 and named it after the Ebola river in northern DRC, which is close to the town Yambuku, where the disease occurred for the first time. Since then the virus has reemerged

mainly in Central Africa and has caused outbreaks in DRC (1995), Gabon (1996/1997 and 2001/2002) and Uganda (2000/2001). One reported case occurred in West Africa in Ivory Coast in 1994, where EBOV was transmitted to a human from an infected chimpanzee from the Tai Forest (Le Guenno et al., 1995).

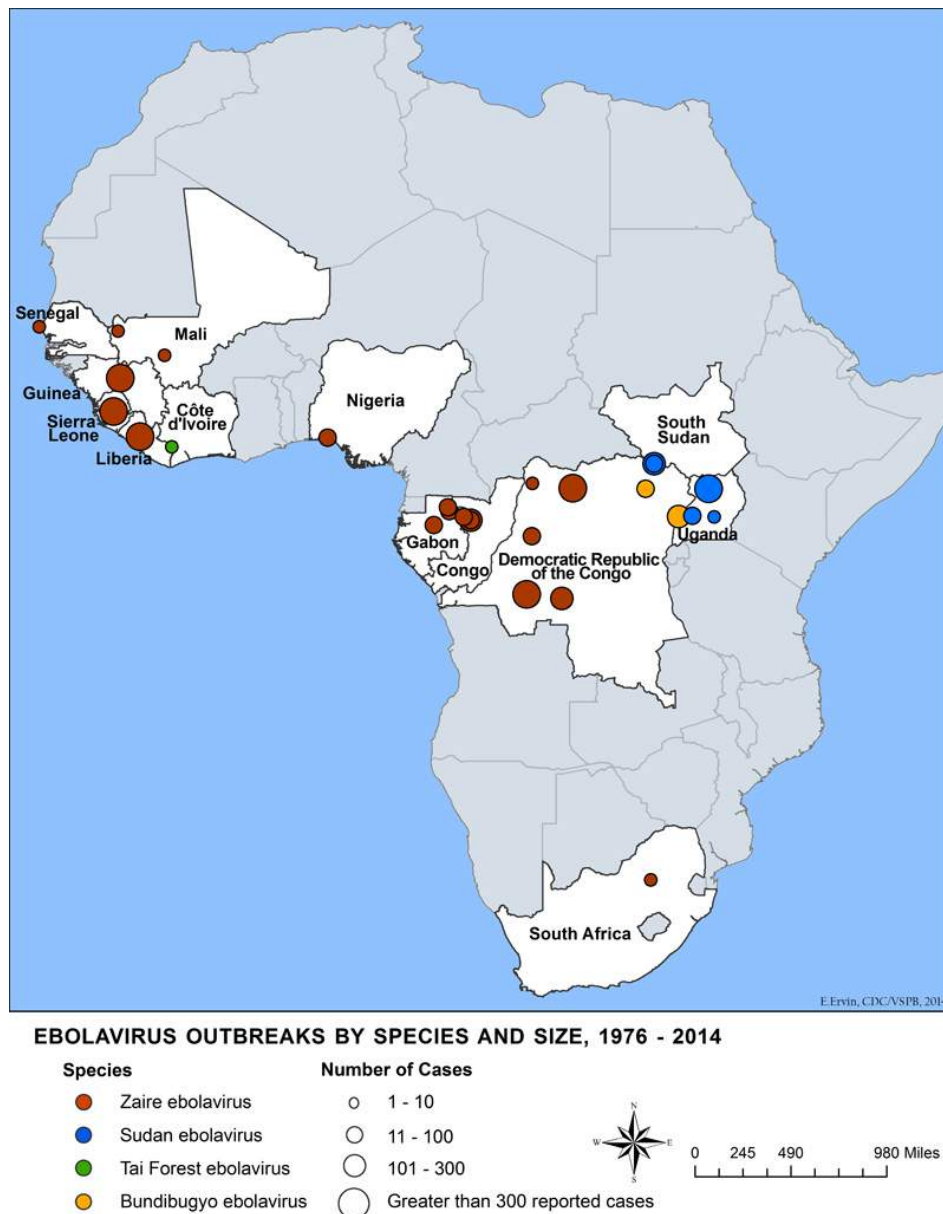


**Figure 7: Geographical distribution of ebolavirus outbreaks in Africa from 1976 – 2014** The map depicts Ebolavirus outbreaks by species and number of cases in Africa from 1976 until 2014 (map from <http://www.cdc.gov/vhf/ebola/outbreaks/history/distribution-map.html>).

In March 2014, Ebola virus was detected for the first time in Guinea in West Africa and spread to the neighboring countries Liberia (March, 2014) and Sierra Leone (May, 2014). Small numbers of cases were also reported in Nigeria, Mali and

Senegal. Furthermore, single cases were exported for the first time to Europe and the United States. For the most affected countries 3,804 cases (2,536 deaths) were documented in Guinea, 10,676 cases (4809 deaths) in Liberia and 14,124 cases (3,956 death) in Sierra Leone (<http://apps.who.int/ebola/current-situation/ebola-situation-report-2-march-2016>). With 28,639 total cases (11,316 deaths) in the three countries this was the biggest EBOV outbreak since its discovery in 1976. In January 2016, West Africa was declared EBOV-free by the WHO. This declaration was followed by sporadic EVD cases attributed epidemiologically to sexual transmission from long-term survivors or vertical transmission through breast milk feeding (Mate et al., 2015; Nordenstedt et al., 2016).

### **3.2.3 Ecology**

EVD is a zoonosis with a still unknown reservoir species. Fruit bats have been suggested as a natural reservoir for filoviruses (Leroy et al., 2005), and this hypothesis was strengthened when Marburg virus was isolated from the Egyptian fruit bat *Rousettus aegyptiacus* (Towner et al., 2009). The possibility of EBOV persistence in fruit bats arose from the detection of viral RNA and antibodies in three species of fruit bats, even though they were never simultaneously detected in the same animal (Leroy et al., 2005). However, EBOV has never been isolated from bats. It is believed that transmission from the natural reservoir to accidental hosts, such as humans and apes, is a rare event. The reservoir species is most likely asymptotically infected; shedding of the virus might be induced by changes of the environment, stress or pregnancy (Feldmann and Geisbert, 2011). Human infection might occur by hunting bush meat, either bats or apes, or entering caves with infected bats in the case of Marburg virus. The initial human infection then leads to further human-to-human transmission via direct contact with infected body fluids. Human outbreaks are usually caused by a single spillover event, even though multiple spillover events have been also described (Baize et al., 2014; Leroy et al., 2004).

### **3.2.4 Clinical symptoms**

The incubation period for EVD is 2 – 21 days with an average of 8 – 10 days (<http://www.cdc.gov/vhf/ebola/symptoms/index.html>). Initial symptoms are rather

nonspecific, including fever, muscle pain and headache. Then, systemic disease manifestations, including gastrointestinal (diarrhea and vomiting), vascular, respiratory and neurological symptoms appear (Feldmann and Geisbert, 2011). In some cases maculopapular rash and hemorrhage have been reported. Laboratory findings include leukopenia, lymphopenia and neutrophilia indicating inflammatory responses, decreased platelet levels and prolonged prothrombin (PT) and partial thromboplastin times (PTT) showing coagulation abnormalities, and elevated levels of serum transaminase concentrations marking liver damage. In fatal cases, patients often die from hypovolemia and multiorgan failure.

Even though EVD is highly pathogenic, case fatality rates of 30 – 90% also imply survival rates of 10 – 70% without a specific antiviral treatment. This raises the question of which are the immune correlates of protection against EVD, a major goal of current EBOV research.

### **3.3 Pathogenesis and host immune response to EVD**

EBOV infects a broad range of cell types in various tissues by binding to cell surface lectins and other sugar-recognizing molecules (e.g. T-cell immunoglobulin and mucin domain 1 (TIM-1)) that are expressed on many cells. EBOV entry in infected cells occurs through macropinocytosis and requires interaction of the virus GP with the endosomal receptor Nieman-Pick C1 (NPC1) to facilitate membrane fusion (Côte et al., 2011; Carette et al., 2011). Immunohistochemistry (IHC) analysis of patient and non-human primate tissues revealed the infection of endothelial cells, fibroblasts, hepatocytes and epithelial cells indicating a broad cell tropism (Zaki et al., 1999; Geisbert et al., 2003a). This allows virus replication in various tissues and subsequently necrosis of tissues such as spleen, liver and adrenal glands. While those pathological findings are directly virus-induced, a second indirect mechanism that results from the interaction of the virus with the immune system appears to be crucial as well (Mahanty and Bray, 2004). Massive viral replication in combination with a dysregulated immune response is likely to cause severe EVD.



### **3.3.1 Inhibition of the IFN-I response**

The IFN-I response is the first line of defense upon viral infection and leads to the establishment of an antiviral state in infected and bystander cells. Basler and colleagues could show that the viral protein VP35 was able to inhibit the induction of IFN $\beta$  by blocking the transcription factor IFN regulatory factor 3 (IRF3) (Basler et al., 2003). The same research group could further demonstrate that the other IFN antagonist, VP24, was able to block IFN mediated induction of an antiviral state (Reid et al., 2006). Targeting both, production and response to IFN, presumably allows replication to high titers and unhampered spread of the virus throughout the body. While all cell types are able to produce type I IFNs, cells of the innate immune system are specialized in sensing viral components. EBOV might specifically target the response of innate immune cells, such as macrophages and DCs, as demonstrated in several studies, which showed that EBOV infected monocyte-derived human macrophages and DCs failed to produce IFN $\alpha$  (Mahanty et al., 2003; Gupta et al., 2001; Bosio et al., 2003).

### **3.3.2 Infection of macrophages and DCs**

Several studies analyzing tissue sections of infected rodents or non-human primates (NHPs) support the idea that macrophages and DCs might be early targets of viral replication (Connolly et al., 1999, Davis et al., 1997, Geisbert et al., 2003b). Since these cells have important roles for innate and adaptive immunity, their infection might result in a dysfunctional immune response (Fig. 8).

It was demonstrated that infected macrophages produce various proinflammatory cytokines, chemokines and nitric oxide early after infection, which might contribute to a strong systemic inflammatory response (Gupta et al., 2001, Hensley et al., 2002). In EVD patients dysregulated inflammatory responses have been associated with fatal outcome (Baize et al., 1999; Villinger et al., 1999; Schieffelin et al., 2014). It was further suggested that the synthesis of tissue factor by macrophages might contribute to coagulation abnormalities observed in infected NHPs (Geisbert et al., 2003c). Taken together, macrophages have been implicated in the hypotension and the septic shock like syndrome observed in EVD patients.

EBOV is thought to enter the host via mucosal surfaces and lesions in the skin. The location of non-lymphoid DCs at peripheral tissues, including skin and mucosa, and

their migration capacity has suggested that DCs might be potential viral vessels contributing to EBOV dissemination. Furthermore, several studies using human monocyte-derived DCs have shown that EBOV infection leads to their impairment. It was shown that EBOV infection blocks secretion of proinflammatory cytokines and inhibits up-regulation of the T cell co-stimulatory molecules CD80, CD86 and CD40. Furthermore, EBOV-infected monocyte-derived DCs fail to prime naïve T cells (Mahanty et al., 2003, Bosio et al., 2003). As mentioned previously, infected DCs fail to produce IFN $\alpha$  probably due to efficient interference of the virus with the type I IFN response. It has been further suggested this might also impact DC maturation (Yen et al., 2014). These findings suggest a key role of DCs during EBOV pathogenesis. Nevertheless, the relevance *in vivo* has not been demonstrated so far.

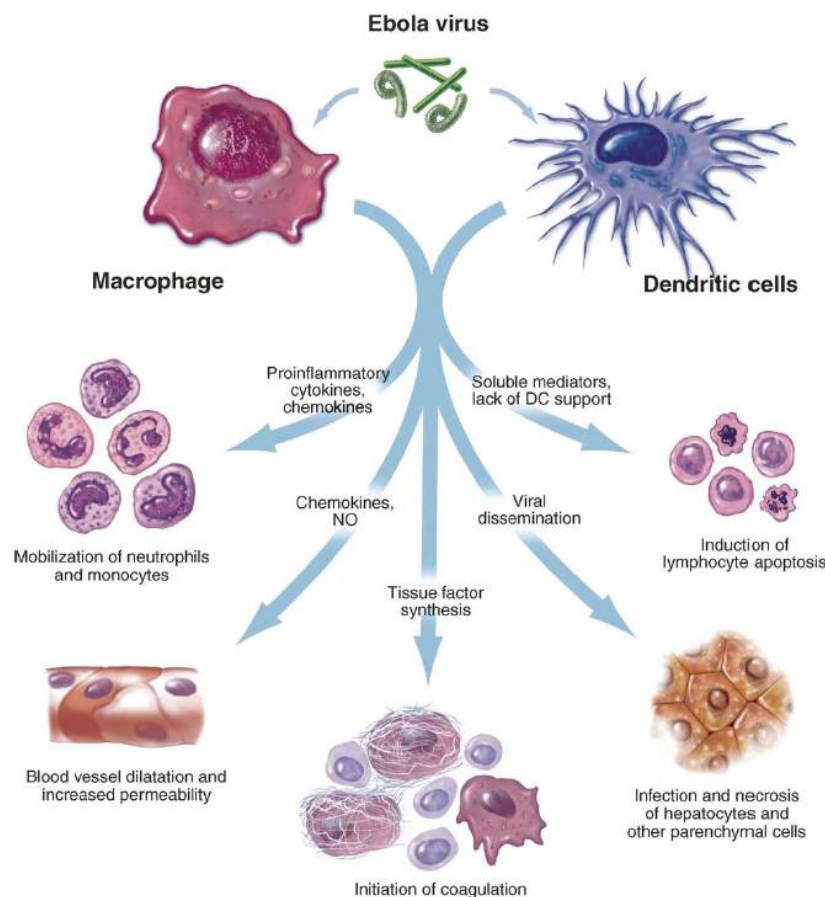


**Figure 8: Role of macrophages and DCs during EBOV pathogenesis** Macrophages and DCs, cells of the innate immune system, are thought to be early targets of EBOV infection. The infection of macrophages likely induces the production of proinflammatory cytokines, chemokines and nitric oxide, which leads to the recruitment of neutrophils and monocytes and increases vascular permeability. The synthesis of tissue factor is believed to cause coagulation abnormalities. The infection of DCs might result in viral dissemination and induction of lymphocyte apoptosis. Furthermore, disseminated virus infects hepatocytes and other parenchymal cells leading to necrosis (schematic from Bray and Geisbert, 2005).

### **3.3.3 Role of B and T lymphocytes**

*In vivo* and *in vitro* studies have demonstrated massive T lymphocyte loss due to apoptosis during EBOV infection (Bradfute et al., 2010, Gupta et al., 2007). Furthermore, apoptosis of lymphocytes was correlated with fatal outcome of EBOV infected patients (Baize et al., 1999; Wauquier et al., 2010). A defective antibody response was further observed in fatal human cases (Baize et al., 1999). Taken together, these data suggest an immune suppression during EBOV infection, which might be partially explained by the impairment of DCs. In contrast to that, a study in mice using mouse-adapted EBOV revealed functional EBOV-specific CD8 T cell responses during lethal EBOV infection, despite substantial T cell loss (Bradfute et al., 2008). Furthermore, the absence of EBOV induced T cell apoptosis in B-cell lymphoma 2 (Bcl-2) transgenic mice, which overexpress the anti-apoptotic protein Bcl-2, did not prevent lethal outcome (Bradfute et al., 2010). In addition, a recent study with EBOV survivors demonstrated a robust EBOV-specific T and B cell response during EVD (McElroy et al., 2015). Although some of the patients developed lymphopenia, McElroy and colleagues observed proliferation and activation of CD8 T cells characterized by double expression of HLA-DR and CD38. Even though the exact functions of B and T cells during EVD remain elusive, several studies in NHPs and rodents have demonstrated critical roles for both, antibodies and CD8 T cells, in vaccine-induced protection (Warfield et al., 2005, Sullivan et al., 2011).

### **3.4 Animal models for EBOV**

The recent EBOV outbreak in West Africa has advanced testing of vaccines and antiviral treatments. But even though several vaccines are in clinical trials and components blocking viral replication have been successfully tested in animal models, to date, no licensed vaccine or antiviral drug exists (Henao-Restrepo et al., 2015; Tapia et al., 2016; Oestereich et al., 2014). A better understanding of the host immune response to EVD *in vivo* is therefore crucial and requires the establishment of adequate animal models.

### **3.4.1 Non-human primates**

The gold-standard models for EBOV research are NHPs, which have been proposed to best reflect pathological features of human EVD due to the fact that they are closely related to humans. Experimentally infected rhesus and vervet monkeys develop lethal illness characterized by weight loss, anorexia, skin rash and high viremia and succumb to the infection 5 – 8 days post-infection (Bowen et al., 1978). Viral titers are detected in several organs, such as spleen, liver and lung, which also show signs of acute necrosis (Baskerville et al., 1978). An elaborate study with cynomolgus macaques evaluated pathogenesis of EBOV infection (Geisbert et al., 2003a). In this study, researchers noted neutrophilia and lymphopenia, proinflammatory cytokines and elevated nitrate levels marking a strong inflammatory response. Furthermore, hematology revealed decreased platelet levels and increased fibrin degradation products (D-dimers), which imply coagulation abnormalities. Elevated aspartate aminotransferase (AST) levels in serum indicated cell damage. The described pathological features are comparable to those observed in human patients even though disease progression is faster and 100% lethal in NHPs.

Despite the fact that NHP research has improved our understanding of EBOV pathogenesis, it is restricted due to ethical reasons and therefore immunological studies are limited. Small animal models, such as hamster or mouse, are essential for advancing EBOV basic research as well as therapies.

### **3.4.2 Mouse models**

Even though EBOV causes lethal illness in newborn mice, adult immunocompetent laboratory mice, such as C57BL/6 or BALB/c, are resistant to EBOV infection by any inoculation route, like intraperitoneal (i.p.) or subcutaneous (s.c.) (van der Groen et al., 1979). Therefore, efforts were made to adapt EBOV to the mouse species. The sequential passage of the human EBOV isolate from 1976 in newborn mice, generated a mouse-adapted EBOV (maEBOV) that was lethal for adult C57BL/6 or BALB/c mice via i.p. inoculation, but interestingly not via the s.c. or intramuscular (i.m.) route (Bray et al., 1998, Table 1). Similar to NHPs, pathological features of maEBOV infection in immunocompetent mice included systemic spread of the virus,

necrosis in liver and spleen and proinflammatory cytokine production. Mice succumb to infection 5 – 8 days after challenge.

In order to study non-adapted EBOV, mice with defects in the innate or adaptive immune response have been utilized. Various human EBOV isolates have been demonstrated to cause lethal illness in IFNAR<sup>-/-</sup> or STAT1<sup>-/-</sup> knockout mice via different inoculation routes (Bray et al., 2001; Raymond et al., 2011; Lever et al., 2012). EBOV and Sudan virus (SUDV) inoculated i.p. caused death in IFNAR<sup>-/-</sup> mice within 5 – 7 days post-infection. Interestingly, the degree of lethality varied between virus isolates. A different EBOV isolate from 1995 caused illness, but was not lethal, while Reston virus (RESV) and Tai Forest virus (TAFV) did not cause illness in IFNAR<sup>-/-</sup> mice (Bray et al., 2001). Researchers could further demonstrate that anti-IFN $\alpha$ / $\beta$  treatment rendered BALB/c mice susceptible to some human EBOV isolates.

**Table 1: Susceptibility of immunocompetent mice and mice with defects in either adaptive or innate immunity to mouse-adapted EBOV or non-adapted EBOV**

<b>Immune Defect</b>	<b>Strain</b>	<b>Mouse-ad i.p.</b>	<b>Mouse-ad s.c.</b>	<b>Non-ad i.p.</b>	<b>Non-ad s.c.</b>
<b>None</b>	BALB/c, C57BL/6	+	–	–	–
<b>Innate</b>	IFNAR <sup>-/-</sup>	+	+	+	+
	Stat1 <sup>-/-</sup>	+	+	+	+
<b>Adaptive</b>	SCID	+	+	+	+
	Rag-2	+	+	+	+

According to these data it is evident that the IFN-I response is crucial for protection against lethal EBOV infection in mice, suggesting that EBOV adaptation might result from a virus variant that was able to evade the mouse IFN-I response. To determine the virulence factors in mice, the viral genome of maEBOV was sequenced and compared to the human isolate revealing 8 amino acid changes. The generation of recombinant viruses containing original and mouse-adapted genes revealed VP24 to be crucial for viral evasion of the murine IFN response (Ebihara et al., 2006). In line with these findings, VP24 has been demonstrated to interfere with IFN induced resistance to EBOV infection (Reid et al., 2006). However, the other interferon antagonist VP35 was shown to be not critical for virulence in mice in this study.

Severe combined immunodeficiency (SCID) or recombination-activating gene 2 (Rag-2) mice, which lack mature lymphocytes, are also susceptible to EBOV and SUDV infection succumbing to the disease 3 – 4 weeks post-infection. However, when SCID mice are treated with anti-IFN $\alpha$ / $\beta$  antibodies, disease progression is comparable to infected IFNAR<sup>-/-</sup> mice indicating that innate immunity is crucial for early control of viral replication and spread, while the adaptive immune response is responsible for virus elimination (Bray et al., 2001).

The models presented here shed light on key mechanisms of resistance to EBOV infection in mice, but do not allow studying the kinetics of a functional immune response in an immunocompetent host.

## 4 Aims of this thesis

Understanding the physiology of the host immune response to viral infections is crucial for the development of successful vaccines and post-exposure therapies. The mouse as a model organism has provided essential knowledge for the basic understanding of human infectious diseases. However, immunocompetent mice are not susceptible to EBOV infection, and therefore IFNAR<sup>-/-</sup> knockout mice have been utilized in the past to study EBOV pathogenesis. Due to the fact that they lack a major antiviral defense mechanism, they are not suitable to study EBOV immunity. As a consequence, very little is known about EBOV immunity *in vivo*. In addition, systemic administration of the virus for experimental EBOV infection in mice has been the standard inoculation route. However, since EBOV is thought to enter its host via peripheral tissues, including mucosa or the skin, systemic inoculation does not mimic the natural course of EBOV infection.

In order to study EBOV immunology at the portals of viral entry it was of great importance to first establish natural routes of EBOV infection. Based on the need for immunocompetent mouse models, the second aim was to generate chimeric mice that were susceptible to non-adapted EBOV but were also able to mount a functional hematopoietic immune response. Ultimate goal was the generation of two models, that would allow studying, both murine and human immune responses to EBOV infection, respectively.

It is long suspected that DCs, which are key mediators of adaptive immunity, might contribute to the severity of EVD. However, this has never been tested *in vivo*. The third aim was to utilize the established models to investigate the role of DCs on EBOV immunity and pathophysiology *in vivo*. The goal was to analyze the contribution of the different DC subsets and correlate findings in the murine system with data from the humanized mouse model. Finally, data from experimental animal infections were further compared to human data obtained in the context of the EBOV outbreak in Guinea from 2014 and 2015.





## 5 Results

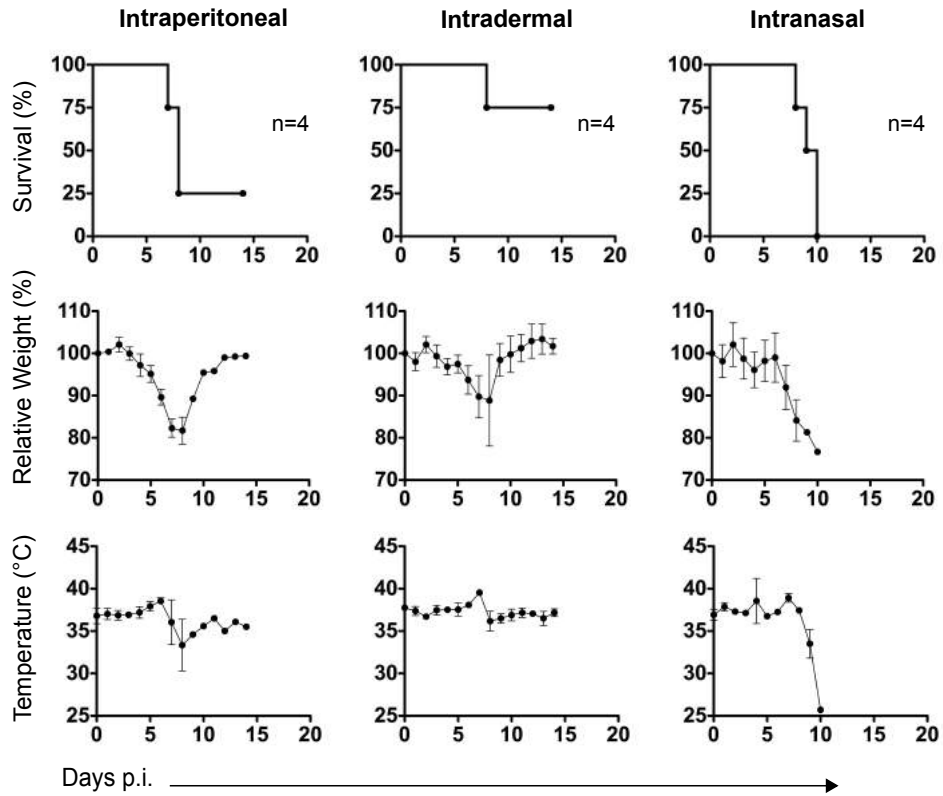
### 5.1 Natural routes of EBOV infection in IFNAR<sup>-/-</sup> knockout mice

#### 5.1.1 IFNAR<sup>-/-</sup> mice are susceptible to natural routes of EBOV infection

EBOV transmission mainly occurs via contact exposure to infectious body fluids (Dowell et al., 1999). It is thought that the virus enters the host via mucosal surfaces and small lesions in the skin. IHC assays of postmortem skin specimens from an EBOV outbreak in Kikwit, DRC revealed EBOV antigen in the skin (Zaki et al., 1999). However, these natural routes of infection have not been considered in previous animal models of EBOV pathogenesis. Utilizing the mouse as a model system, most pathogenesis studies have been carried out in knockout mice that lack the interferon- $\alpha$  and  $\beta$  receptor (IFNAR<sup>-/-</sup>). Bray and colleagues demonstrated that IFNAR<sup>-/-</sup> mice were highly susceptible to i.p. inoculation of non-adapted EBOV (Bray et al., 2001). Since immune responses are initiated at the natural portals of viral entry it was of great importance to establish natural EBOV infection in IFNAR<sup>-/-</sup> knockout mice, which would lead to systemic dissemination of the virus.

Viral entry via the skin was mimicked by injecting the virus intradermal/subcutaneous (i.d./s.c.) and intranasal (i.n.) administration was utilized to mimic entry via the respiratory mucosa. Both routes were compared to systemic i.p. inoculation. IFNAR<sup>-/-</sup> mice were inoculated with 1000 focus forming units (FFU) of EBOV, which was the standard inoculation dose in previous animal models (Bray et al., 2001). Temperature and body weight were measured daily to monitor signs of morbidity and mortality. Heparin blood was collected at indicated time points to determine viremia and serum to analyze AST levels.

A



B

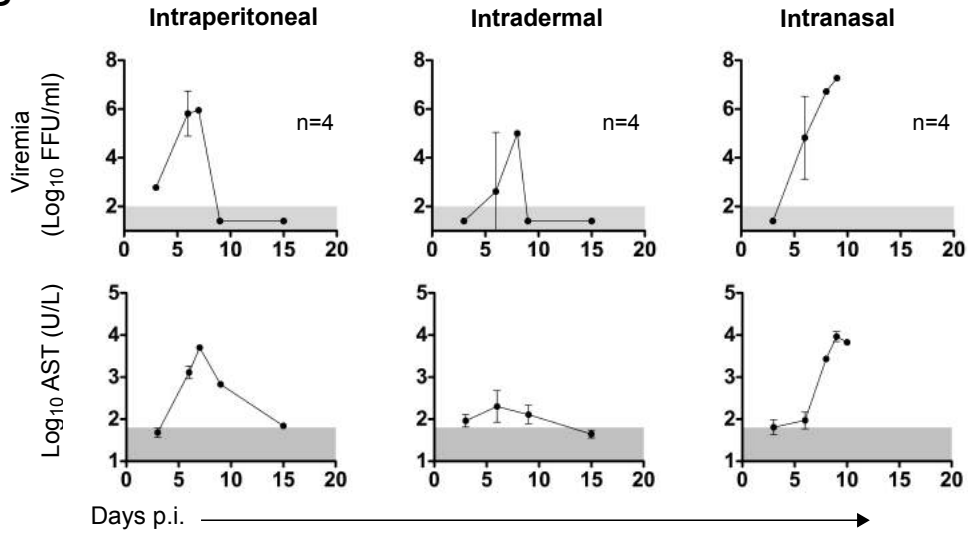


**Figure 9: Natural routes of EBOV infection** IFNAR<sup>-/-</sup> mice were infected ip., i.d./s.c. or i.n. with 1000 FFU of EBOV. For i.d./s.c. administration at the base of the tail, animals were shaved prior to infection. For i.n. inoculation, virus inoculate was applied to the nostrils of the mice. Infected animals were monitored daily, measuring weight and temperature (A), and heparin blood and serum were collected at indicated time points, for determination of viremia and AST levels, respectively. Viremia was determined via focus formation assay, AST levels were analyzed using a colorimetric assay kit for a reflotron (B). The normal range for AST and the limit of detection for viremia are shaded in grey. Mean and standard deviation are shown.

As expected, animals inoculated i.p. showed significant weight loss around day 6 post-infection and 75% of infected mice succumbed to the disease at days 7 and 8 post-infection (Fig. 9A). After 6 days post-infection animals revealed systemic infection indicated by viremia in blood and had elevated AST levels, a sign of cell damage (Fig. 9B). In comparison, the i.d./s.c. administration of EBOV at the back of the tail resulted in reduced mortality and lower viremia and AST levels. I.n. infection via nostrils was 100% lethal and animals had to be sacrificed 8 – 10 days post-infection. Six days post-infection, animals exhibited high viremia and AST levels. Taken together, these results indicated that IFNAR<sup>-/-</sup> mice were susceptible to EBOV infection via all three routes analyzed. Interestingly, a high degree of protection was observed when the virus was administered via the skin (i.d./s.c.). Since intranasal inoculation provides a system of mucosal infection leading to systemic dissemination of EBOV and high mortality, this system was chosen for further studies.

### **5.1.2 Mucosal infection leads to local and systemic EBOV replication**

To further characterize the course of EBOV infection after mucosal infection, the kinetics of viral replication was determined in lung, as part of the respiratory system where early viral replication might take place, and in spleen, which is highly affected by EBOV replication in NHPs (Geisbert et al., 2003). IFNAR<sup>-/-</sup> mice were infected i.n. with 1000 FFU of EBOV and starting on day 1 post-infection, two animals were euthanized every 2 days. Heparin blood for viremia analysis and serum for evaluation of AST levels were collected and lung and spleen were harvested to investigate local and systemic replication, respectively. The experiment was carried out in parallel in C57BL/6 mice (referred to as Bl6 mice) in order to compare viral replication in immunodeficient and immunocompetent animals.

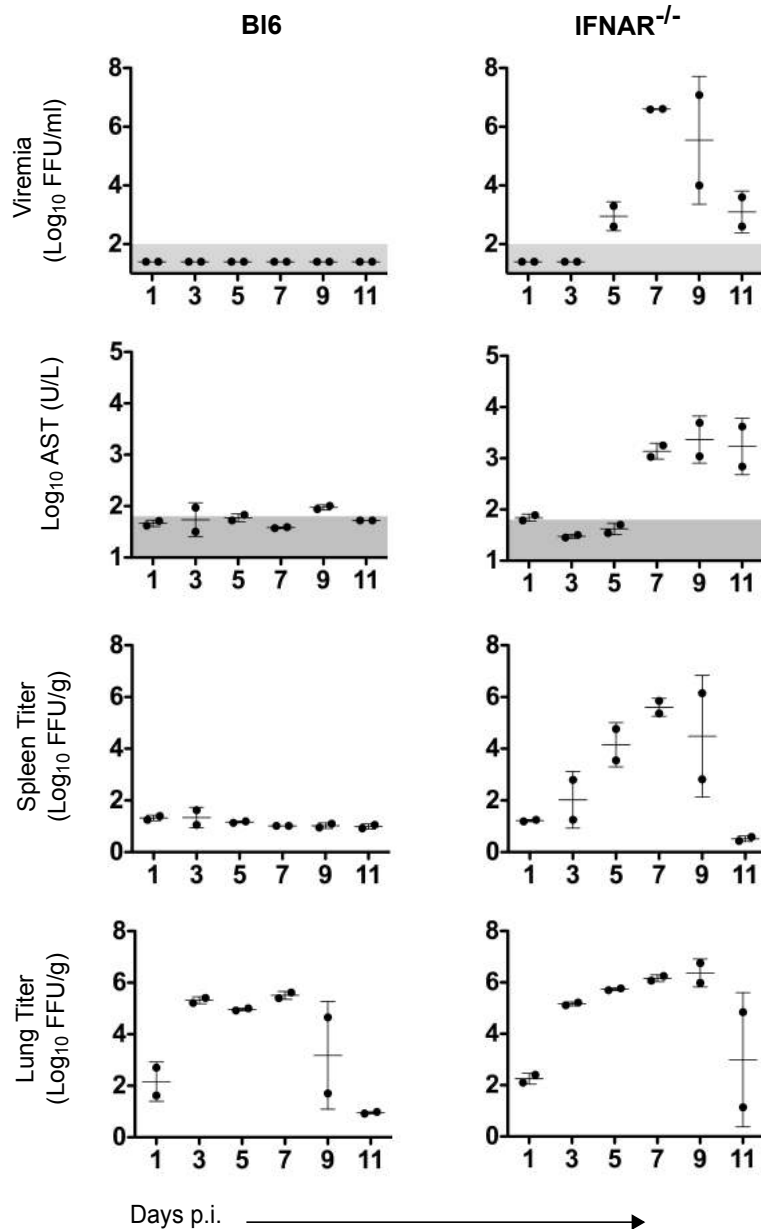


**Figure 10: Kinetic of EBOV replication in IFNAR<sup>-/-</sup> and B16 mice** IFNAR<sup>-/-</sup> and B16 mice were inoculated i.n. with 1000 FFU of EBOV. Starting on day 1 post-infection, 2 animals per group were sacrificed every 2 days. Heparin blood and serum were collected for viremia and AST, lung and spleen were taken for organ titers. AST levels were measured using a colorimetric assay kit for a reflotron and viremia and organ titers were determined via focus formation assay. The grey bar is showing the normal range for AST and the limit of detection for viremia. Graphs are presented with mean and standard deviation.

As expected, no viral replication was detected in blood and spleen over the course of infection in B16 mice, AST levels were not elevated (Fig. 10). Infected B16 animals did not show disease symptoms such as weight loss or changes in body temperature (data not shown). However, significant viral replication was observed 3 days post-infection in the lung and remained detectable up to day 9 post-infection. The virus was cleared from the lung of infected animals 11 days post-infection. In contrast,

IFNAR<sup>-/-</sup> mice exhibited systemic infection starting on day 5 post-infection demonstrated by viremia, viral titers in spleen and elevated AST levels starting on day 7. IFNAR<sup>-/-</sup> mice showed comparable lung titers to BL6 mice. One out of two animals cleared the virus from the lung at day 11 post-infection.

This experiment demonstrated that BL6 mice were resistant to EBOV infection, while IFNAR<sup>-/-</sup> mice were systemically infected after i.n. inoculation. However, local replication at the entry site of the virus was observed in BL6 mice from day 3 until day 9 post-infection revealing susceptibility of murine cells non-adapted EBOV independently of the IFN-I response. These findings are in line with previously published data that IFN signaling is crucial for controlling viral dissemination but also indicate that local EBOV replication occurs in IFN competent systems.

## **5.2 Establishment of immunocompetent mouse models susceptible to EBOV**

Since immunocompetent C57BL/6 mice are resistant to non-adapted EBOV, most EBOV research has been carried out in IFNAR<sup>-/-</sup> knockout mice. However, due to their lack of the main antiviral defense mechanism, IFNAR<sup>-/-</sup> mice are not suitable to study the immune response to viral infections. As part of the second aim of this thesis a murine chimeric mouse model was established that was susceptible to non-adapted EBOV but that also retained hematopoietic immunocompetence.

### **5.2.1 EBOV infection in bone marrow chimeric mice**

It is evident that the type I IFN response is essential for the resistance to EBOV infection in mice, but it is unclear which cells are important for this response. In general, all body cells are capable of producing and responding to type I IFN, but the IFN response of immune cells is especially important for controlling viral infections. Bone marrow chimeric mice were utilized to dissect the role of hematopoietic cells, which include most immune cells, and non-hematopoietic cells, such as stromal and epithelial cells, in resistance to EBOV infection. The basis of bone marrow transplantation is that pluripotent hematopoietic stem cells (HSCs) from the bone marrow are very sensitive to irradiation. Thus, depletion of HSCs by irradiation allows transplantation of donor bone marrow cells. This permits the generation of chimeric mice where the lack of the interferon receptor is confined to either hematopoietic (BL6 IFNAR<sup>-/-</sup>) or non-hematopoietic (IFNAR<sup>-/-</sup> BL6) cells. However, it has to be noted that

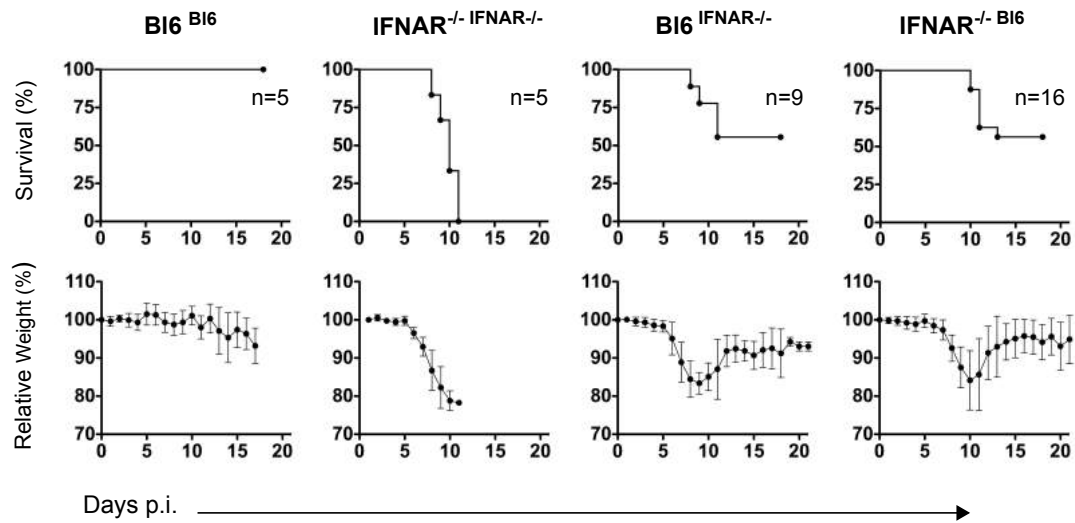
some lung-resident macrophages are yolk sac-derived and radioresistant and therefore cannot be depleted via irradiation (Perdiguero and Geissmann, 2015).

Chimeric mice were generated by lethal irradiation of either B16 or IFNAR<sup>-/-</sup> recipient mice followed by heterologous transplantation of bone marrow from IFNAR<sup>-/-</sup> or B16 donor mice, respectively. Control chimeras (B16<sup>B16</sup> and IFNAR<sup>-/-</sup> IFNAR<sup>-/-</sup>) with homologous transplantation were generated as well. Engraftment of donor cells was analyzed 4 weeks post transplantation. Cells from donor and recipient mice could be distinguished using donor congenic mice that possess different alleles of the hematopoietic marker CD45, namely CD45.1 and CD45.2. In this experiment, C57BL/6\_Ly5.1 mice expressed CD45.1, while IFNAR<sup>-/-</sup> mice expressed CD45.2. Chimeric mice with an engraftment >85% of donor CD45<sup>+</sup> cells were infected i.n. with 1000 FFU of EBOV and monitored over the course of infection. Survival and weight loss were measured daily, viremia and AST levels were analyzed at indicated time points.

While B16<sup>B16</sup> chimeras were not susceptible to EBOV infection, IFNAR<sup>-/-</sup> IFNAR<sup>-/-</sup> chimeras were highly susceptible to the infection with a lethality rate of 100% (Fig. 11). This result was line with previous experiments and demonstrated that the chimerism did not affect disease outcome. Both, heterologous IFNAR<sup>-/-</sup> B16 and B16<sup>IFNAR<sup>-/-</sup></sup> chimeras were susceptible to EBOV infection but showed enhanced survival compared to IFNAR<sup>-/-</sup> IFNAR<sup>-/-</sup> control chimeras (Fig. 11). These findings revealed that both, hematopoietic and non-hematopoietic cells were important for IFN-mediated protection. Interestingly, B16<sup>IFNAR<sup>-/-</sup></sup> chimeras exhibited high viremia, while IFNAR<sup>-/-</sup> B16 had low or no viremia indicating an important role of hematopoietic cells in controlling viral dissemination.

The IFNAR<sup>-/-</sup> B16 chimeric mouse thus represents a novel semi immunocompetent model that is susceptible to non-adapted EBOV and possesses functional hematopoietic immunity allowing the study of the kinetic of the immune response to EBOV *in vivo*.

A



B

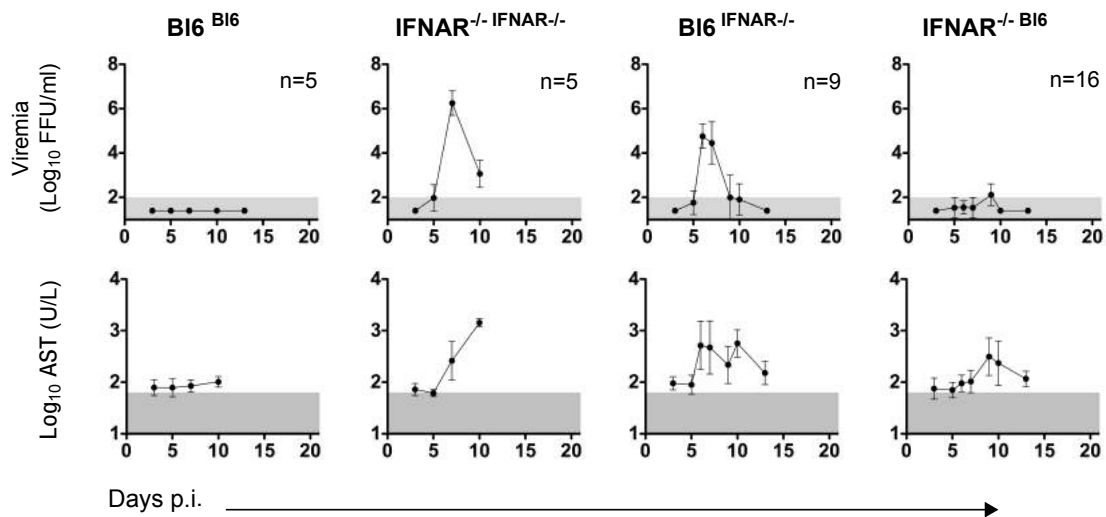


**Figure 11: Course of EBOV infection in  $IFNAR^{-/-}$  Bl6 and Bl6  $IFNAR^{-/-}$  chimeric mice** Four weeks post transplantation, chimeric Bl6<sup>Bl6</sup>,  $IFNAR^{-/-}$   $IFNAR^{-/-}$ , Bl6  $IFNAR^{-/-}$  and  $IFNAR^{-/-}$  Bl6 mice were infected i.n. with 1000 FFU of EBOV. Survival and relative weight loss were controlled daily, blood and serum were collected at indicated time points for determination of viremia and AST levels, respectively. The normal range for AST and the limit of detection for viremia are shaded in grey. Mean and standard deviation are shown.

## 5.2.2 EBOV infection in humanized NSG-A2 mice

The  $IFNAR^{-/-}$  Bl6 chimeric mouse provides a useful tool for understanding the kinetics of the immune response to EBOV in the context of the murine immune system. Even though murine and human immunity is closely related, findings in the murine system do not necessarily translate to humans. Furthermore, EBOV infected mice do not exhibit all pathological features of human EVD. The only animals closely mimicking

human EBOV infection are NHPs. Due to ethical reasons only end point experiments are conducted in NHPs. However, in order to study immunity to a pathogen it is crucial to understand the kinetics of the immune response since it is a highly complex biological process. It was therefore of great importance to develop a ‘humanized’ mouse model that was susceptible to non-adapted EBOV and furthermore mimicked pathological features of EVD. In addition, this model allowed comparison and validation of findings from the murine model in the context of the human immune response.

### ***Generation of humanized NSG-A2 mice***

The general principle of ‘humanized’ mice is based on the engraftment of human tissue, hematopoietic stem cells (HSCs) or peripheral-blood mononuclear cells (PBMCs) into severely deficient recipient mice that tolerate the transplant (Shultz et al., 2007). A variety of humanized mouse models have been developed in the past that demonstrated to be useful systems to study the infection of numerous viruses (Bente et al., 2005; Melkus et al., 2006).

In the present study, non-obese diabetic (NOD)/severe combined immunodeficiency (scid)-interleukin-2 (IL-2) receptor- $\gamma$  chain knockout (NSG) mice were utilized as immunodeficient recipients. NSG mice exhibit severe defects in innate immunity and lack of T and B cells that permit long-term engraftment of human cells (Ishikawa et al., 2005). Furthermore, the expression of human HLA-A2.1 guarantees the development of functional human T cells from HLA-A2.1 donors in humanized NSG-A2 mice, which was demonstrated previously by Shultz and colleagues (Shultz et al., 2010). The reconstitution of the human immune system was achieved by the transplantation of CD34<sup>+</sup> hematopoietic stem cells (HSCs) obtained from human cord blood from HLA-A2.1 donors into sub-lethally irradiated NSG-A2 mice.

**Table 2: Engraftment of human hematopoietic cells comparing male and female NSG mice**

<b>CD45<sup>+</sup> cells (% of Singlets)</b>	<b>Female 1</b>	<b>Female 2</b>	<b>Male 1</b>	<b>Male 2</b>
Blood	18.7	N/A	16.8	N/A
Bone Marrow	41.9	80.1	15.8	24.1
Spleen	56.1	60.3	51.2	49.0
Lung	32.1	37.8	25.8	19.9



First optimization experiments were carried out in NSG mice that did not express HLA-A2.1. However, for all following infection experiments NSG-A2 mice were utilized to ensure functional T cell responses. For optimal engraftment, male and female NSG mice were compared, freshly thawed and cultured HSCs were used and lethal and sub-lethal irradiation was tested. The engraftment of human immune cells was analyzed in lymphoid and peripheral organs 8 weeks post transplantation by staining of the hematopoietic marker CD45 using multicolor flow cytometry. Best engraftment in lymphoid (blood, bone marrow and spleen) and peripheral organs (lung) was achieved with sub-lethally irradiated female NSG mice and the transplantation of freshly thawed HSCs (Table 2). Therefore for further studies only female animals were used for the transplantation with freshly thawed cells. Lethal irradiated NSG mice died shortly after irradiation and transplantation. The engraftment in male NSG mice was lower compared to female NSG mice. Cells from the human myeloid and lymphoid lineage were further investigated with lineage specific markers. In all lymphoid organs B and T cells and myeloid cells like monocytes could be found (Fig. 12).

### Bone Marrow

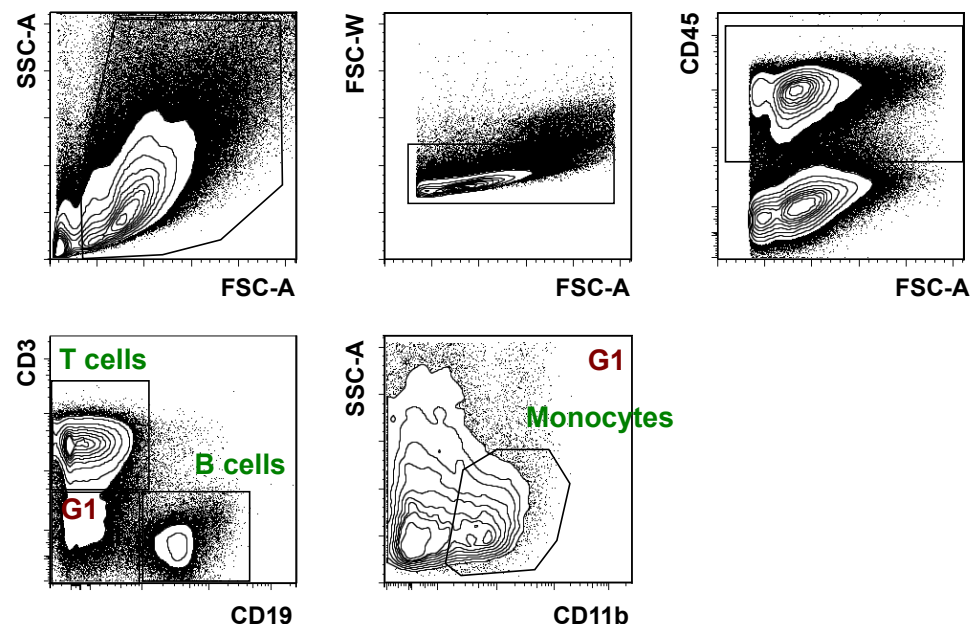


**Figure 12: Engraftment of lymphoid and myeloid cells in bone marrow of huNSG mice** Humanized NSG mice were sacrificed 8 month post-transplantation. The bone marrow was extracted and analyzed for the presence of human cells with flow cytometry using antibodies directed against human cell surface markers. The gating strategy for bone marrow of one animal is presented. The first gate excludes debris and the second excludes doublets. In the third gate human CD45 hematopoietic cells are selected. From there, CD3 and CD19 markers were used to identify T and B cells, respectively. Monocytes were characterized as CD3 and CD19 double negative cells, which were positive for CD11b.

In order to investigate the immune response to EBOV infection at the natural portals of entry, it was important to analyze the presence of antigen-presenting cells (APCs) at peripheral tissues (e.g. lung). Antigen-presenting cells are defined as positive for HLA-DR and negative for the Lineage markers CD3, CD19 and CD56 that are expressed by T cells, B cells and NK cells, respectively. Within the APC population monocytes, monocyte-derived DCs and macrophages as well as conventional DCs can be distinguished. Conventional DCs are CD14 and CD16 negative, and express the markers CD141 and CD11c. CD141<sup>+</sup> DCs and CD11c<sup>+</sup> DCs were detected in all lungs analyzed (Fig. 13). Furthermore, CD14<sup>+</sup> myeloid cells, which include monocytes, monocyte-derived macrophages and DCs, as well as CD16<sup>+</sup> myeloid cells were identified as well.

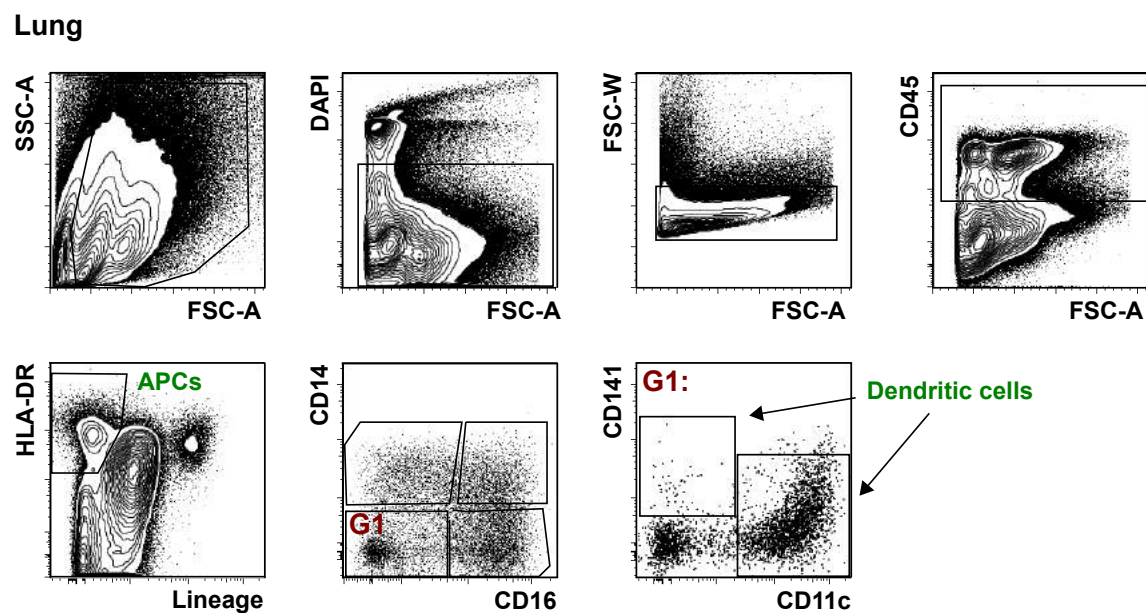


**Figure 13: Engraftment of antigen-presenting cells in lungs of huNSG mice** Lungs of huNSG mice were collected 8 weeks post transplantation. A single cell suspension was created and cells were stained for flow cytometry. The gating strategy of myeloid cells in the lung of one animal is presented. Briefly, debris, doublets and dead cells were excluded with the first three gates. Then human hematopoietic cells were selected using the CD45 marker. Antigen-presenting cells were defined as CD45<sup>+</sup>, HLA-DR<sup>+</sup> and Lineage negative. Lineage included T cells (CD3), B cells (CD19) and NK cells (CD56). The APC gate included CD16<sup>+</sup> monocytes, CD14<sup>+</sup> monocytes, CD14<sup>+</sup> monocyte-derived DCs and macrophages and dendritic cells, which were negative for CD14 and CD16, and expressed CD11c or CD141.

In summary, the repopulation of human cells of lymphoid and myeloid origin was found in bone marrow, spleen and blood of all animals analyzed. Furthermore, also peripheral tissues showed engraftment of lymphoid cells, as well as APCs. Nevertheless, there is room for improvement of this model, since animals that were

transplanted at the same time showed high variations in numbers of engrafted lymphoid and myeloid cells. This might lead to variations in the response to EBOV infection.

### ***Humanized NSG-A2 mice are highly susceptible to EBOV infection***

To analyze whether huNSG-A2 mice were susceptible to EBOV infection, mice were infected i.p. with 1000 FFU of EBOV and monitored over the course of infection. Heparin blood was collected to determine viremia and spleen, kidney, liver, lung and brain were taken at the time of death to analyze histopathology and viral organ titers. I.p. administration was chosen, in order to compare findings with those from previous reports that used small animal models of EBOV infection. NSG-A2 mice with low engraftment of hematopoietic cells (20-40% in peripheral blood leukocytes) were compared to high engrafted animals (>40% in peripheral blood leukocytes). Animals inoculated with PBS served as controls (Mock).

It was observed that huNSG-A2 mice were susceptible to EBOV infection and that the severity of the infection was correlated with the percentage of human cells (Fig. 14A). Infected animals started to lose body weight around day 7 post-infection. While the lethality for low engrafted mice was 75%, all high engrafted mice succumbed to the EBOV infection within 20 days. This reflected the incubation period and length of disease course typically observed in humans (Schieffelin et al., 2014). Low and high engrafted mice displayed a systemic infection indicated by viremia in blood starting around day 6 post-infection (Fig. 14B). Furthermore, both low and high engrafted animals had similar titers in spleen, kidney, liver, lung and brain suggesting that mouse cells also support viral replication. Immunofluorescence staining of liver sections revealed that mouse hepatocytes supported viral replication (Fig. 14C).

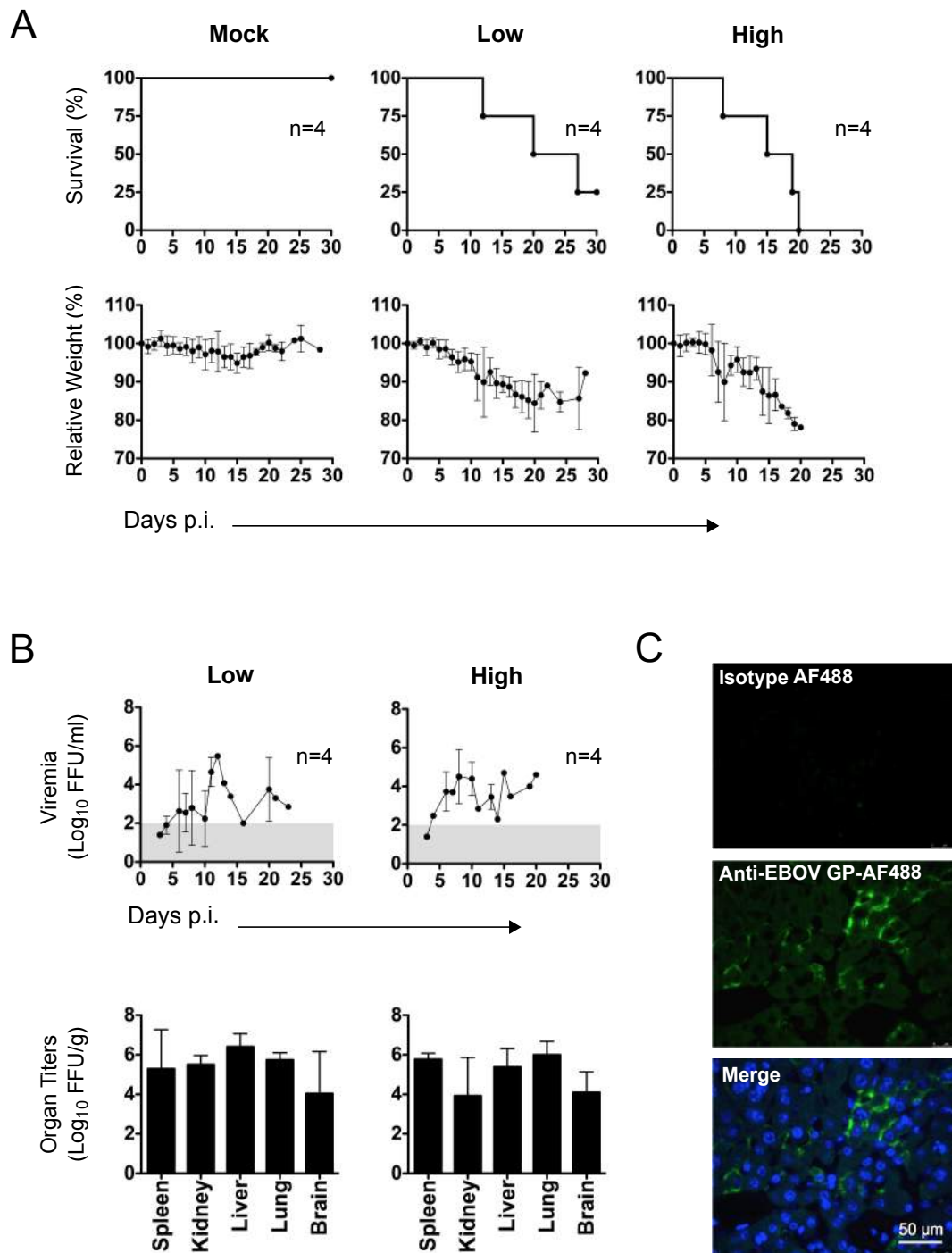


**Figure 14: EBOV infection in humanized NSG-A2 mice** HuNSG-A2 mice were inoculated i.p. with 1000 FFU of EBOV or PBS (mock control) and monitored daily for survival and relative weight loss over the course of infection (A). Viremia was determined at indicated time points and viral titers of spleen, kidney, liver, lung and brain were analyzed at the time of death (B). The grey bar indicates the limit of detection for viremia. Mean and standard deviation are shown. For immunofluorescence staining of liver sections an anti-EBOV Glycoprotein antibody labeled with AlexaFluor488 (AF488) was used to stain infected cells, DAPI was used to stain nuclei. The merged picture is an overlay of EBOV and DAPI staining. Tissue sections were also stained with an isotype control antibody for AF488 (C).

The model presented here is susceptible to non-adapted EBOV and presents systemic infection with high viral titers and high lethality that also has been observed in human patients.

***EBOV infected huNSG-A2 mice reproduce pathological findings of human EVD***

To further investigate the pathological features of huNSG-A2 mice during EBOV infection, AST levels as a sign of cell damage were analyzed. In comparison to mock infected animals, both, low and high engrafted animals displayed elevated AST levels (Fig. 15A). Moreover, necropsies showed splenomegaly and liver steatosis (fatty liver) and in one out of 6 animals focal hemorrhage and necrosis in the liver was observed (Fig. 15B). Histology of tissue sections further demonstrated lymphocyte infiltration in spleen and droplet steatosis in liver (Fig. 15C).

Thus, huNSG-A2 mice infected with non-adapted EBOV reproduce key features of EBOV pathology previously observed in human patients and NHPs (Geisbert et al., 2003a).

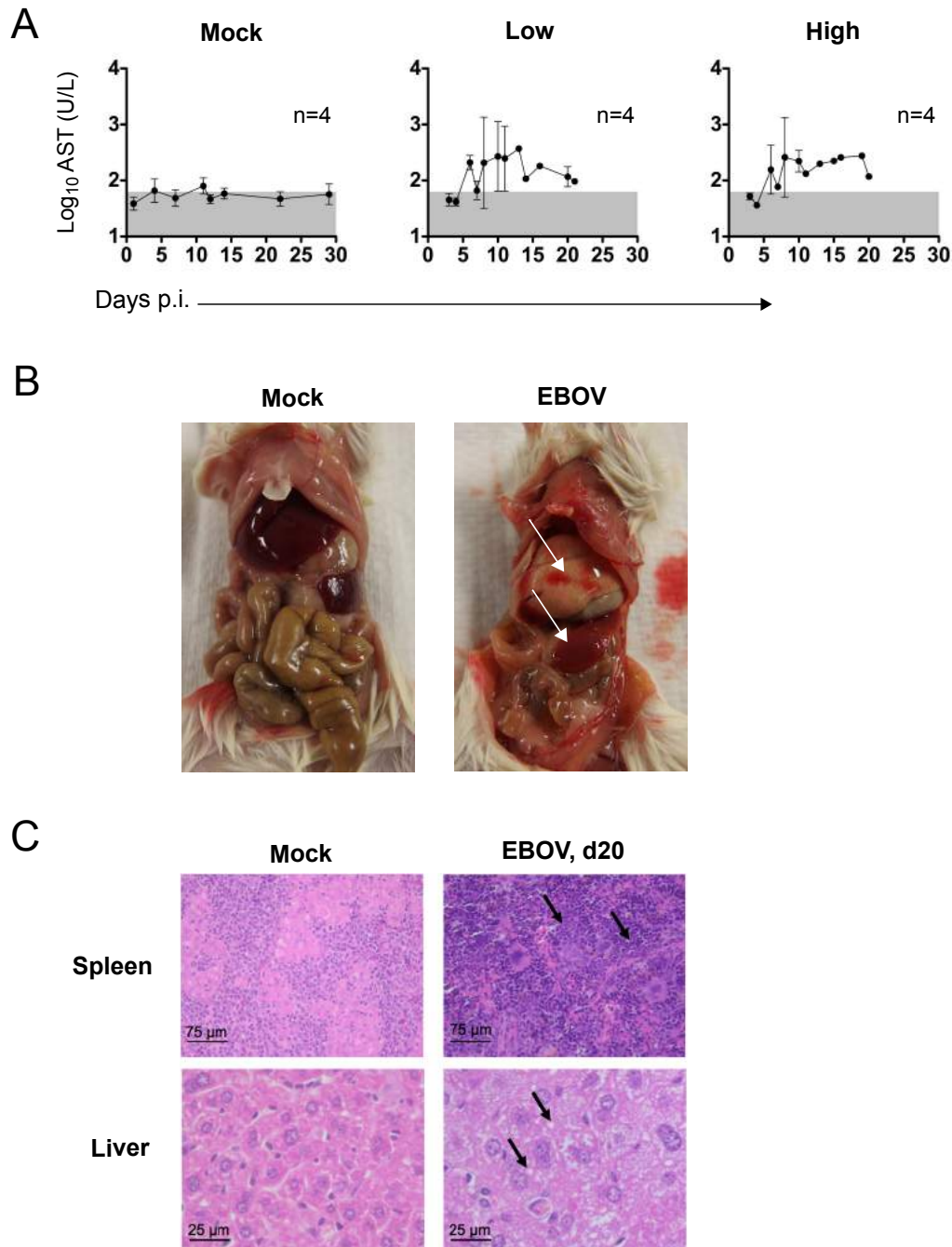


**Figure 15: Pathological features of EBOV infection** AST levels in serum were analyzed using a colorimetric assay kit for a reflatron (A). The normal range for AST is shaded in grey. Graphs show mean and standard deviation. Necropsies of mock and EBOV infected huNSG-A2 mice are shown (B). The upper arrow indicates focal hemorrhage, the lower arrow shows splenomegaly. Histology of spleen and liver sections of mock and EBOV infected animals is presented. The black arrows in spleen indicate lymphocyte infiltration, in liver the arrows indicate droplet steatosis (C).

## ***Presence of human cells is directly correlated with pathology in EBOV infected huNSG-A2 mice***

To dissect whether the human immune system contributed to EBOV pathogenesis in huNSG-A2 mice, non-transplanted NSG-A2 mice or mice with transplanted mouse bone marrow cells (moNSG-A2) were inoculated i.p. with 1000 FFU of EBOV and monitored over the course of infection.

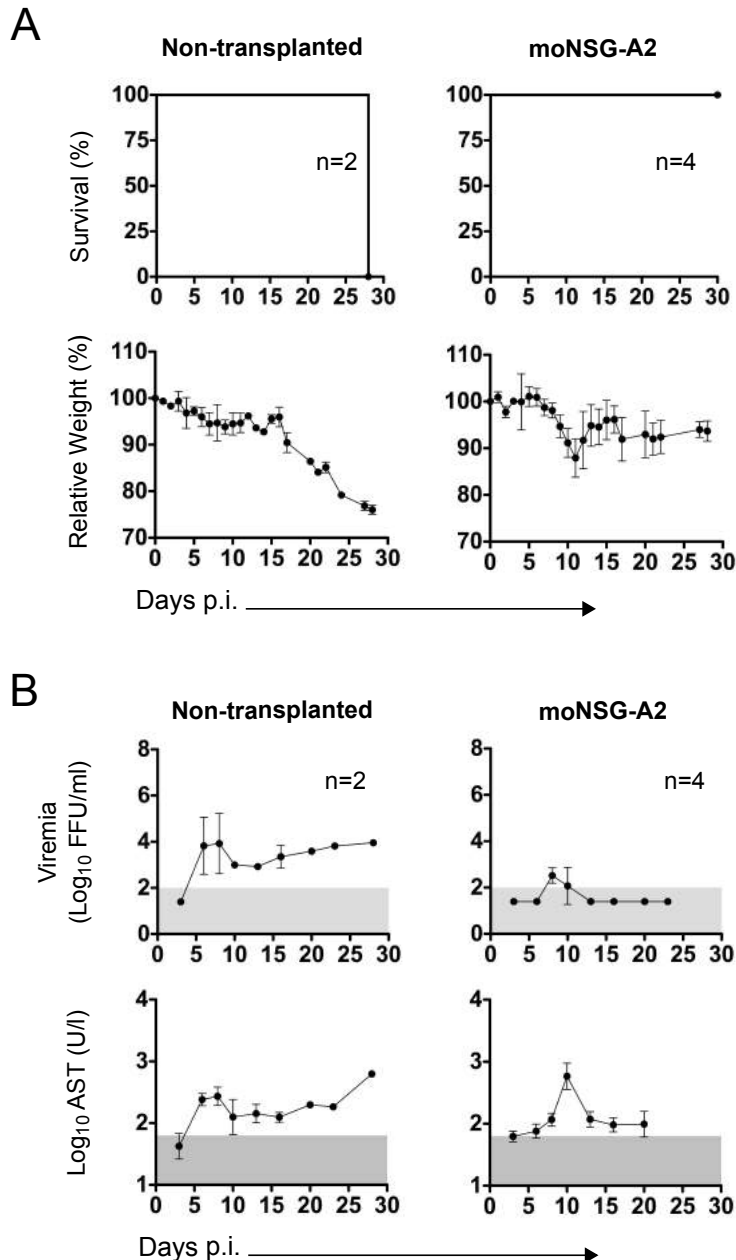


**Figure 16: EBOV infection in non-transplanted NSG-A2 and moNSG-A2 mice** Non-transplanted NSG-A2 and moNSG-A2 mice were infected i.p. with 1000 FFU of EBOV. Survival and relative weight loss were monitored daily (A). Viremia and AST levels were analyzed at indicated time points. The grey bars show the limit of detection for viremia and the normal range for AST levels. Mean and standard deviation are shown.

Non-transplanted NSG-A2 mice lost weight progressively and succumbed to EBOV 4 weeks after infection with unresolved viremia and elevated AST levels (Fig. 16). Presumably due to defects in innate and adaptive immunity, non-transplanted NSG-A2 mice were not able to control the infection. This was in contrast to moNSG-A2 mice, which exhibited moderate body weight loss, low viremia and slightly elevated AST levels around day 10 post-infection, but recovered from the infection with 100% survival.

These findings suggest that mouse hematopoietic cells are able to control EBOV infection, even though early EBOV replication can occur due to defects in the innate response of non-hematopoietic cells of NSG-A2 recipients. Moreover, these data demonstrate that human hematopoietic cells account for the degree of EBOV infection severity observed in huNSG-A2 mice. The data presented in figures 14 – 16 were generated in close collaboration with Lisa Oestereich and published in 2015 as a co-first author publication (Lüdtke et al., 2015).

### ***Hu-NSG-A2 mice are highly susceptible to intranasal EBOV infection***

Similar to the murine IFNAR<sup>-/-</sup> Bl6 model, a more natural route of infection was established for huNSG-A2 mice which would allow analyzing the immune response at the entry site of the virus. HuNSG-A2 mice were inoculated i.n. with 1000 FFU of EBOV and relative weight loss and survival was monitored. Moreover, heparin blood was collected at indicated time points and viral titers in several organs were determined at the time of death. HuNSG-A2 mice were engrafted with 35 – 75% of human hematopoietic cells in peripheral blood.

The i.n. infection of huNSG-A2 mice led to a faster and more homologous disease course compared to i.p. inoculation, with animals succumbing to infection between day 8 and 13 post-inoculation (Fig. 17A). High viremia was observed in all animals between days 8 and 13 as well as high viral titers in spleen, kidney, liver and lung at the time of death (Fig. 17B). Furthermore, infection with the Mayinga variant of EBOV was compared to a new EBOV variant, Makona, isolated during the 2014 – 2015 EBOV outbreak in West Africa. It could be seen that the infection with the Makona variant resulted in reduced mortality with a survival rate of approximately 60% (Fig. 17C).



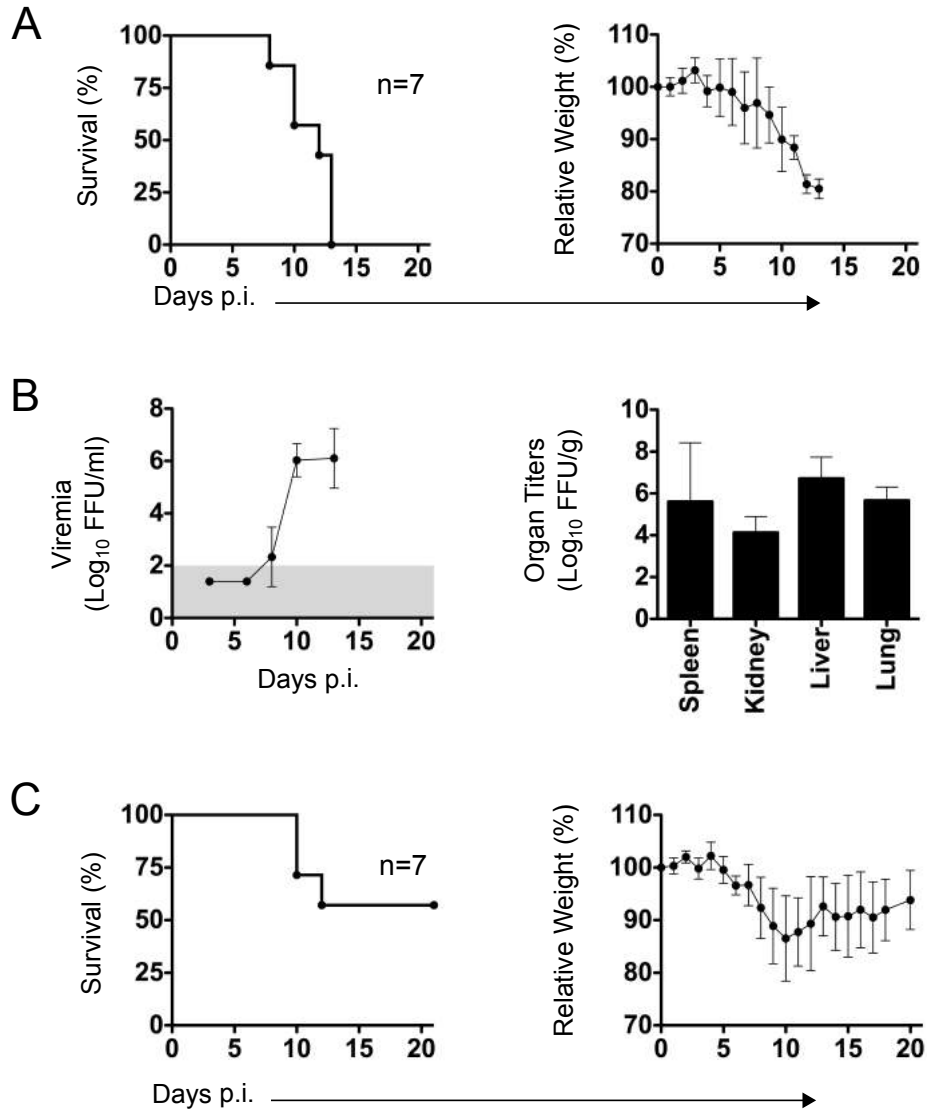


**Figure 17: Intranasal EBOV infection of humanized NSG-A2 mice** HuNSG-A2 mice were inoculated i.n. with 1000 FFU of EBOV. Survival and relative weight loss were examined daily (A), viremia was analyzed at indicated time points, organ titer at the time of death (B). HuNSG-A2 mice were also inoculated i.n. with 1000 FFU of the Makona EBOV variant (C). The grey bar indicates the level of detection for viremia and graphs show mean and standard deviation.

These findings showed that huNSG-A2 mice were highly susceptible to EBOV administered i.n. with a 100% lethal outcome. Therefore, mucosal administration of EBOV was chosen for further immunology studies in huNSG-A2 mice. Moreover, huNSG-A2 mice were also susceptible to the Makona variant of EBOV with reduced mortality. These data are in line with recently published data that showed a delay in disease progression of Makona in NHPs suggesting reduced pathogenicity of the new West African variant (Marzi et al., 2015).

## 5.3 Investigation of EBOV immunity *in vivo*

### 5.3.1 EBOV immunity in bone marrow chimeric mice

Due to the lack of small immunocompetent animal models, there is very little known about EBOV immunity *in vivo*. Upon viral infection the host immune response is initiated, which can be generally divided into innate and adaptive immunity. Innate immunity is crucial for the control of early viral replication and the initiation of an adaptive immune response that mediates clearance of the virus and leads to long-lasting protective immunity. Since this highly complex physiological process involves the interplay of a variety of body cells in lymphoid and non-lymphoid organs, kinetic studies are necessary to understand immunity to viral pathogens. The third aim of this thesis was therefore to investigate the kinetics of the immune response during EBOV infection *in vivo* utilizing the established immunocompetent IFNAR<sup>-/-</sup> Bl6 model.

#### ***IFNAR<sup>-/-</sup> Bl6 mice sustain lower systemic replication than IFNAR<sup>-/-</sup> IFNAR<sup>-/-</sup> mice***

To be able to correlate immunological findings with pathophysiological data, viremia, organ titers and AST levels were determined at early (day 4), intermediate (day 7) and late (day 9) time points post-infection for IFNAR<sup>-/-</sup> Bl6 and IFNAR<sup>-/-</sup> IFNAR<sup>-/-</sup> chimeras. The latter were included in the experiment in order to determine IFN-I dependency in hematopoietic-mediated immunity to EBOV.

Consistent with the data presented in Figure 11, IFNAR<sup>-/-</sup> Bl6 chimeras had no viremia, while IFNAR<sup>-/-</sup> IFNAR<sup>-/-</sup> mice exhibited systemic infection starting at day 7 post-infection (Fig. 18). On day 9, both IFNAR<sup>-/-</sup> Bl6 and IFNAR<sup>-/-</sup> IFNAR<sup>-/-</sup> chimeras had elevated AST levels indicating cell damage. Replicating virus was observed in the lungs of both chimeras at all three time points evaluated. At day 7 post-infection, titers in liver and spleen were observed in both chimeras, while IFNAR<sup>-/-</sup> Bl6 mice had a ten-fold reduction in viral titers compared to IFNAR<sup>-/-</sup> IFNAR<sup>-/-</sup> mice. After 9 days post-infection, IFNAR<sup>-/-</sup> Bl6 chimeras had significant lower titers in spleen, liver and kidney compared to IFNAR<sup>-/-</sup> IFNAR<sup>-/-</sup> chimeras, which exhibited titers around 10<sup>5</sup> in these organs.

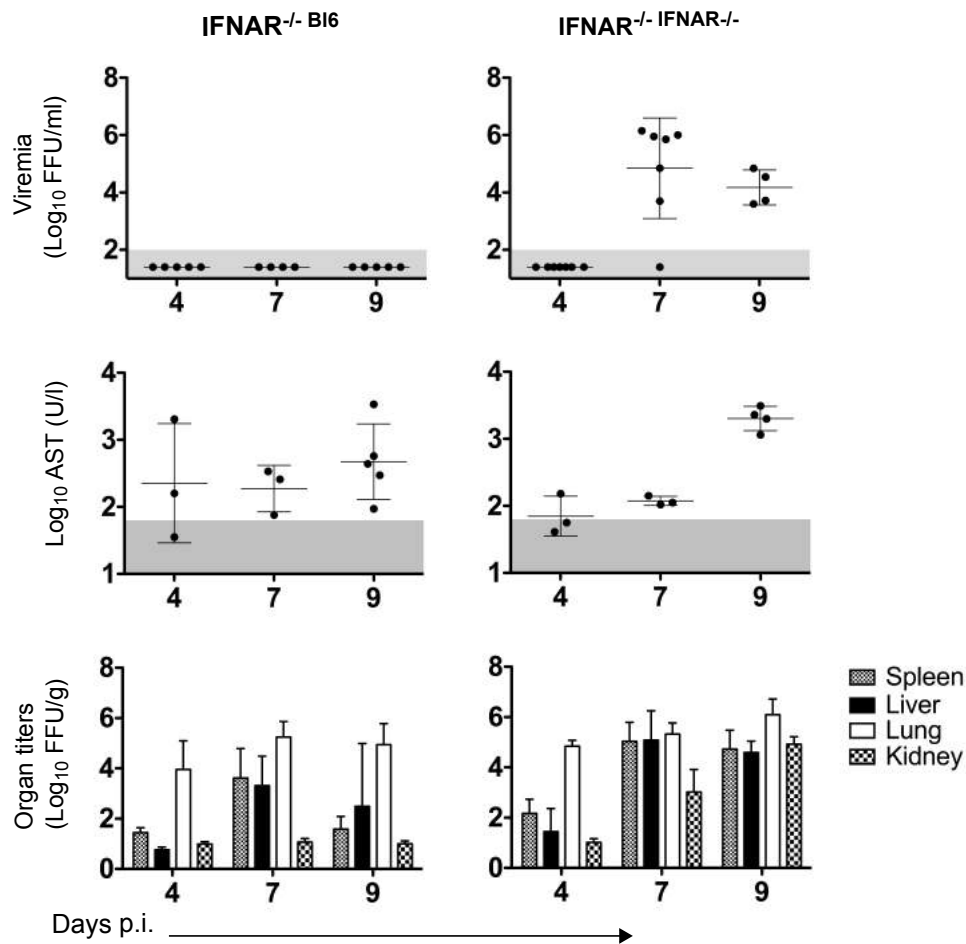


**Figure 18: Course of EBOV replication in IFNAR<sup>-/-</sup> Bl6 and IFNAR<sup>-/-</sup> IFNAR<sup>-/-</sup> chimeras** IFNAR<sup>-/-</sup> Bl6 and IFNAR<sup>-/-</sup> IFNAR<sup>-/-</sup> chimeras were infected i.n. with 1000 FFU of EBOV. 3 – 9 animals of each group were sacrificed on days 4, 7 and 9 post-infection. Heparin blood and serum were collected for viremia and AST levels, respectively. Spleen, liver, lung and kidney were taken to determine organ titers. The grey bars show the limit of detection for viremia and the normal range for AST levels. Mean and standard deviation are shown.

Viral replication in several organs occurred in IFNAR<sup>-/-</sup> Bl6 chimeras but to a lower extent than in IFNAR<sup>-/-</sup> IFNAR<sup>-/-</sup> mice. These data further suggested that cells of hematopoietic origin might play an important role in controlling viral dissemination. In agreement with this hypothesis, IFNAR<sup>-/-</sup> Bl6 mice were able to clear the virus in spleen and liver in contrast to IFNAR<sup>-/-</sup> IFNAR<sup>-/-</sup> mice. The fact that no viral replication was detected in blood but in several organs of IFNAR<sup>-/-</sup> Bl6 chimeras, might be explained by the sensitivity of the focus formation assay. It is possible that low viral copies in blood of IFNAR<sup>-/-</sup> Bl6 animals cannot be detected with this assay. This would imply that low levels of circulating virus are sufficient to establish infection after reaching peripheral organs with available target cells.

### ***Inflammatory myeloid cells are increased during EBOV infection***

Myeloid cells such as neutrophils and monocytes, are among the first cells to be recruited to the sites of infection. During viral infections neutrophils have been demonstrated to be both protective as well as to enhance disease severity (Daher et al., 1986; Perrone et al., 2008). In the steady state, monocytes replenish some subsets of tissue DCs as well as tissue macrophages. Upon inflammatory stimulus, monocytes can be massively recruited to the sites of infection mediating clearance of some viral infections, while increasing the pathology of other viruses (Lim et al., 2011; Aldridge et al., 2009). In order to investigate the inflammatory response to EBOV infection, cellularity of myeloid was investigated in both chimeras over the course of infection using multicolor flow cytometry.

Both chimeras exhibited an increase in the percentage of neutrophils within the CD45<sup>+</sup> population of peripheral blood over the course of infection (Fig. 19A). This increase in neutrophil frequencies was higher in IFNAR<sup>-/-</sup> IFNAR<sup>-/-</sup> chimeras. Furthermore, a strong increase of neutrophil frequencies was also observed in the lungs of IFNAR<sup>-/-</sup> IFNAR<sup>-/-</sup> mice indicating a stronger inflammatory response in those chimeras. Percentages of monocytes in blood increased in IFNAR<sup>-/-</sup> Bl6 mice until day 7, but decreased at day 9. IFNAR<sup>-/-</sup> IFNAR<sup>-/-</sup> mice had no significant changes in monocyte frequencies at days 4 and 7 post-infection, but the frequencies dropped at day 9 post-infection. The percentages of monocytes in lung was not altered over the course of infection, but a significant increase of CD11b<sup>+</sup> cells that expressed intermediate levels of MHCII was observed in IFNAR<sup>-/-</sup> Bl6 and IFNAR<sup>-/-</sup> IFNAR<sup>-/-</sup> chimeras. This population could be further divided according to their Ly6C expression, indicating that both Ly6C<sup>hi</sup> and Ly6C<sup>low</sup> CD11b<sup>+</sup> MHCII<sup>int</sup> populations increased over time (data not shown). These cells are probably 'activated' monocytes displaying an intermediate phenotype between infiltrating monocytes and dendritic cells induced by EBOV infection. In line with this, an increase on the percentage of DCs was observed in both chimeras.

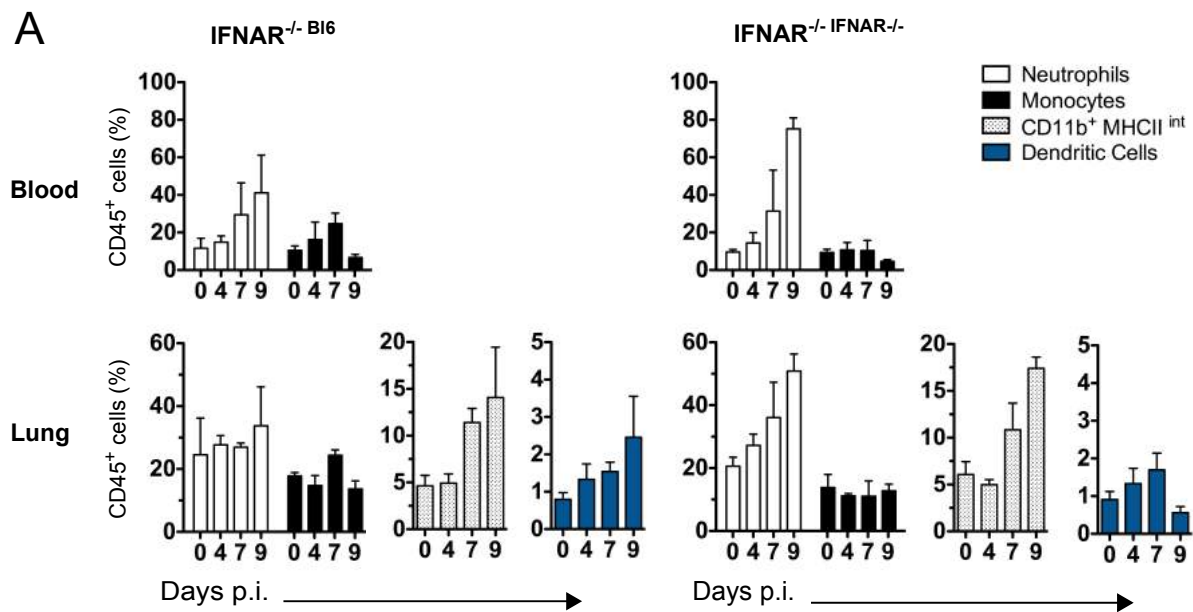


**Figure 19: Cellularity of myeloid and lymphoid populations over the course of EBOV infection** IFNAR<sup>-/-</sup> Bi6 and IFNAR<sup>-/-</sup> IFNAR<sup>-/-</sup> chimeras were infected i.n. with 1000 FFU of EBOV. Three animals of each group were sacrificed on days 4, 7 and 9 post-infection. Three uninfected animals of each group were analyzed as day 0. Blood and lungs were taken and processed for multicolor flow cytometry. Graphs represent the frequencies of myeloid cells within the CD45<sup>+</sup> population. Mean and standard deviation are shown.

Taken together, these results indicated that IFNAR<sup>-/-</sup> IFNAR<sup>-/-</sup> chimeras had a stronger inflammatory neutrophil response than IFNAR<sup>-/-</sup> Bi6 chimeras, which might explain to some extent the more severe disease outcome. Second, EBOV infection induced a strong increase of 'activated' monocytes cells in lungs of both chimera that might contribute to pathogenesis as well.

### ***Dendritic cells and macrophages are infected early after EBOV infection***

It has been proposed for a long time that macrophages and DCs might be early targets of EBOV replication. Studies by Geisbert and colleagues have detected EBOV antigen in 'dendritiform cells' that also stained positive for DC-SIGN, a C-type lectin expressed on some DCs (Geisbert et al., 2003a). *In vitro* data further showed that human monocyte-derived DCs infected with EBOV were not able to upregulate T cell-costimulatory molecules and failed to prime naïve T cells (Mahanty et al., 2003; Bosio et al., 2003).

However, monocyte-derived DCs cannot reproduce the variety of DC subsets *in vivo*. DCs can be divided into subsets based on their development and function. In non-lymphoid tissue, such as lung, two major subsets are found: CD103<sup>+</sup> and CD11b<sup>+</sup>

DCs. The function of non-lymphoid DCs is to scan the tissue in order to sense invading pathogens. The encounter of antigen, for example from replicating virus, leads to DC activation and migration to the tissue draining lymph nodes in order to present viral antigen to naïve T cells and thereby to initiate adaptive immunity. The presence of DCs at the entry site of EBOV, such as skin and mucosa, as well as their high migration potential led us to hypothesize that DCs might serve as viral vessels contributing to dissemination of the virus and moreover that the failure to initiate an adaptive immune response by priming of naïve T cells might further contribute to a dysfunctional immune response causing severe EVD.

Infection of DCs was addressed at days 4, 7 and 9 post-infection in  $IFNAR^{-/-}$  <sup>Bl6</sup> and  $IFNAR^{-/-}$   $IFNAR^{-/-}$  chimeras and compared to other myeloid cell populations, such as neutrophils, monocytes and tissue-resident alveolar macrophages. A cocktail of two monoclonal anti-EBOV-Glycoprotein (anti-EBOV-GP) antibodies conjugated with a fluorochrome (Alexa Fluor 488) was utilized to detect EBOV infected cells via immunofluorescence and flow cytometry. The principle of the assay is that EBOV replication in the cell leads to the expression of GP on the cell surface.

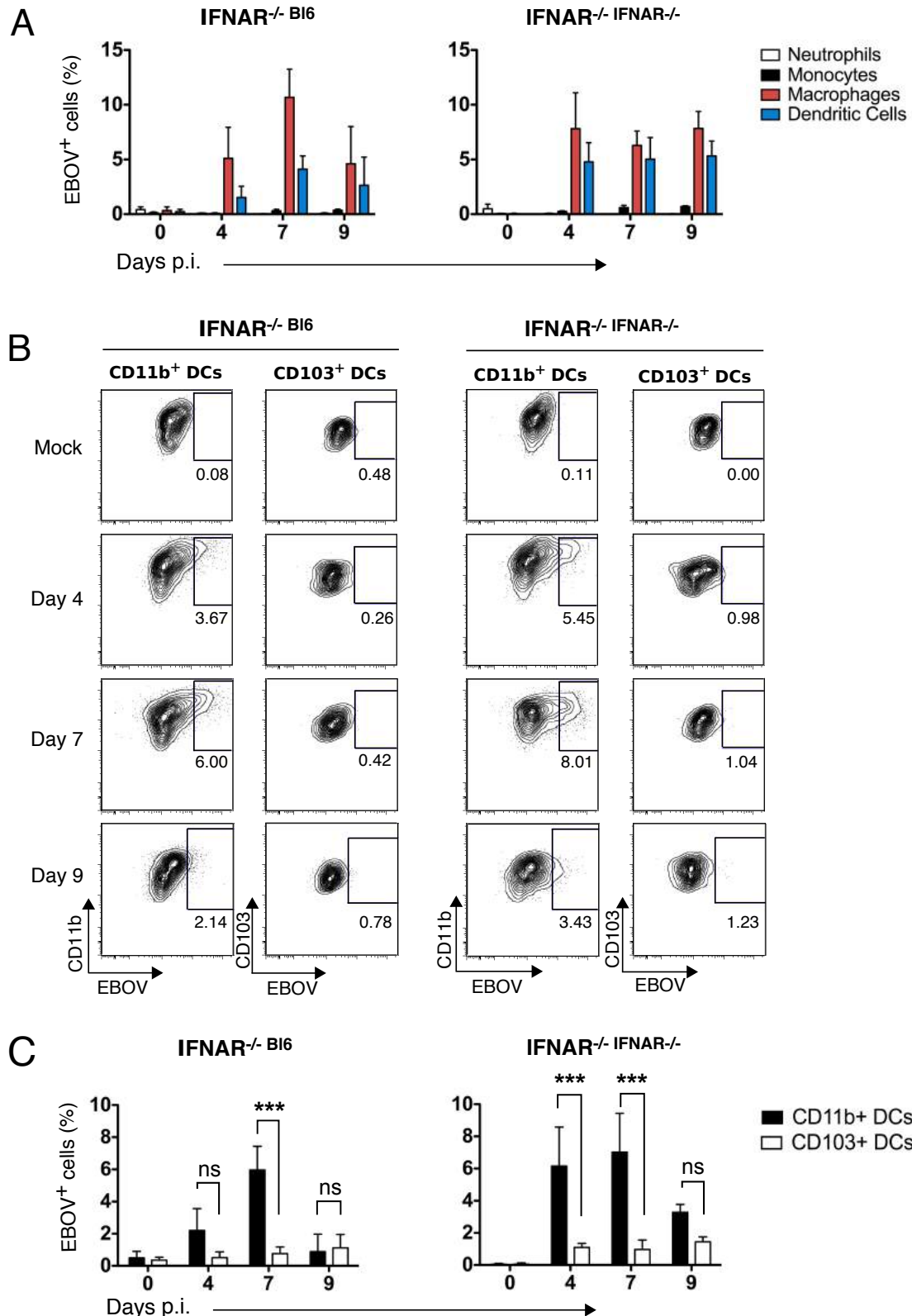


**Figure 20: Infection of myeloid populations during EBOV infection** Chimeric IFNAR<sup>-/-</sup> B16 and IFNAR<sup>-/-</sup> IFNAR<sup>-/-</sup> mice were infected i.n. with 1000 FFU of EBOV. Three animals of each group were sacrificed on days 4, 7 and 9 post-infection. Three uninfected animals of each group were analyzed as day 0 (mock). Lungs were collected to create a single cell suspension. Infection of neutrophils, monocytes, alveolar macrophages and dendritic cells was analyzed using multicolor flow cytometry (A). Representative plots (B) and graphs (C) show EBOV infection of dendritic cell subsets, CD103<sup>+</sup> and CD11b<sup>+</sup> DCs. Infected cells were identified using a cocktail of two monoclonal antibodies against the EBOV glycoprotein. Mean and standard deviation are shown. Statistical analysis was done with 2way ANOVA analysis.

Infection of cells was observed starting at day 4 post-infection in IFNAR<sup>-/-</sup> Bl6 and IFNAR<sup>-/-</sup> IFNAR<sup>-/-</sup> chimeras (Fig 20A). Interestingly, infection was IFN independent, even though the percentage of EBOV<sup>+</sup> cells was higher in IFNAR<sup>-/-</sup> IFNAR<sup>-/-</sup> mice. Alveolar macrophages and DCs were found to be infected in IFNAR<sup>-/-</sup> Bl6 and IFNAR<sup>-/-</sup> IFNAR<sup>-/-</sup> chimeras starting on day 4 post-infection and remained infected up to day 9 post-infection. The occurrence of infected macrophages and DCs coincided with viral replication in lungs of IFNAR<sup>-/-</sup> Bl6 and IFNAR<sup>-/-</sup> IFNAR<sup>-/-</sup> chimeras. Conversely, infection of neutrophils and monocytes was not observed at any of the time points analyzed.

The data reveal that macrophages and DCs are early targets of viral replication and that their infection is independent of IFN.

### ***CD11b<sup>+</sup> DCs, but not CD103<sup>+</sup> DCs are targets of EBOV infection***

The fact that DCs were infected led to the next step, which was to determine whether both or only one of the two major DC subsets, CD103<sup>+</sup> and CD11b<sup>+</sup> DCs, were infected. Interestingly, only the CD11b<sup>+</sup> DC sub-population was infected, while infection of CD103<sup>+</sup> DCs was not demonstrated at any of the time points analyzed (Fig. 20B and C). Infection of CD11b<sup>+</sup> DCs and protection of CD103<sup>+</sup> DCs was IFN independent. The peak of infected CD11b<sup>+</sup> DCs was seen at day 7 post-infection for IFNAR<sup>-/-</sup> Bl6 chimeras and at day 4 and 7 for IFNAR<sup>-/-</sup> IFNAR<sup>-/-</sup> chimeras. The differences in infection rates between CD11b<sup>+</sup> DCs and CD103<sup>+</sup> DCs were significant at this time points. Infection of CD11b<sup>+</sup> DCs on day 7 also correlated with viral titers in liver and spleen.

The results of this chapter identify CD11b<sup>+</sup> DCs as the infected subset within the DC population, while infection of CD103<sup>+</sup> DCs is not observed. Moreover, the data reveal that monocytes are not infected, which is in line with previously published data (Martinez et al., 2013).

### ***Both, conventional and monocyte-derived CD11b<sup>+</sup> DCs are infected***

Martinez and colleagues have shown previously that monocytes are not susceptible to EBOV infection, but association of the virus to monocytes induced their differentiation into DCs, which allowed viral entry (Martinez et al., 2013). This led to the next question of whether infected CD11b<sup>+</sup> DCs were of monocytic origin. CD11b<sup>+</sup>



DCs were originally classified according to their Ly6C expression into a conventional (resident) and a monocyte-derived subpopulation. The Ly6C<sup>hi</sup> CD11b<sup>+</sup> DC population is derived from infiltrating monocytes from the blood, while lung resident CD11b<sup>+</sup> DCs express low levels of Ly6C.

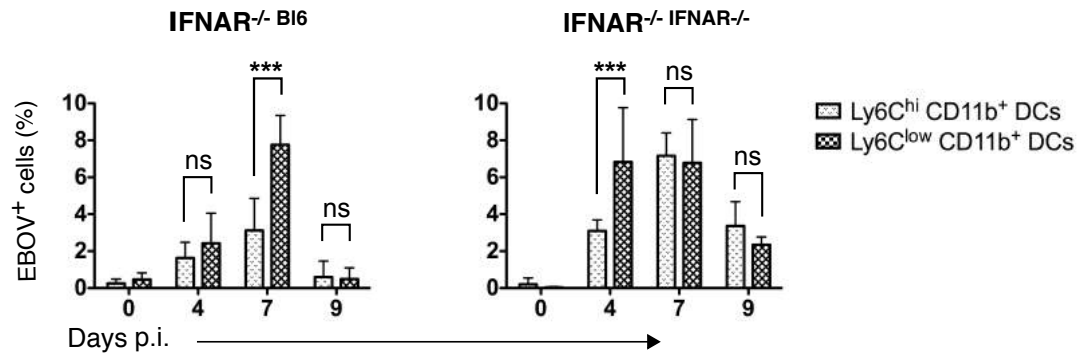


**Figure 21: Ly6C<sup>hi</sup> and Ly6C<sup>low</sup> CD11b<sup>+</sup> DCs are infected during EBOV infection** Chimeric IFNAR<sup>-/-</sup> Bl6 and IFNAR<sup>-/-</sup> IFNAR<sup>-/-</sup> mice were infected i.n. with 1000 FFU of EBOV. Three animals of each group were sacrificed on days 4, 7 and 9 post-infection. Three uninfected animals of each group were analyzed as day 0 (mock). Lungs were collected to create a single cell suspension. Infection of Ly6C<sup>hi</sup> and Ly6C<sup>low</sup> CD11b<sup>+</sup> dendritic cells was analyzed using multicolor flow cytometry. The graphs show mean and standard deviation of EBOV+ cells. Statistical analysis was done with 2way ANOVA analysis.

Analysis of the Ly6C expression in infected CD11b<sup>+</sup> DCs showed that both, Ly6C<sup>hi</sup> and Ly6C<sup>low</sup> CD11b<sup>+</sup> DCs, were infected (Fig. 21). The percentage of EBOV cells was higher in Ly6C<sup>low</sup> CD11b<sup>+</sup> DCs compared to Ly6C<sup>hi</sup> CD11b<sup>+</sup> DCs and this was significant for IFNAR<sup>-/-</sup> Bl6 mice at day 7 and for IFNAR<sup>-/-</sup> IFNAR<sup>-/-</sup> mice at day 4.

However, the sole distinction of conventional and monocyte-derived CD11b<sup>+</sup> DCs via Ly6C is not sufficient, since the marker is down regulated upon tissue entry (Merad et al., 2013). Recently, Plantinga and colleagues have distinguished between conventional and monocyte-derived CD11b<sup>+</sup> DCs using the markers MAR-1 and CD64 (Plantinga et al., 2013). Applying this gating strategy it was further investigated whether conventional and/or monocyte-derived CD11b<sup>+</sup> were infected. Since the infection of CD11b<sup>+</sup> DCs was independent of IFN signaling, IFNAR<sup>-/-</sup> knockout mice were utilized to answer this question. Immunological data were also compared to viremia and organ titers in lung and spleen.

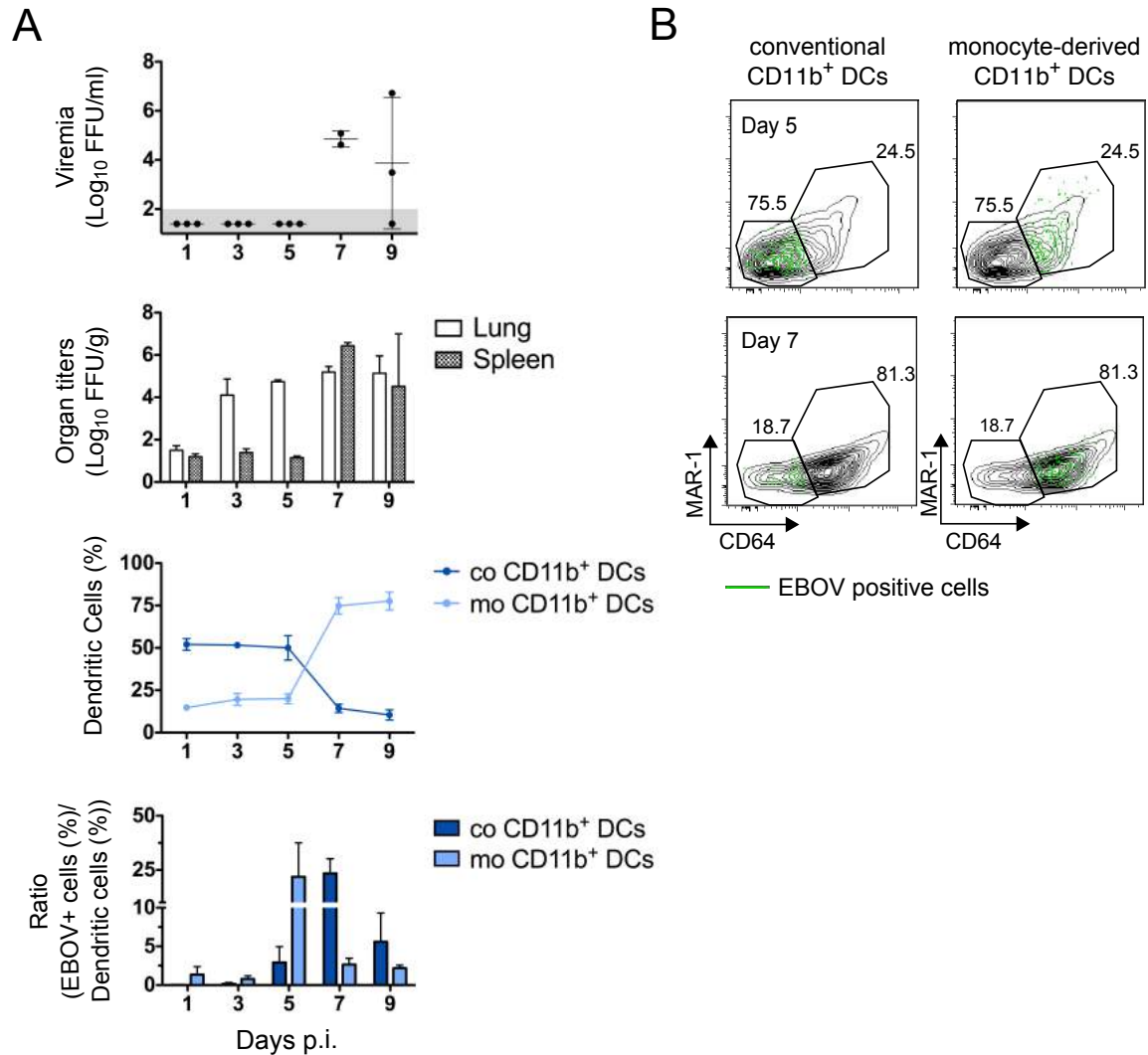


**Figure 22: Monocyte-derived and conventional CD11b<sup>+</sup> DCs are infected during EBOV infection** IFNAR<sup>-/-</sup> knockout mice were infected i.n. with 1000 FFU of EBOV. On days 1, 3, 5, 7 and 9, three animals were sacrificed and blood was collected for viremia and lung and spleen were taken for viral titers. Lung was also processed for multicolor flow cytometry. Frequencies of conventional CD11b<sup>+</sup> DCs (co CD11b<sup>+</sup> DCs) and monocyte-derived CD11b<sup>+</sup> DCs (mo CD11b<sup>+</sup> DCs) within the DC population are shown. The ratios of EBOV+ cells and the frequencies of co or mo CD11b<sup>+</sup> DCs were determined. Representative plots show Mar-1 and CD64 gating to distinguish conventional from monocyte-derived DCs. Green dots represent EBOV positive cells within each population.

IFNAR<sup>-/-</sup> knockout mice were viremic at day 7 post-infection, which coincided with viral titers in spleen (Fig. 22). As previously observed, animals exhibited lung titers starting at day 3. EBOV infection of DCs first occurred at day 5 post-infection and was detected in CD11b<sup>+</sup> DCs that were of monocytic origin (Fig. 22A+B). However, at day 7 post-infection, a shift on the population of infected cells was observed and conventional CD11b<sup>+</sup> DCs were the main EBOV positive population. At the same time, a shift in frequencies of monocyte-derived CD11b<sup>+</sup> DCs and conventional CD11b<sup>+</sup> DCs was observed. From day 5 to day 7, frequencies of monocyte-derived

CD11b<sup>+</sup> DCs within the DC population increased 3-fold, consequentially, the frequencies of conventional CD11b<sup>+</sup> DCs were decreased. This massive increase of monocyte-derived CD11b<sup>+</sup> DCs presumably explains the lower infection rates of this subpopulation at day 7. Consequently the decrease of conventional CD11b<sup>+</sup> DCs probably resulted in a higher infection rate of this subpopulation at day 7.

These data indicate that EBOV infection occurs first in monocyte-derived CD11b<sup>+</sup> DCs. Moreover, EBOV infection induces a strong increase of frequencies of this subset at day 7 post-infection. These results provide further support for the hypothesis that inflammatory monocytes upon tissue entry differentiated into monocyte-derived CD11b<sup>+</sup> DCs, which might contribute to EBOV dissemination and pathogenesis.

### ***Inflammatory monocytes play a role in EBOV pathogenesis***

In order to further dissect the role of infiltrating monocytes and monocyte-derived DCs on EBOV pathogenesis and viral dissemination, IFNAR<sup>-/-</sup> CCR2<sup>-/-</sup> chimeras were generated. CCR2 is a chemokine receptor that controls monocyte exit from the bone marrow and recruitment to the sites of inflammation. Therefore, in CCR2<sup>-/-</sup> knockout mice monocyte-derived DCs are significantly reduced (Serbina et al., 2003).

IFNAR<sup>-/-</sup> CCR2<sup>-/-</sup> chimeras were infected i.n. with 1000 FFU of EBOV. Relative weight and survival was monitored over the course of infection. No differences in relative weight loss and survival could be observed (Fig. 15A). In addition, viremia and AST levels were comparable between IFNAR<sup>-/-</sup> Bl6 and IFNAR<sup>-/-</sup> CCR2<sup>-/-</sup> chimeras.

A second approach to dissect the role of inflammatory monocytes on viral dissemination was to deplete monocytes in IFNAR<sup>-/-</sup> knockout mice utilizing an anti-Ly6C antibody. Since Ly6C is also expressed on neutrophils the antibody depletes both monocytes and neutrophils. Therefore as a control, neutrophils alone were depleted using an anti-Ly6G antibody. Animals were infected i.n. with 1000 FFU of EBOV and then depleted 3 and 5 days post-infection. Depletion efficiency was analyzed at days 5 and 7 post-infection.

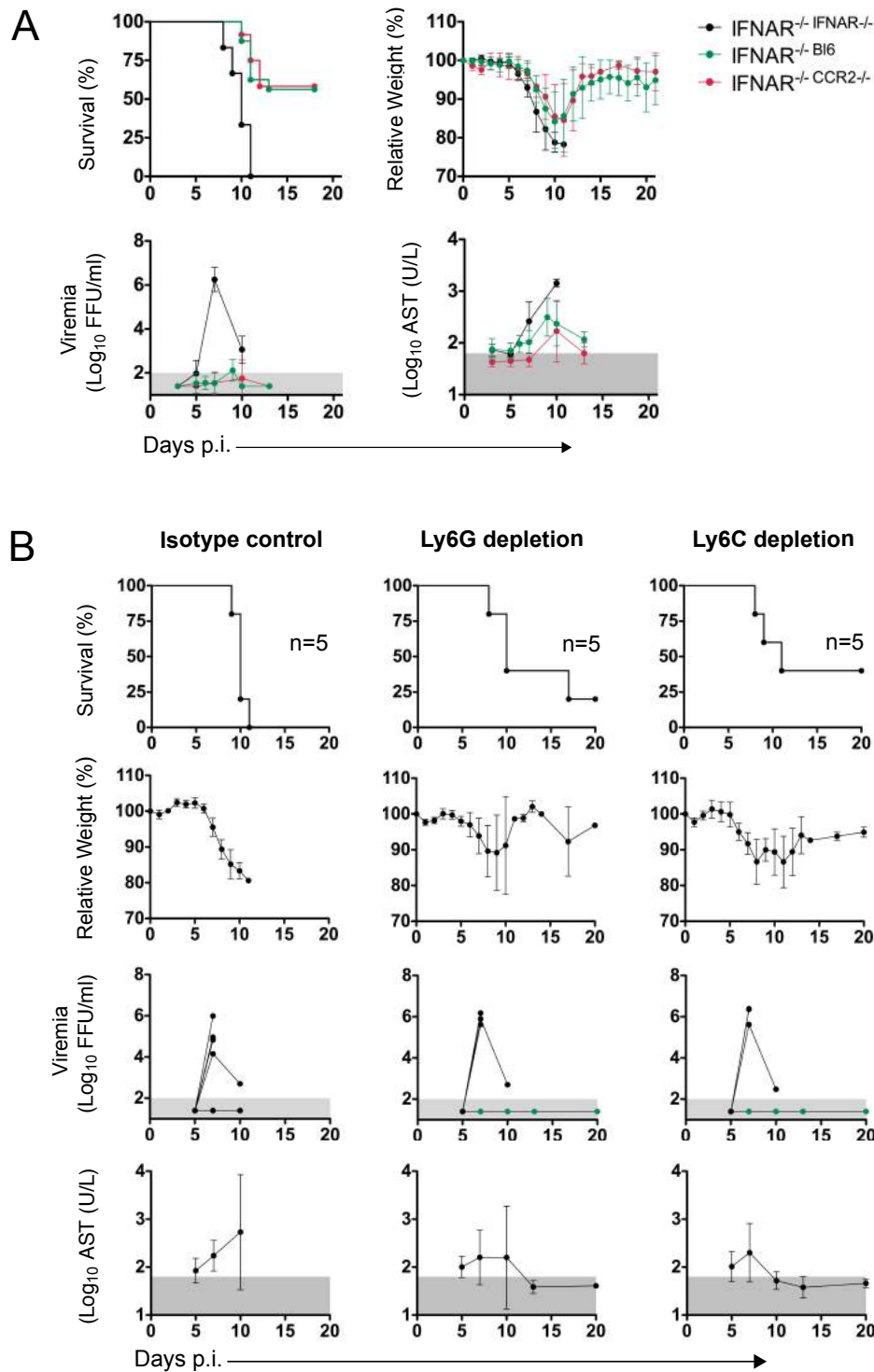


**Figure 23: Role of monocytes during EBOV infection** IFNAR<sup>-/-</sup> CCR2<sup>-/-</sup> chimeras (n=12) were infected i.n. with 1000 FFU of EBOV. Relative weight loss, survival viremia and AST levels were compared to previously obtained data from IFNAR<sup>-/-</sup> IFNAR<sup>-/-</sup> mice (n=5) and IFNAR<sup>-/-</sup> Bl6 mice (n=16) (A). For monocyte and neutrophil depletion, IFNAR<sup>-/-</sup> knockout mice were infected i.n. with 1000 FFU of EBOV. Mice were depleted with anti-Ly6C and anti-Ly6G antibodies on days 3 and 5 post-infection. Survival and relative weight loss were monitored daily, viremia and AST levels were determined as indicated (B). The graphs show mean and standard deviation. The grey shaded areas indicate the limit of detection for viremia and the normal range for AST levels. Surviving animals are labeled in green.

In line with previous data, IFNAR<sup>-/-</sup> knockout mice infected with EBOV displayed a 100% lethal phenotype in the presence of an isotype control antibody. Strikingly, Ly6C depletion in EBOV infected IFNAR<sup>-/-</sup> knockout mice resulted in 40% protection suggesting that inflammatory Ly6C<sup>hi</sup> monocytes contribute to disease severity (Fig. 23B). The depletion of neutrophils alone with an anti-Ly6G antibody resulted in a 20% survival indicating that neutrophils also might contribute to EBOV pathogenesis. Due to different outcomes within the depletion groups, the depletion efficiency of Ly6C<sup>+</sup> monocytes in blood was analyzed. It was observed that in animals that survived EBOV infection, Ly6C<sup>hi</sup> monocytes were efficiently depleted both at day 5 and 7 post-infection, while animals with lethal outcome recovered levels of circulating Ly6C<sup>hi</sup> monocytes by day 7 (Fig. 24). This was also seen for neutrophils. The depletion efficiency also correlated with viremia. Animals in which Ly6C<sup>hi</sup> monocytes were efficiently depleted did not have viremia at any time point analyzed, while animals, who recovered blood Ly6C<sup>hi</sup> monocytes on day 7, viremia in blood was also observed.

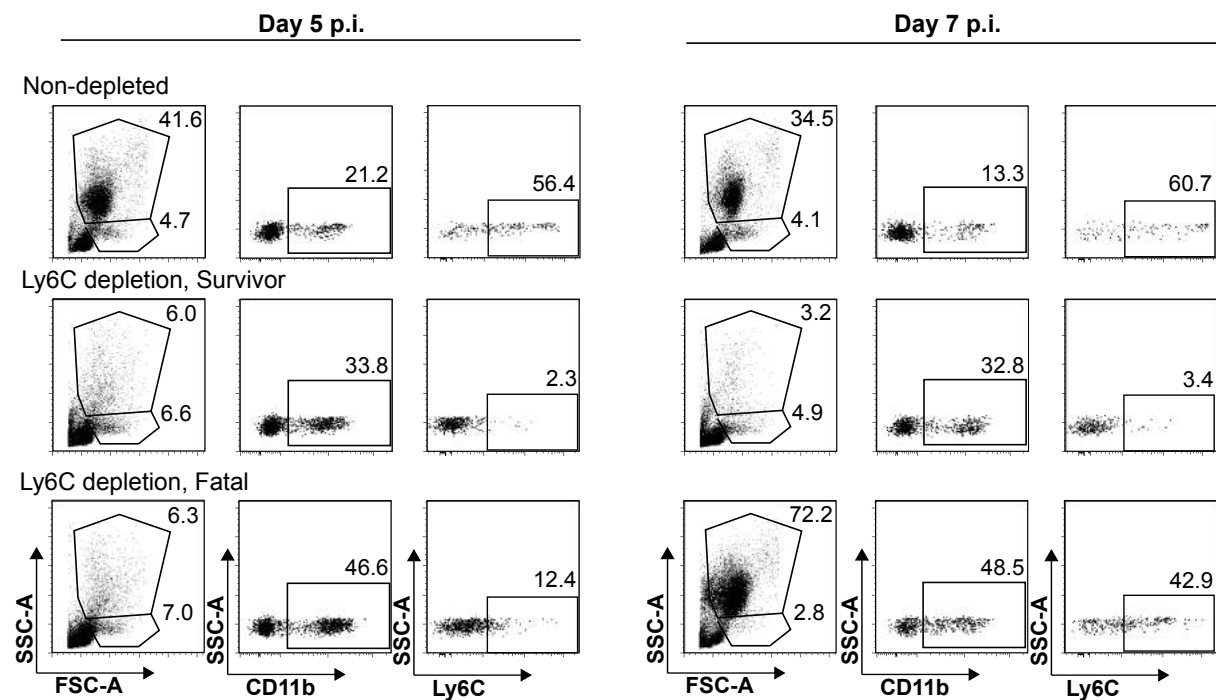


**Figure 24: Depletion of monocytes in IFNAR<sup>-/-</sup> knockout mice** Depletion efficiency of Ly6C<sup>+</sup> monocytes in blood of EBOV infected IFNAR<sup>-/-</sup> knockout mice was addressed at days 5 and 7 post-infection using flow cytometry. Representative plots of non-depleted, and Ly6C depleted animals (Survivor and fatal) are shown. The gating was done as followed: In the first gate, neutrophils were gated as SSC<sup>high</sup> and monocytes as SSC<sup>low</sup>. The second gate defined CD11b<sup>+</sup> monocytes and the third gate, Ly6C<sup>high</sup>, CD11b<sup>+</sup> monocytes.

These data suggest that Ly6C<sup>hi</sup> monocytes might contribute to EBOV disease severity and might furthermore have a role on EBOV dissemination. However, depletion of neutrophils also enhanced survival of EBOV infected mice indicating a role of neutrophils on EBOV pathogenesis.

### ***T cells are protective during EBOV infection***

Previously obtained data in IFNAR<sup>-/-</sup> Bl6 chimeras have indicated that the adaptive immune system might have an important role in controlling viral dissemination. Studies have revealed that fatal EVD is associated with loss of lymphocytes and defective antibody responses. However, recent data revealed that neutralizing antibodies did not develop early during infection and therefore are not likely to contribute to protection against EBOV (Luczkowiak et al., 2016). In contrast, it was recently demonstrated that EBOV survivors displayed robust EBOV-specific T cell responses (McElroy et al., 2015). This led to the hypothesis that T cells might be crucial for controlling EBOV dissemination and clearance.

In order to analyze the role of T cells in protection against EBOV infection, CD4 and/or CD8 T cells were depleted in IFNAR<sup>-/-</sup> Bl6 chimeras prior to infection. Animals were then infected i.n. with 1000 FFU of EBOV and monitored for relative weight loss and survival. Viremia and AST levels were measured at indicated time points. At the time of death, organ titers were determined to evaluate viral dissemination. The depletion of either CD4 or CD8 T cells did not significantly change the outcome of EBOV infection in IFNAR<sup>-/-</sup> Bl6 chimeras (Fig. 25A). While a 50% survival was observed with isotype control treatment, 60% survival was seen after CD4 depletion and 40% after CD8 depletion. However, when both, CD4 and CD8 T cells, were depleted, the protection was lost and 100% lethality was observed. Moreover, CD4 and CD8 depleted mice showed higher viral titers in spleen and liver (Fig. 25B), indicating enhanced viral dissemination.

These data demonstrate an important role of both CD4 and CD8 T cells in controlling viral dissemination and pathogenesis during EBOV infection. Therefore, protection is likely to be dependent on a synergistic effect of CD4 and CD8 T cells. These results further implicate that functional dendritic cells are able to prime antigen-specific T cells inducing adaptive immunity. Due to the fact that CD103<sup>+</sup> DCs seem to be

protected from infection, they are putative candidates for initiating T cell responses during EBOV infection.

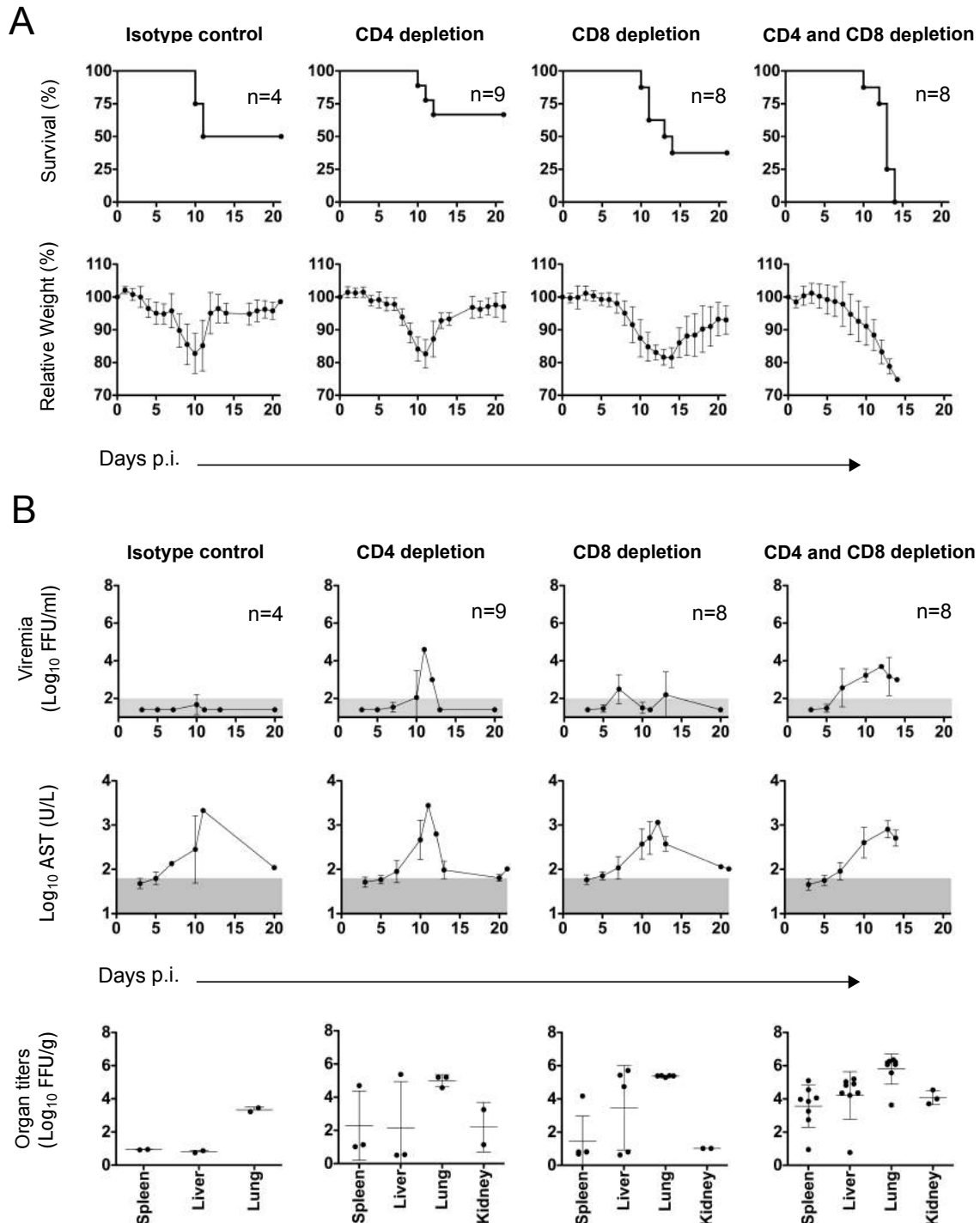


**Figure 25: T cells are protective during EBOV infection** IFNAR<sup>-/-</sup> Bl/6 mice were depleted with anti-CD4 or anti-CD8 or anti-CD4 and anti-CD8 antibodies three days and one day prior to infection. Depletion of T cells was verified using flow cytometry. Mice were infected i.n. with 1000 FFU of EBOV. Survival and relative weight loss were controlled daily, blood and serum were collected at indicated time points for determination of viremia and AST levels, respectively. At the time of death, spleen, liver, lung (and kidney) titers were determined. The normal range for AST and the limit of detection for viremia are shaded in grey. Mean and standard deviation are shown.

### 5.3.2 EBOV immunity in humanized NSG-A2 mice

The IFNAR<sup>-/-</sup> Bl6 chimeric model demonstrated that CD11b<sup>+</sup> DCs are early targets of viral replication, while CD103<sup>+</sup> DCs are presumably protected from EBOV infection. The data further suggested that infected CD11b<sup>+</sup> DCs might be partly of monocytic origin. The next step was to investigate infection of myeloid cells in the context of the human immune response utilizing huNSG-A2 mice.

HuNSG-A2 mice were infected i.n. with 1000 FFU of EBOV. Animals were sacrificed at day 6 and day 10 post-inoculation and infection of lung myeloid populations was analyzed using a cocktail of two monoclonal anti-EBOV-GP antibodies as described above. Due to the high variations of percentages of myeloid cell populations in huNSG-A2 mice, changes in frequencies due to EBOV infection have to be evaluated with caution. Nevertheless, the data suggested that CD14<sup>+</sup> myeloid cells, which are likely to be macrophages or monocyte-derived DCs, showed reduced frequencies over the course of infection (Fig. 26B) (Collin et al., 2013). Furthermore, they are infected on day 6 and day 10 post-infection (Fig. 26C). While frequencies of CD14<sup>+</sup> population were decreased, an increase of CD16<sup>+</sup> myeloid cells was observed. These cells also expressed CD11c and thus were consistent with human non-classical monocytes (MacDonald et al., 2002). However, in mock-infected animals very small numbers could be observed and therefore, the background of the anti-GP antibody could not be measured. It was not possible therefore to determine whether these cells were infected. In addition, classical DC populations CD141<sup>+</sup> DCs and CD1c<sup>+</sup> DCs could not be identified in huNSG-A2 mice.

Taken together, these data suggest that CD14<sup>+</sup> DCs or macrophages are likely to be early targets of EBOV replication in huNSG-A2 mice. These results confirm findings on the murine IFNAR<sup>-/-</sup> Bl6 chimeric model, since CD14<sup>+</sup> DCs are likely to be the human counterparts of murine monocyte-derived CD11b<sup>+</sup> DCs (Haniffa et al., 2013).



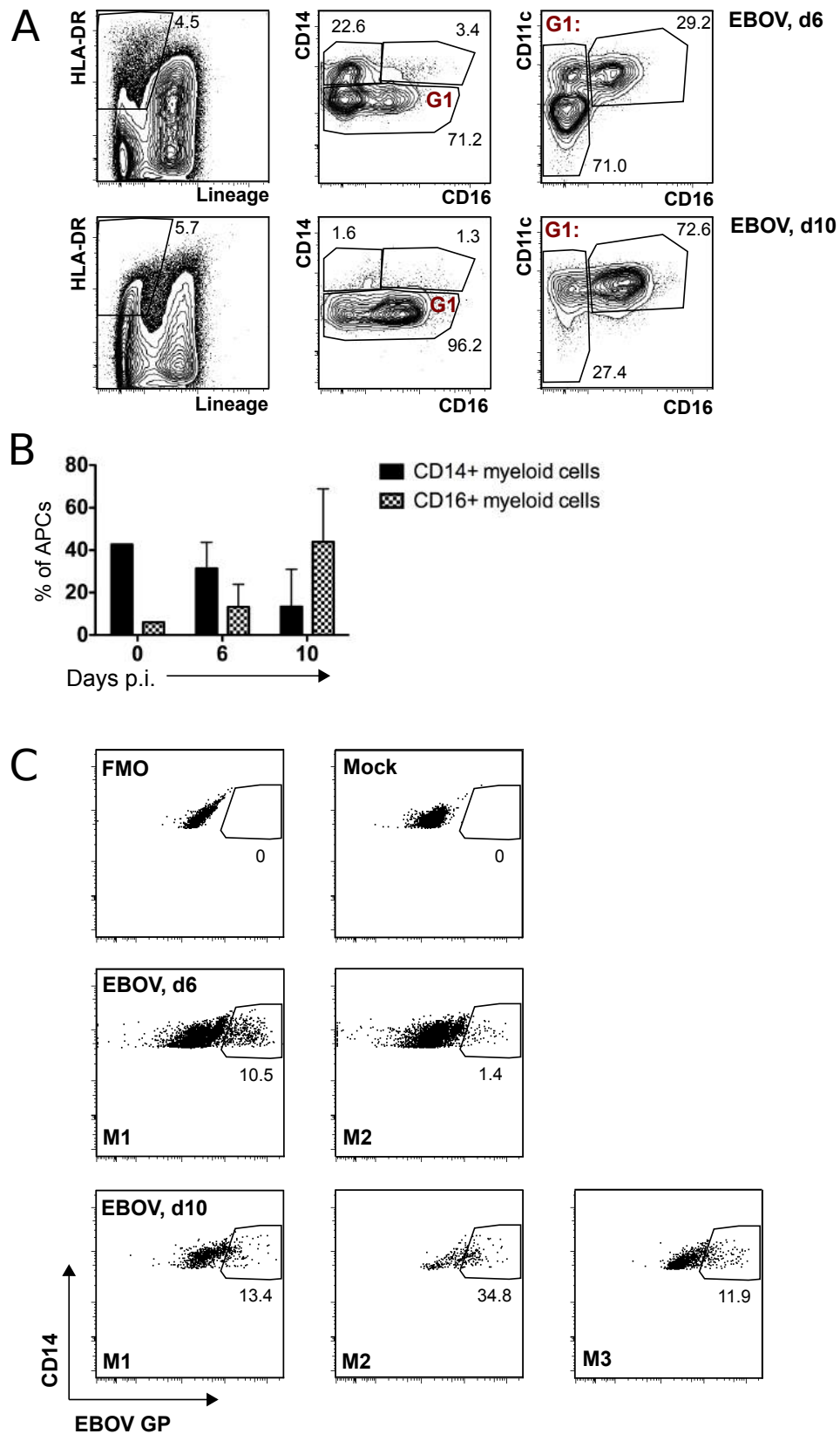


**Figure 26: EBOV infection of myeloid cells in lungs of huNSG-A2 mice** HuNSG-A2 mice were infected i.n. with 1000 FFU of EBOV. Lungs were harvested on day 6 and day 10 post inoculation and infection of lung myeloid cells was analyzed using multicolor flow cytometry. Graphs (B) show frequencies of myeloid subsets with the APC gate and representative plots show gating (A) and representative plots of each mouse (C) of EBOV infection in CD14+ cells. Infected cells were identified using a cocktail of two monoclonal antibodies against the EBOV glycoprotein. Mean and standard deviation are shown.

## 5.4 Analysis of APCs during human EVD

Human peripheral blood leukocytes consist of a heterogeneous population of myeloid cells, including different monocyte subsets and subsets of precursor DCs. Monocytes in human blood can be subdivided into classical CD14<sup>+</sup> monocytes, non-classical CD16<sup>+</sup> monocytes and double positive CD14<sup>+</sup> CD16<sup>+</sup> monocytes (Saha and Geissmann, 2011). Both monocyte subsets expressing CD14 are believed to mediate antimicrobial activity, while non-classical CD16<sup>+</sup> monocytes have been assigned a patrolling function in the endothelium of blood vessels and furthermore have been implicated in antiviral responses (Serbina et al., 2008; Cros et al., 2010). Tissue CD141<sup>+</sup> and CD1c<sup>+</sup> DCs are the major human DC subsets that are distinguished based on their development and probably also on their function. However, the distinct functions of CD141<sup>+</sup> and CD1c<sup>+</sup> DCs are still under investigation (Segura et al., 2013a). Precursors of both subsets can be found in human blood.

The phenotype and function of monocytes and DCs in peripheral blood of EVD patients has not been investigated yet. Since they might have crucial roles on EBOV immunity and pathogenesis, it was of great importance to investigate the blood myeloid populations of EVD patients. In the context of the recent EBOV outbreak in West Africa our laboratory had the chance to conduct immunological analyses in Guinea using leftover diagnostic samples from EVD patients diagnosed by the EML. First, monocyte and DC subsets concentrations in first samples of EVD patients were compared to acute patients that tested negative for EBOV. A significant loss of circulating CD16<sup>+</sup> monocytes was observed in EVD patients compared to other acute febrile patients (Fig. 27A). The concentrations of CD14<sup>+</sup> and CD14<sup>+</sup> CD16<sup>+</sup> monocytes as well as CD1c<sup>+</sup> DCs were also reduced in comparison with other febrile controls (Fig. 27A+B).



It could be seen that concentrations of CD14<sup>+</sup> and CD16<sup>+</sup> monocytes were positively correlated with the Ct value (threshold cycle), which is a surrogate of the viral load (Fig. 27C). Low Ct value (hence high viral load) was correlated with loss of CD14<sup>+</sup> and CD16<sup>+</sup> monocytes. This was further underlined when grouping of all analyzed samples according to their Ct values demonstrated a significant loss of CD16<sup>+</sup> monocytes in high viremic EVD patients (Ct < 25) compared to low viremic patients (Ct > 33) and convalescent EVD patients that have been EBOV positive previously (Fig. 27D). In patients with high viral loads (Ct < 25) a reduction of CD14<sup>+</sup> monocytes was also observed.

*In vitro* studies have indicated that EBOV impairs activation of monocyte-derived DCs and that this inhibition is mediated via the IFN antagonist protein VP35 (Mahanty et al., 2003; Yen et al., 2014). However, effects of EBOV on the activation status of APCs *in vivo* have not been studied. This was addressed in peripheral blood of EVD patients via quantification of the expression levels of HLA-DR. It was demonstrated in a previous study on Influenza virus that HLA-DR expression on CD14<sup>+</sup> monocytes was associated with their activation status (Diao et al., 2014).

The data showed that, in fact, high viremic patients (Ct < 25) displayed significant lower HLA-DR expression on CD14<sup>+</sup> and CD16<sup>+</sup> monocytes compared to convalescent EVD patients and other acute patients (Fig. 28A). The analysis of longitudinal samples of individual EVD patients indicated that surviving EVD patients had low expression levels of HLA-DR early during infection, but gained higher HLA-DR expression during the course of disease (Fig. 28B). Clearance of the virus was associated with high HLA-DR expression. In contrast, fatal EVD patients displayed low HLA-DR expression during the whole course of disease. These findings indicate that monocytes, especially CD16<sup>+</sup> monocytes, might in fact have a role in EBOV induced immunosuppression.

The data presented in figures 27 – 28 were generated in close collaboration with Paula Ruibal and Beate Becker-Ziaja and submitted for publication in March 2016 as a co-first author publication.

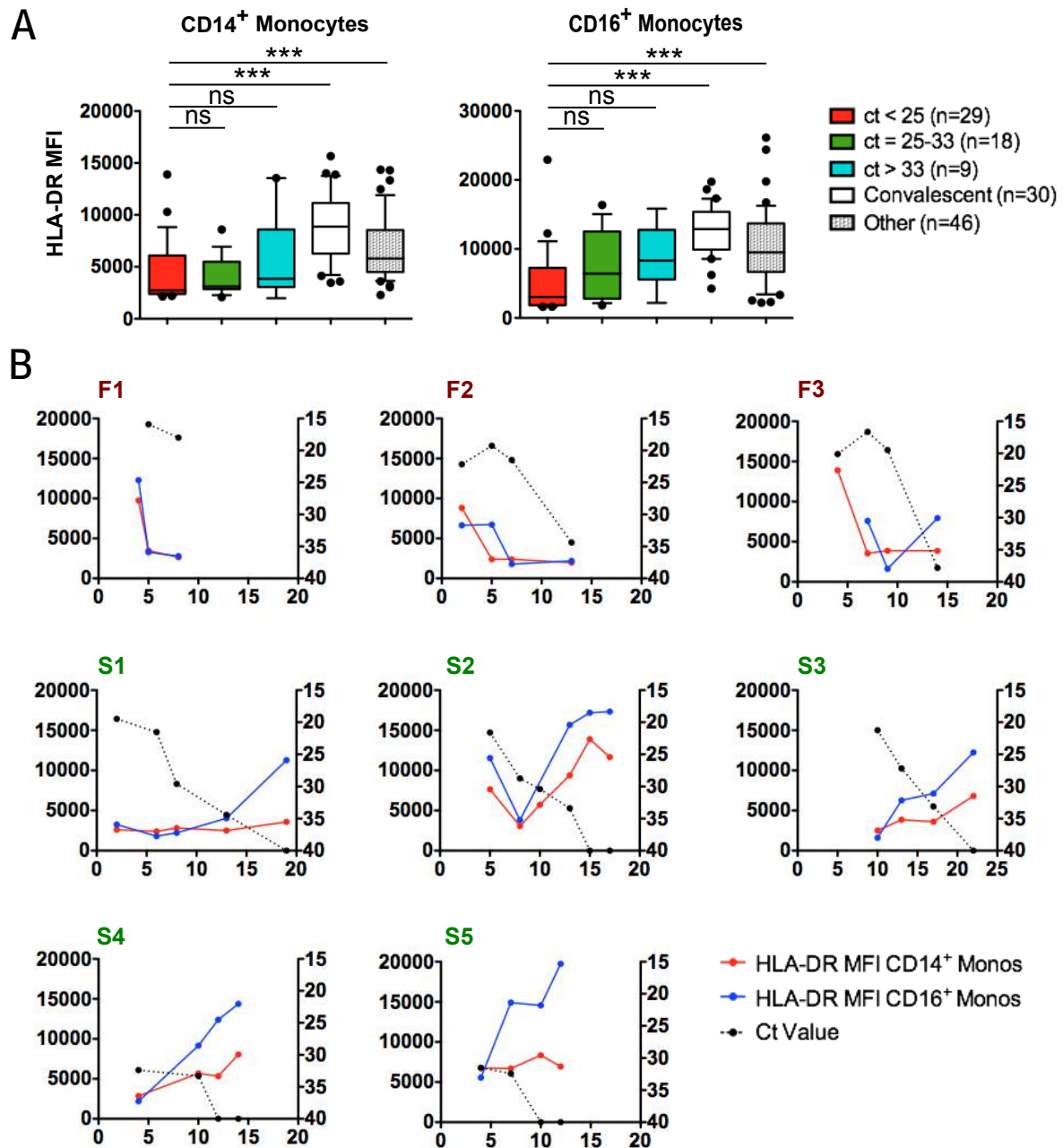


**Figure 28: HLA-DR expression of CD14<sup>+</sup> and CD16<sup>+</sup> Monocytes** HLA-DR Median fluorescence intensity (MFI) on CD14<sup>+</sup> and CD16<sup>+</sup> monocytes grouped depending on their Ct values: red: Ct < 25, green: Ct = 25-33, turquoise: Ct > 33. These were further compared to convalescent EBOV patients (white) and other acute patients negative for EBOV (grey) (A). Longitudinal analysis of HLA-DR MFI and Ct value of three fatal EVD patients (F1-3) and five EBOV survivors (S1-5) (B). Graphs represent mean and standard deviation. Statistical analysis was performed using Kruskal-Wallis test.



## 6 Discussion

Due to the lack of small immunocompetent animal models and the restriction of EBOV research to BSL4 containment, very little is known about the immune response to EBOV and its contribution to EVD pathophysiology. It has been long suspected that EBOV might specifically target DCs as a mechanism of immune evasion contributing to severe EVD, yet this has not been demonstrated *in vivo*.

The goal of the present study was to improve basic understanding of EBOV immunology focusing on the role of DCs and their contribution to EBOV immunity and pathogenesis. In order to achieve this goal, the first aim was to establish natural routes of EBOV infection that would lead to systemic dissemination of the virus. The second aim was to generate immunocompetent mouse models that were susceptible to non-adapted EBOV and allowed the formation of a functional hematopoietic-derived immune response against EBOV. Utilizing both, natural routes of infection and immunocompetent mouse models then led to the third aim, which was to investigate the role of DCs during the immune response to EBOV infection *in vivo*.

### 6.1 Natural routes of EBOV infection

EVD epidemiology data collected during the last 40 years and in particular during the recent outbreak in West Africa suggests that EBOV naturally infects humans via mucosal surfaces and lesions in the skin (Feldmann and Geisbert, 2011). At these natural portals of viral entry local tissue cells, including DCs, initiate the immune response (Christensen and Thomsen, 2009). However, experimental EBOV infection of mice is usually achieved by systemic administration of the virus. In fact, i.p. inoculation of EBOV is the standard route of administration in mice with defects in innate or adaptive immunity. Bray and colleagues demonstrated high susceptibility of IFNAR<sup>-/-</sup> knockout mice to i.p. inoculation of non-adapted EBOV (Bray et al., 2001). However, this route of infection does not reflect the natural entry of EBOV into its host. Most importantly, systemic administration prevents early encounter of tissue-resident DCs with viral antigen. Since severe EVD is associated with high viral loads in blood and several organs, we hypothesized that local EBOV infection of the mucosa or skin might lead to systemic spread of EBOV throughout the body. To

more closely mimic this more natural course of EBOV infection, two novel application routes were established.

First, the virus was administered via the nostrils (i.n.) of the mice leading to exposure of the mucosa of the respiratory tract. The lung possesses tissue-resident DCs, namely CD103<sup>+</sup> DCs and CD11b<sup>+</sup> DCs that are important for lung-mediated immune responses (Lambrecht and Hammad, 2012). I.n. administration of non-adapted EBOV led to a severe course of disease in IFNAR<sup>-/-</sup> mice, with 100% lethality and high viremia. This administration route was selected for further experiments, because local administration led to systemic dissemination of the virus and high lethality, which allowed studying DC immunity at the portals of viral entry with a severe course of disease as seen in many human EBOV infections.

Secondly, EBOV was administered i.d./s.c. in order to mimic viral entry via the skin. This was achieved by inoculation of the virus at the base of the tail. Previous studies had already demonstrated susceptibility of IFNAR<sup>-/-</sup> mice to s.c. inoculation, however the virus is administered below the dermis and epidermis, body sites that contain important tissue-resident DCs that mediate skin-derived immunity (Merad et al., 2008). Inoculation at the base of the tail achieves injection into the dermis (even though injection below the dermis cannot be excluded) and is therefore an improvement to solely s.c. administration, since the virus will be more efficiently exposed to DCs that are resident in the dermis. The data showed that i.d./s.c. inoculation of EBOV in IFNAR<sup>-/-</sup> mice resulted in a milder course of disease with enhanced survival and lower viremia compared to i.p. or s.c. inoculation.

The fact that EBOV infection of the respiratory mucosa led to a severe course of disease, while skin infection resulted in enhanced survival, suggests a protective role of skin immune cells to EBOV infection. The skin contains dermal CD103<sup>+</sup> DCs and CD11b<sup>+</sup> DCs, which are related to those present in the lung. In addition, a unique DC subset, called Langerhans cell (LC) is found in the epidermis. LCs do not share developmental origin with other DC subsets, since they originate from embryonic fetal liver monocytes and yolk sac-derived macrophages (Hoeffel et al., 2012). A role for LCs in tolerance induction has been suggested, however, LCs also have been implicated in mediating antiviral immunity (Kaplan et al., 2005; King and Kesson, 2003). In fact, it has been demonstrated that infection of LCs with West Nile virus (WNV), which is transmitted to humans via mosquitoes, led to their activation and migration to the skin draining lymph nodes (Johnston et al., 1996; Johnston et al.,



2000). This suggests that LCs might actually be involved in the induction of antiviral T cell responses. The role of LCs during EBOV infection is not known, however, the detection of EBOV antigen in the epidermis of skin specimens suggested that LCs might be targets of EBOV infection (Zaki et al., 1999). Since LCs are not present in lung, they might be responsible for the unique protection observed upon administration of EBOV to the skin.

## **6.2 Establishment of immunocompetent mouse models**

### **6.2.1 EBOV in bone marrow chimeric mice**

The fact that immunocompetent laboratory inbred mice, such as BALB/c or B6 mice are not susceptible to non-adapted EBOV has hampered EBOV studies in mice until researchers adapted EBOV to the murine host. Sequential passage of EBOV in newborn mice resulted in maEBOV that was highly virulent in adult BALB/c or B6 mice (Bray et al., 1998). However, adaptation of EBOV to the mouse introduced mutations into the viral genome and therefore experimental maEBOV infection in mice might not translate into EVD pathophysiology in humans. Furthermore, the variety of *ebolavirus* variants and species cannot be studied in BALB/c or B6 mice. A different approach to study non-adapted EBOV was then made by Bray and colleagues, who demonstrated high susceptibility of IFNAR<sup>-/-</sup> or STAT<sup>-/-</sup> knockout mice to several species of non-adapted EBOV by several routes (Bray et al., 2001). But even though this allowed studying non-adapted EBOV, IFNAR and STAT are essential components of the antiviral IFN response and therefore these knockout mice are not suitable to study immunology to EBOV.

The susceptibility of IFNAR<sup>-/-</sup> or STAT<sup>-/-</sup> knockout mice to non-adapted EBOV strongly supports the idea that the IFN-I response is crucial for protection against EBOV infection in mice. This is further strengthened by the findings that treatment with IFN antibodies renders immunocompetent mice susceptible to EBOV and that adaptation of EBOV to the mouse as a host leads to changes in one of the virus IFN antagonist proteins, namely VP24 (Ebihara et al., 2006; Reid et al., 2006). All body cells are able to produce IFN-I and respond to it, however it is not clear which cellular compartment is critical for IFN-I mediated protection against EBOV infection.

In order to dissect the cellular compartment responsible for IFN-I mediated protection, we generated bone marrow chimeric mice, where the IFNAR knockout was confined to either hematopoietic (B16<sup>IFNAR<sup>-/-</sup></sup>) or non-hematopoietic cells (IFNAR<sup>-/-</sup> B16). Hematopoietic cells are derived from hematopoietic BM progenitors that can be generally derived into lymphoid and myeloid progenitors. Myeloid progenitors give rise to immune cells participating in innate immune responses, such as neutrophils, monocytes, macrophages and DCs, while lymphoid progenitors give rise to T and B lymphocytes, key mediators of the adaptive immune response. Even though some tissue-resident populations are derived independently from the bone marrow, most of the adult immune system comprises of hematopoietic cells. Non-hematopoietic cells include for example stromal and epithelial cells that also have important roles in IFN-I signaling, when infected.

The obtained data revealed that B16<sup>IFNAR<sup>-/-</sup></sup> chimeras as well as IFNAR<sup>-/-</sup> B16 chimeras following i.n. infection with non-adapted EBOV exhibited enhanced survival compared to IFNAR<sup>-/-</sup> IFNAR<sup>-/-</sup> chimeras, where neither hematopoietic nor non-hematopoietic cells could respond to IFN signaling. These results suggest that functional IFN-signaling within the hematopoietic as well as non-hematopoietic compartments is equally important for protection against EBOV infection. However, a major difference was that B16<sup>IFNAR<sup>-/-</sup></sup> showed high viremia, while IFNAR<sup>-/-</sup> B16 had low or no viremia over the course of infection. This strongly supports the idea that hematopoietic immunity regulates viral dissemination but does not seem to be sufficient for complete protection against EBOV, since around 50% of IFNAR<sup>-/-</sup> B16 chimeras did not survive.

The advantage of the IFNAR<sup>-/-</sup> B16 chimeric mouse is that it supports productive infection of non-adapted EBOV and at the same time possesses functional hematopoietic immunity allowing the investigation of the hematopoietic-derived immune response to EBOV *in vivo*. In this model, different *ebolavirus* species can be investigated without adaptation. This also is an advantage for testing antivirals or vaccine candidates. Furthermore, this model opens up possibilities for other chimeric models, where modifications of the hematopoietic compartment could allow further dissection of the roles of different immune cells on EBOV immunity. For example, the transplantation of BM from conditional knockout mice, such as Langerin-DTR or

CD11b-DTR, would permit depletion of Langerin<sup>+</sup> or CD11b<sup>+</sup> cells, respectively, in order to investigate their role during EBOV infection.

### **6.2.2 EBOV in humanized mice**

It is generally accepted that the mouse as a model system is very important for the understanding of human diseases. However, the mouse does not reflect all pathological features of human EVD due to the high species specificity of EBOV, which is likely to result from evasion of the host IFN-I response. A novelty in the field of infectious diseases is the humanized mouse, a severe immunodeficient mouse that allows engraftment of human tissues or cells. For several human viral pathogens, such as Dengue virus (DENV), Epstein-Barr virus (EBV) or human immunodeficiency virus (HIV), the humanized mouse has proven to be a useful tool to investigate human immune responses to these pathogens (Jaiswal et al., 2009; Shultz et al., 2010, Brainard et al., 2009).

As part of this thesis, a humanized mouse model was established for non-adapted EBOV infection. NSG mice were utilized as immunodeficient recipients that permitted long-term engraftment of human cells due to severe defects in innate and adaptive immunity. They furthermore expressed human HLA-A2.1 to facilitate development of functional T cells from HLA-A2.1 donors. Humanized NSG-A2 mice were generated via transplantation of human HSCs into sub-lethally irradiated NSG-A2 mice. Transplanted HSCs gave rise to all hematopoietic-derived immune cells in lymphoid as well as non-lymphoid tissues.

The results presented here demonstrated high susceptibility of humanized NSG-A2 mice to non-adapted EBOV and furthermore showed that the severity of the infection was dependent on the percentage of engrafted human cells. EBOV infected humanized NSG-A2 mice exhibited high viremia and viral titers in several organs, similar to severe human EVD. Several pathological features of human EVD were also reflected by EBOV infection in humanized mice, including liver steatosis and necrosis, splenomegaly and in rare cases focal hemorrhage. The data further revealed that huNSG-A2 mice were also susceptible to the Makona variant of EBOV isolated from a human case of the 2014/2015 outbreak in West Africa, albeit with higher survival rates. These data are in line with recently published study that

showed a delay in disease progression of EBOV Makona in NHPs indicating reduced virulence of the new West African variant (Marzi et al., 2015).

These data indicate that huNSG-A2 mice might also translate the differences in lethality of different EBOV variants or species. It would therefore be important to also investigate the course of disease of other *ebolavirus* species such as RESTV, which is thought to be nonpathogenic for humans. In fact, the huNSG-A2 mouse could serve as a platform to test pathogenicity of new *ebolavirus* strains or species.

It was further shown that NSG-A2 mice without BM transplantation were susceptible to EBOV infection, but they succumbed to the disease after 4 weeks post-infection. This was probably due to unresolved viremia since NSG-A2 mice have severe defects in innate and adaptive immune responses. In contrast, transplantation of bone marrow from BL6 mice into NSG-A2 (moNSG-A2) mice resulted in 100% survival.,

Taken together, these data indicate that the pathology seen in huNSG-A2 mice are caused by the presence of human immune cells because they are responsible for faster disease progression compared to the course of disease in NSG-A2 mice without BM transplantation and furthermore, for high lethality in contrast to NSG-A2 mice with murine hematopoietic cells. In addition, immunofluorescence staining of the liver revealed that mouse hepatocytes were infected, which further demonstrates that even though viral replication takes place in human and murine cells, the human immune system probably fails to protect these animals. It remains to be determined, which interactions of EBOV with the immune system in particular are causing the disease pathology.

As demonstrated by others, the EBOV proteins VP24 and VP35 efficiently inhibit IFN-I responses and furthermore mutations in VP24 have been shown to be crucial for adaption to mice (Basler et al., 2003, Reid et al., 2006, Ebihara et al., 2006). One way of addressing the contribution of VP24 to disease pathology would be to infect huNSG-A2 mice with EBOV containing a mutation in VP24 that caused mouse adaptation. Furthermore, it would be important to determine whether macrophages and DCs serve as early targets of EBOV, which has been long suspected, and investigate their role on pathogenesis. The latter could be achieved by their depletion or by inhibiting viral entry into these cells. It would also be interesting to analyze cytokine levels in huNSG-A2 mice to determine whether strong inflammatory responses as seen in human EVD patients are causing the severity in huNSG-A2

mice. Finally, even though high lethality is observed in huNSG-A2 mice, it would be important to know whether these animals mount functional EBOV specific T cell or antibody responses and if yes, whether these responses can be modified to induce protection to EBOV. If this was not the case, then the next question would be to determine why huNSG-A2 mice fail to mount EBOV specific adaptive immunity. It was recently demonstrated that DENV infection in humanized mice induced a humoral and virus-specific T cell response (Jaiswal et al., 2012).

### **6.3 EBOV Immunity**

Limited immunological data have been collected in the past from human EVD cases and experimental infected NHPs. However, no *in vivo* kinetic studies have been conducted to investigate the complexity of the immune response to EBOV infection. The models established here were utilized for the third aim, which was to investigate EBOV immunology at the portals of viral entry and to determine the role of DCs on EBOV pathogenesis.

#### **6.3.1 Inflammatory response during EBOV infection**

Upon infection, viral replication at peripheral tissue sites is detected by receptors of the innate immune response called PRRs that are expressed by local tissue cells (Takeuchi and Akira, 2010). Among those tissue cells are macrophages, which are mainly involved in cytokine and chemokine production to attract other innate effector cells such as neutrophils and monocytes that mediate proinflammatory responses.

The investigation of pro-inflammatory effector cells, such as neutrophils and monocytes, revealed a strong inflammatory response in the lung of EBOV infected chimeric mice. IFNAR<sup>-/-</sup> IFNAR<sup>-/-</sup> chimeras with IFN-I deficient hematopoietic cells and non-hematopoietic cells displayed stronger infiltration of neutrophils into the lung and exhibited stronger neutrophilia in blood with up to 80% of hematopoietic cells being neutrophils at late time points post-infection compared to IFNAR<sup>-/-</sup> B16 chimeras. Even though neutrophils have been implicated in protection against some viral pathogens, they can also contribute to pathology, as seen in a study of influenza virus infection showing strong infiltration of neutrophils into the lung and high levels of pro-inflammatory cytokines contributing to severe lung inflammation (Perrone et al., 2008). It is not clear why IFNAR<sup>-/-</sup> IFNAR<sup>-/-</sup> chimeras had stronger neutrophil responses

that IFNAR<sup>-/-</sup> Bl6 mice, however, it is possible that other hematopoietic cells regulate neutrophil recruitment, which depends to a great extent on IFN-I. In fact, another study of influenza virus infection showed strong neutrophilia in IFNAR<sup>-/-</sup> mice in contrast to Bl6 mice. The authors suggested that the production of chemokines by IFN-I deficient monocytes induced massive neutrophil recruitment (Seo et al., 2011). The more severe lung pathology in EBOV infected IFNAR<sup>-/-</sup> IFNAR<sup>-/-</sup> mice could, to some extent, account for their higher susceptibility as shown previously in other models of infection such as highly pathogenic influenza virus (Perrone et al., 2008). It would be important to determine cytokine levels in lungs of EBOV-infected chimeras. Importantly, these findings are in line with the neutrophilia observed in human EVD patients as well as in experimental infected NHPs (Geisbert et al., 2003a).

The second interesting observation was that monocytes, that expressed intermediate levels of MHCII, accumulated over the course of infection in the lungs of EBOV-infected chimeras. These 'activated' monocytes were increased 3-fold at late time points post-infection in both types of chimeric mice. An increase of DC frequencies in lungs was also observed, even though in IFNAR<sup>-/-</sup> IFNAR<sup>-/-</sup> chimeras this increase was reduced at later time points post-infection. Taken together these data suggest infiltration of inflammatory monocytes into the lung that might differentiate into monocyte-derived DCs. However, whether they have a protective role or rather contribute to disease pathology is unclear.

### **6.3.2 EBOV infection of lung DCs**

Tissue-resident DCs are sentinels of the immune system patrolling peripheral tissues for invading pathogens. Once they detect virus replication in the periphery, they migrate to the tissue-draining lymph nodes in order to present viral antigen to naïve T cells that differentiate into effector T cells mediating viral clearance and long-lasting immunity. In the murine lung two major DC subsets, can be distinguished, namely CD103<sup>+</sup> DCs and CD11b<sup>+</sup> DCs. They are derived from different lineages and also have been assigned different roles during the antiviral immune response of the respiratory tract. Lung CD103<sup>+</sup> DCs are thought to have superior cross-presentation abilities compared to CD11b<sup>+</sup> DCs and therefore were suggested as key mediators of CD8 T cell responses (Ho et al., 2011). Moreover, during Influenza virus infection CD103<sup>+</sup> DCs were shown to be crucial for viral clearance from the lung

(GeurtsvanKessel et al., 2008). Lung CD11b<sup>+</sup> DCs in the lung comprise of a resident population and a monocyte-derived population in the steady state, however during inflammation infiltrating monocytes contribute to an increase of monocyte-derived CD11b<sup>+</sup> DCs (Munoz-Fontela et al., 2011; Cao et al., 2012). Their contribution to immunity against respiratory viral infections is still unclear, however researchers have demonstrated the ability of CD11b<sup>+</sup> DCs to induce both, CD4 and CD8 responses (Ballesteros-Tato et al., 2010; Kim and Braciale, 2009). The individual roles of CD103<sup>+</sup> DCs and CD11b<sup>+</sup> DCs during EVD have never been investigated.

The data presented here showed for the first time EBOV infection of lung DCs *in vivo*. In fact, DCs were found to be equally infected in both, IFNAR<sup>-/-</sup> IFNAR<sup>-/-</sup> and IFNAR<sup>-/-</sup> Bl6 chimeras. In comparison to other myeloid cell populations, alveolar macrophages were also infected, in contrast to monocytes and neutrophils that were not infected at any time point analyzed. Strikingly, only the CD11b<sup>+</sup> DC subset was found to be infected by EBOV, while infection of CD103<sup>+</sup> DCs in IFNAR<sup>-/-</sup> IFNAR<sup>-/-</sup> and IFNAR<sup>-/-</sup> Bl6 chimeras was not demonstrated. This marks a major difference to a recent study, which reported IFN-I induced protection of CD103<sup>+</sup> DCs from infection with Influenza virus (Helft et al., 2012).

The findings in the present study suggest cell-type specificity of EBOV infection rather than IFN-I dependency. EBOV cell tropism is likely to be dependent on cell surface receptors that facilitate viral entry. Viral attachment factors such as the C-type lectins DC-SIGN or human macrophage galactose- and N-acetylgalactosamine-specific C-type lectin (hMGL) have been implicated in EBOV entry (Alvarez et al., 2002; Takada et al., 2004). In favor of this hypothesis is the fact that CD103<sup>+</sup> DCs lack CD209, the mouse equivalent of DC-SIGN, on their surface, while CD11b<sup>+</sup> DCs do express CD209 (Hashimoto et al., 2011). DC-SIGN belongs to the family of PRRs and is involved in pathogen recognition (Geijtenbeek and Gringhuis, 2009). However, many viruses, including HIV, Dengue and measles virus, exploit their ability to bind DC-SIGN to favor viral entry (Tassaneetrithep et al, 2003; Mesman et al., 2012; Geijtenbeek et al, 2000). The fact that lung macrophages also express DC-SIGN further supports the idea that EBOV entry into certain cell types depends on their expression of cell surface receptors (Soilleux et al 2002).

Due to their migration capacity CD11b<sup>+</sup> DCs might indeed serve as viral vessels contributing to EBOV dissemination. The most likely route of dissemination is via the lymphatics, since lung CD11b<sup>+</sup> DCs migrate to the mediastinal lymph nodes.

However, the analysis of lymph nodes during EBOV infection did not reveal EBOV positive CD11b<sup>+</sup> DCs at any time point analyzed. A possible explanation might be that the virus kills its target cells before they reach their destination. However, it is also possible that difficulties at the isolation of mediastinal lymph nodes in the BSL-4 affected the experiment outcome. Therefore, another way of detecting infected DCs in the lymph nodes would be immunofluorescence staining of lymph node sections of EBOV infected mice. A further improvement for the detection of EBOV dissemination would be to utilize recombinant EBOV expressing a fluorescent tag such as GFP. Finally, a different approach would be to prevent migration of DCs, which could be achieved with the generation of IFNAR<sup>-/-</sup> CCR7<sup>-/-</sup> chimeras. CCR7 controls DC migration to the lymph nodes and CCR7<sup>-/-</sup> knockout mice have been demonstrated to lack migratory DCs (Ohl et al., 2004). In IFNAR<sup>-/-</sup> CCR7<sup>-/-</sup> mice, CD11b<sup>+</sup> DCs would not be able to carry infectious virus to the lymph nodes.

### ***Role of monocyte-derived DCs on EBOV pathogenesis***

In this study, it was further shown that infected CD11b<sup>+</sup> DCs were partially of monocytic origin. Furthermore, within the CD11b<sup>+</sup> DC compartment, a significant shift in percentages of conventional and monocyte-derived DCs was observed. While during early time points post-infection the majority of CD11b<sup>+</sup> DCs in the lung comprised of conventional DCs, at later time points post-infection most of the CD11b<sup>+</sup> DCs were of monocytic origin. These findings and the fact that monocytes were refractory to EBOV entry is in line with recently published data by the group of Chris Basler. They showed that monocytes were in fact resistant to EBOV entry. However, association of EBOV to monocytes induced their differentiation into monocyte-derived DCs facilitating viral entry (Martinez et al., 2013). This might be a mechanism of the virus to increase its repertoire of target cells. A similar mechanism was recently described for DENV, where inflammatory monocytes were recruited to the skin, the entry site of DENV, which differentiated in monocyte-derived CD11b<sup>+</sup> DCs and became major targets of DENV replication (Schmid and Harris, 2014).

Taken together, the data in this study suggest that upon EBOV infection monocytes infiltrate the lungs and differentiate into monocyte-derived DCs, which also become infected. Whether EBOV induces their differentiation in order to facilitate entry remains to be determined *in vivo*. However, this led to the hypothesis that monocyte-derived DCs might contribute to viral dissemination and EBOV pathogenesis. In order



to further investigate this theory IFNAR<sup>-/-</sup> CCR2<sup>-/-</sup> chimeras were generated. The chemokine receptor CCR2 regulates monocyte exit from the bone marrow and furthermore is essential for infiltration into inflamed tissue. It was demonstrated previously that monocyte-derived DCs are reduced in CCR2<sup>-/-</sup> knockout mice (Serbina et al., 2003). However, when we compared EBOV infection in IFNAR<sup>-/-</sup> B16 chimeras and IFNAR<sup>-/-</sup> CCR2<sup>-/-</sup> chimeras the data revealed no differences in survival or viremia. Engraftment of CCR2<sup>-/-</sup> BM in IFNAR<sup>-/-</sup> recipient mice could not be verified due to the fact that both recipient and donor mice expressed the same isoform of CD45, a feature that is commonly used to distinguish donor from recipient cells via flow cytometry. Therefore, it cannot be excluded that low engraftment might have had an influence on the outcome of the experiment. Therefore, a second approach was to deplete inflammatory monocytes using depleting antibodies. In fact, the depletion of monocytes rescued 40% of EBOV infected IFNAR<sup>-/-</sup> mice in comparison to isotype control-treated animals, where EBOV infection was 100% lethal. These findings indicated a role of monocytes in EBOV pathogenesis, however, the Ly6C depletion antibody also depletes neutrophils, and indeed, Ly6G depletion of neutrophils alone also resulted in enhanced survival (20%) compared to the isotype control. It is possible that due to their contribution to lung immunopathology neutrophil depletion alleviated lung inflammation in our system. In fact massive infiltration of neutrophils into the lungs of EBOV-infected chimeras was observed. In addition, differentiation of monocytes into monocyte-derived DCs might provide more target cells for the virus and this could also further contribute to disease progression. Furthermore, monocyte-derived DCs might as well increase lung pathology similar to what has been observed during Influenza virus infection (Lin et al., 2007). Whether monocyte-derived DCs contribute to viral dissemination remains to be determined. However, other depletion models would further help to understand the role of CD11b<sup>+</sup> DCs on EBOV pathogenesis. For example, transplantation of BM from conditional CD11b-DTR knockout mice into IFNAR<sup>-/-</sup> recipients, would allow depletion of CD11b<sup>+</sup> cells, which is mainly expressed on monocytes and DCs.

### ***EBOV infection of human CD14<sup>+</sup> myeloid cells***

Next, the humanized mouse model was utilized in order to compare and validate findings from the murine chimeric mouse. EBOV infection of huNSG-A2 mice revealed infection of lung CD14<sup>+</sup> myeloid cells. Infection of those cells coincided with

a decrease in their frequencies. Furthermore an increase of CD16<sup>+</sup> CD11c<sup>+</sup> myeloid cells consistent with 'non-classical' was also observed. Due to the lack of additional markers tissue CD14<sup>+</sup> macrophages and DCs could not be explicitly distinguished; therefore, the exact nature of these CD14<sup>+</sup> myeloid cells remains to be determined. In any case, the data from the humanized mouse model obtained here are in line with the findings in the murine chimeric mouse model, which showed infection of both, macrophages and DCs. Interestingly, tissue CD14<sup>+</sup> DCs have been proposed to be the human equivalents of monocyte-derived CD11b<sup>+</sup> DCs (Haniffa et al., 2013). For future experiments it will be important to identify markers for clear distinction of macrophages and DCs to be able to investigate their individual roles. The fact that CD14<sup>+</sup> DCs also express DC-SIGN further supports the idea that DC-SIGN is a crucial entry factor for EBOV *in vivo* (Fehres et al., 2015).

### **6.3.3 Role of IFN-I signaling in hematopoietic immunity to EBOV**

The results of this study demonstrated that a functional IFN-I response in hematopoietic cells led to lower viral loads in blood and probably as a result also lower viral titers in organs, such as spleen and liver. In addition, functional IFN signaling in hematopoietic cells led to viral clearance, while mice with IFN-deficient hematopoietic cells were not able to clear the virus. Taken together, overall lower viral loads probably enhanced survival., This is consistent with human data from the 2014/2015 EBOV outbreak indicating that lower viral loads correlated with increased survival rates (Fitzpatrick et al., 2015, Schieffelin et al., 2014, Lanini et al., 2015).

The IFN-I response is the first line of defense against viral infections. It establishes a state of resistance in infected and surrounding cells, however, IFN-I signaling did not prevent infection of DCs or macrophages. In fact, both cell types were infected in both, IFNAR<sup>-/-</sup> IFNAR<sup>-/-</sup> and IFNAR<sup>-/-</sup> Bl6 chimeras, even though in the latter the percentage of EBOV positive CD11b<sup>+</sup> DCs was lower compared to EBOV infected CD11b<sup>+</sup> DCs in the former. These results suggest that IFN-I signaling did not induce significant protection from EBOV infection in hematopoietic cells.

However, these findings suggest an important contribution of IFN-I on adaptive immunity to EBOV. In fact, previous studies have demonstrated that the IFN-I signaling is necessary for DC activation and antigen-presentation (Longhi et al., 2009; Simmons et al., 2012). Furthermore, an important mechanism called cross-

presentation, describing presentation of viral antigen acquired in the periphery by DCs via MHC I to CTLs, also depends on IFN-I signaling (Joffre et al., 2012). IFN-I signaling can also directly affect T cell responses. In fact, IFN-I was shown have both, pro- and anti-apoptotic effects on T cells depending on the timing of TCR and IFNAR signaling (Crouse et al., 2015). While ‘in-sequence’ signaling (meaning TCR engagement prior to IFNAR signaling) promotes survival and differentiation of T cells, ‘out-of-sequence’ signaling (meaning IFNAR engagement prior to TCR signaling) induces anti-proliferative, pro-apoptotic program in T cells. The lack of IFN-I signaling clearly disturbs this fine regulation of the T cell responses.

In summary, major mechanisms of the adaptive immune response to viral infections are IFN-I dependent, which might explain the better control of viral loads in IFNAR<sup>-/-</sup> Bl6 chimeras and hence there improved survival compared to IFNAR<sup>-/-</sup> IFNAR<sup>-/-</sup> chimeric mice.

#### **6.3.4 Protective role of T cells during EBOV infection**

The data presented here suggested that hematopoietic immunity played an important role in controlling viral dissemination. As discussed above it is likely that adaptive immune responses are responsible for this control. In order to further dissect the protection mediated by hematopoietic immunity, T cells were depleted in IFNAR<sup>-/-</sup> Bl6 chimeras. Depletion of either CD4 or CD8 T cells alone did not affect survival or viral loads, however when both CD4 and CD8 T cells were depleted, the previously observed protection in IFNAR<sup>-/-</sup> Bl6 chimeric mice was lost and 100% lethality was observed. Furthermore, an increase in organ titers at the time of death indicated deficient viral clearance.

These findings demonstrated a protective role of T cells during EBOV infection. A synergistic effect of CD4 and CD8 T cells might be crucial for controlling viral dissemination and reducing EBOV pathogenesis. From this also follows that functional DC responses precede functional T responses. It is possible, that T cell activation is mediated by CD103<sup>+</sup> DCs, whose infection could not be demonstrated. They might cross-present internalized EBOV antigen via MHC I to CTLs, inducing killing of virus-infected cells. This mechanism would require help from activated CD4<sup>+</sup> T cells that induce upregulation of CD80/86 on DCs necessary for efficient cross-presentation to CTLs. The conditional depletion of Langerin<sup>+</sup> cells, which includes

CD103<sup>+</sup> cells in the lung, would shed light on the function of CD103<sup>+</sup> DCs on EBOV immunity. It is possible that infected CD11b<sup>+</sup> DCs are also able to prime CD8 T cells, however, if the observed impairment of monocyte-derived DCs *in vitro* is also true *in vivo*, then these infected cells are not able to induce proper CTL responses. This will require further investigations.

#### **6.4 APCs in peripheral blood of EVD patients**

In the context of the EBOV outbreak in Guinea between 2014 and 2015, our laboratory had the chance to perform immunology studies on leftover diagnostic samples. This unique opportunity allowed phenotyping of monocyte and DC subsets in peripheral blood of EVD patients.

Human blood consists of three monocyte subsets: classical CD14<sup>+</sup> monocytes, double positive CD14<sup>+</sup> CD16<sup>+</sup> monocytes and non-classical CD16<sup>+</sup> monocytes. In addition, precursors of tissue-resident CD141<sup>+</sup> and CD1c<sup>+</sup> DCs are also present in human peripheral blood. Investigation of these myeloid populations in peripheral blood of EVD patients revealed significant loss of CD16<sup>+</sup> and CD14<sup>+</sup> monocytes. It is possible that this was due to their direct infection, even though infected populations in peripheral blood could not be demonstrated. However, experimental infection of huNSG-A2 mice revealed infection and loss of CD14<sup>+</sup> cells, which strengthens the idea that in fact CD14<sup>+</sup> DCs might be targets of productive EBOV infection. Interestingly, an increase of CD16<sup>+</sup> myeloid cells was observed in the lungs of huNSG-A2, which might explain the decrease of this population in peripheral blood of EVD patients. It has been suggested previously that CD16<sup>+</sup> monocytes are patrolling the blood vessels to detect virus-infected cells in order to produce proinflammatory cytokines, while another study reported inflammatory DCs expressing CD16 present in the skin of psoriasis patients (Cros et al., 2010; Hänsel et al., 2011). It is therefore possible that blood CD16<sup>+</sup> monocytes might infiltrate the inflamed tissue during EBOV infection and differentiate in DCs.

Furthermore, monocyte loss was correlated with high viremia and low activation status, indicated by low HLA-DR expression. In fact, EBOV induced inhibition of monocyte-derived DC activation has been demonstrated previously and furthermore, their poor T cell priming capacity (Mahanty et al., 2003). It could be further shown that in fatal cases, HLA-DR expression on monocytes stayed low during disease

progression, while increased HLA-DR expression was observed in survivors, which coincided with viral clearance. These data indicate an immune suppressive mechanism of EBOV on monocyte function that might have an effect on disease pathophysiology.

## **6.5 Proposed model**

It was demonstrated in the present study that lung DCs and alveolar macrophages are early targets of EBOV infection. Local replication of the virus in these cells probably induces a proinflammatory immune response attracting more innate effector cells. Indeed, neutrophil and monocyte recruitment to the lungs was observed. Alveolar macrophages are likely to serve as viral replication sites and moreover, their infection might contribute to massive proinflammatory responses. While EBOV was shown to infect CD11b<sup>+</sup> DCs, infection of CD103<sup>+</sup> DCs was not demonstrated. In addition, a strong increase of monocyte-derived CD11b<sup>+</sup> DCs was seen. Interestingly, both, monocyte-derived and conventional CD11b<sup>+</sup> DCs were infected. In line with another study it is probable that EBOV induces the differentiation of monocytes into monocyte-derived DCs. This would provide additional target cells for the virus. It could not be determined whether monocyte-derived or conventional CD11b<sup>+</sup> DCs contribute to viral dissemination however they are possible candidates due to their migration capacity. Depletion of monocytes reduced fatality in mice, indicating a role in pathogenesis. In contrast, CD103<sup>+</sup> DCs, whose infection was not demonstrated, might actually be able to migrate to the draining lymph nodes in order to prime naïve T cell responses. In fact, CD4 and CD8 T cells were shown to be crucial for the protection mediated by hematopoietic cells.

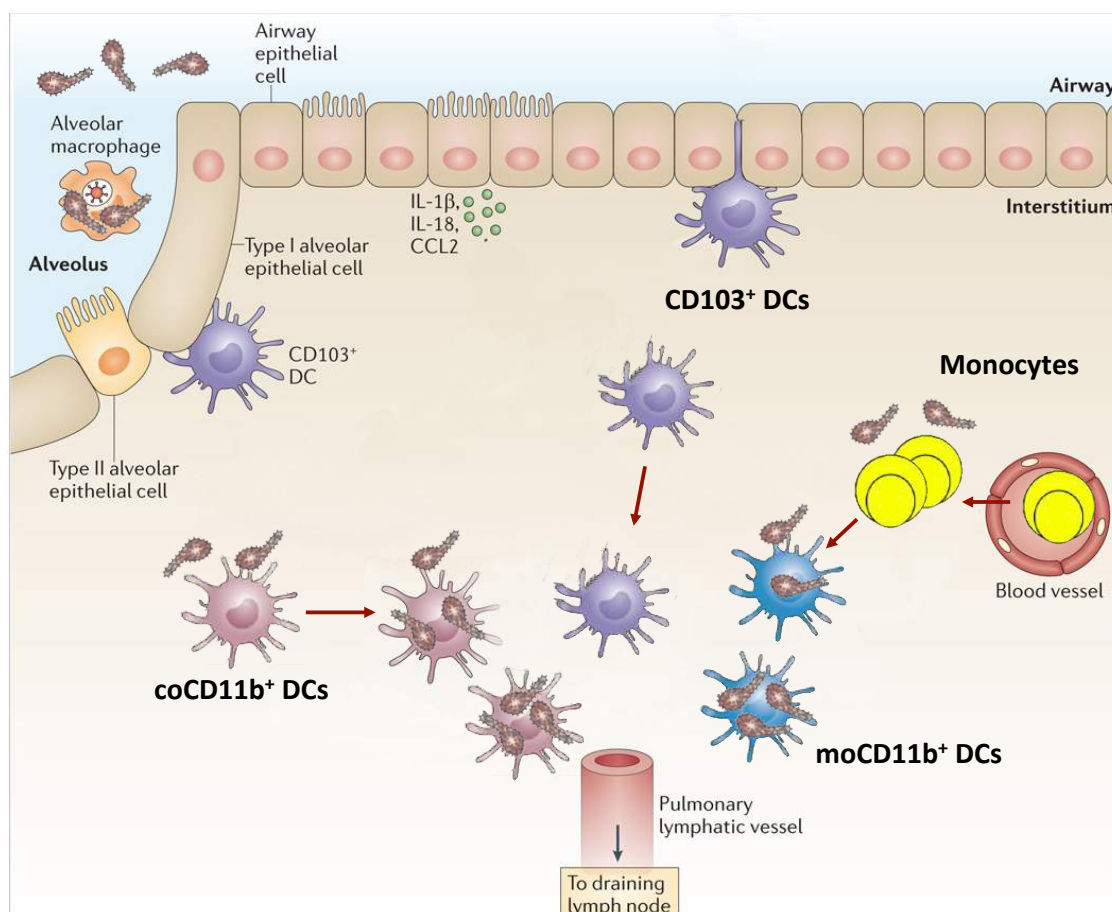


**Figure 29: Proposed model of DC responses to EBOV infection in the respiratory tract** EBOV replicates in alveolar macrophages and CD11b<sup>+</sup> DCs. Inflammatory monocytes that infiltrate the lung upon EBOV infection, differentiate into monocyte-derived CD11b<sup>+</sup> DCs, which are also infected. CD11b<sup>+</sup> DCs might migrate to the lymph nodes and thereby disseminate the virus. CD103<sup>+</sup> DCs are protected from infection and might migrate to the draining lymph nodes to initiate EBOV-virus specific T cell responses (schematic modified from Braciale et al., 2012 and Haniffa et al., 2013).

Studies have suggested that EBOV infection induces immune suppression. Based on the generated data in this study a possible mechanism for EBOV mediated immune suppression is the induction of a suppressive state in DCs. Myeloid suppressive cells were recently characterized in a study on allograft transplantation. Researchers demonstrated that Ly6C<sup>high</sup> monocytes from blood infiltrated the allograft, downregulated Ly6C and upregulated DC-SIGN dependent on CSF1 signaling developing into Ly6C<sup>low</sup> suppressive macrophages that were necessary for tolerance of the transplant by inhibiting CD8 T cells and inducing Treg expansion (Conde et al., 2015).

In fact, EBOV infected CD11b<sup>+</sup> cells could be distinguished into Ly6C<sup>low</sup> and Ly6C<sup>high</sup> CD11b<sup>+</sup> DCs. While Ly6C<sup>high</sup> CD11b<sup>+</sup> DCs are likely to be inflammatory, Ly6C<sup>low</sup> CD11b<sup>+</sup> DCs might exhibit a suppressive phenotype. Attachment of EBOV to

inflammatory  $\text{Ly6C}^{\text{hi}}$  monocytes that infiltrate the lung might induce their differentiation into DCs and viral entry might be facilitated by up regulation of DC-SIGN. Infected  $\text{CD11b}^+$  DCs might down regulate  $\text{Ly6C}$  and become suppressive by inhibiting effector T cell responses. In addition, the observed low activation status of  $\text{CD16}^+$  monocytes in peripheral blood of EVD patients further supports the idea, since these are the equivalents to murine  $\text{Ly6C}^{\text{low}}$  monocytes. Furthermore, this would be in line with our recently obtained data from the EBOV outbreak 2014/2015 that fatal EVD was associated with overexpression of inhibitory molecules CTLA-4 and PD-1 on CD4 and CD8 T cells (Ruibal et al., 2016, in revision). CTLA-4 and PD-1 have been associated with T cell exhaustion, which describes the loss of effector function and the failure to generate memory T cells. These mechanisms might contribute to the failure of the immune system to clear the infection and lead to fatal outcome.

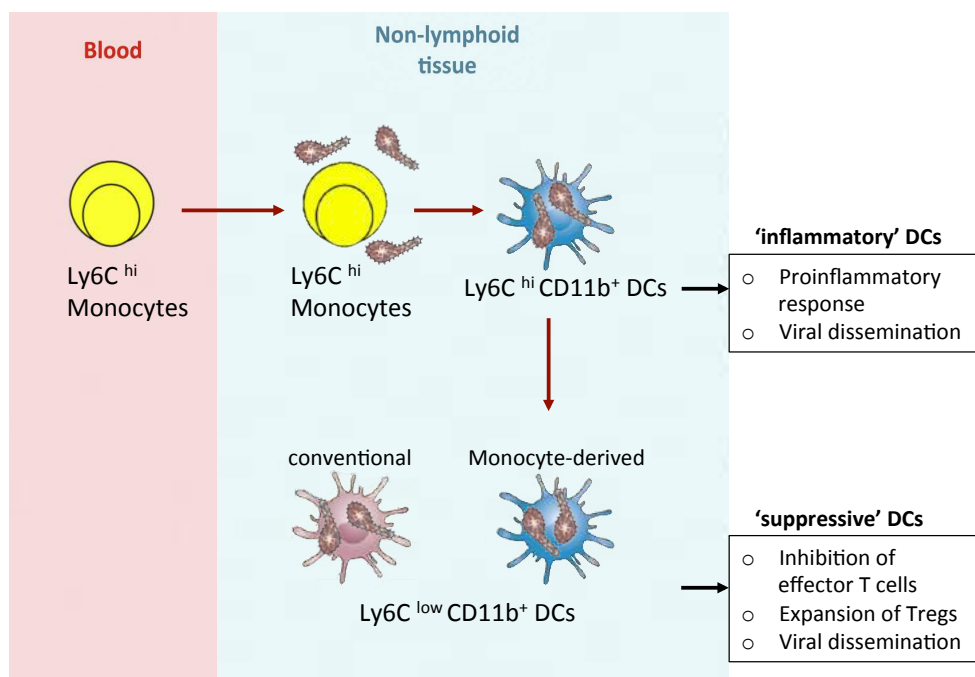


**Figure 30: Possible contributions of DCs on EBOV pathogenesis**  $\text{Ly6C}^{\text{hi}}$  monocytes infiltrate into the inflamed lung, association of EBOV to monocytes might induces their differentiation allowing viral entry. 'Inflammatory'  $\text{Ly6C}^{\text{hi}}$   $\text{CD11b}^+$  DCs might mediate proinflammatory responses or dissemination of the virus, while  $\text{Ly6C}^{\text{low}}$   $\text{CD11b}^+$  DCs might be suppressive by inhibiting effector T cell responses and expanding Tregs (schematic modified from Haniffa et al., 2013 and Braciale et al., 2012).

## 6.6 Outlook

The present study strengthens the idea that DCs have an important role on EBOV pathophysiology *in vivo*. Therefore, they might in fact be important targets for immunotherapy against EVD. DC-SIGN is likely to be a crucial factor for EBOV entry in DCs. It is therefore possible that blocking the receptor would actually prevent infection of DCs, minimize the immune suppression caused by DC infection and facilitate antiviral T cell responses. In addition, blocking the infection of macrophages would probably also reduce the massive inflammatory responses observed during EVD. Possible ways of blocking the interaction of EBOV with DC-SIGN are anti-DC-SIGN antibodies or compounds that bind DC-SIGN. In fact, an *in vitro* study demonstrated efficient inhibition of DC-SIGN mediated EBOV entry via a glycodendritic structure (Lasala et al., 2003). Another possibility to block EBOV entry via DC-SIGN would be to block CSF1 signaling, which is required for DC-SIGN upregulation on myeloid cells (Domínguez-Soto et al., 2011). Anti-CSF-1R antibodies that block CSF-1R activation are already used in anti-tumor therapies (Hume and MacDonald, 2012).

A different approach would be to reverse EBOV induced immune suppression on DCs via CD40L treatment or agonistic CD40 antibodies. The interaction of CD4 T cells with DCs is essential for proper DC activation and is achieved via CD40 - CD40L signaling (Shreedhar et al., 1999). In fact, intense research has been conducted in anti-tumor therapy on DC activation via CD40 signaling (Diehl et al., 1999; van Mierlo et al., 2002). In addition, several studies have demonstrated enhanced immune responses to infections upon CD40 stimulation (Demangel et al., 2001; Zickovich et al., 2014). Interestingly, a recent study showed that non-fatal EBOV cases had significantly higher plasma levels of soluble CD40L (sCD40L) than fatal EBOV cases (McElroy et al., 2014). The authors suggested that sCD40L might indicate repair of altered endothelium, however, it is also possible that sCD40L induces activation of DCs (Martinson et al., 2004).

Understanding the interactions of EBOV with the human immune system will allow specific targeting of the immune response to induce protective and long lasting immunity against EBOV.



## 7 Material

### 7.1 General consumables

General consumables were obtained from Eppendorf, Sarstedt, Greiner Bio One, Qiagen, Thermo Scientific, Miltenyi, Sigma and Carl Roth.

### 7.2 Viruses

Most infection experiments were carried out using *Zaire ebolavirus* isolate from 1976 (Ebola virus H.sapiens-tc/COD/1976/Yambuku-Mayinga). In one experiment the Makona variant of *Zaire ebolavirus* (Ebola virus h.sapiens-wt/GIN/2014/Makona) from the 2014/2015 outbreak in West Africa was used.

### 7.3 Cell lines

Vero E6 cells, derived from kidneys of African green monkeys, were utilized for virus amplification and focus formation assays.

### 7.4 Mouse colonies

Name	Source
C57BL/6	Jackson Laboratories
C57BL/6_Ly5.1	Jackson Laboratories
IFNAR <sup>-/-</sup>	Gift from Friedrich Loeffler Institute
CCR2 <sup>-/-</sup>	Jackson Laboratories
NSG-A2	Jackson Laboratories
NSG	Jackson Laboratories

## 7.5 Reagents, buffers and kits

Name	Company
Collagenase D	Roche
DnaseI	Sigma
Red Blood Cell Lysis Buffer	BD
BD Cytofix/Cytoperm Plus Golgi Plug	BD
Baytril 2,5%	Bayer
Triton X-100	Roth
Formaldehyde (37%)	Roth
Dulbecco's Phosphate Buffered Saline (PBS)	Sigma
Live/Dead Fixable Blue Dye	Molecular Probes
Live/Dead Zombie Dye	BioLegend
Alexa Fluor 488 Antibody Labeling Kit	Invitrogen
Human Cord Blood CD34 Positive Selection Kit	Stemcell Technologies
TMB substrate solution	Mikrogen Diagnostik
Biocoll	Biochrom

## 7.6 Media and solutions

Name	Content	
Growth medium (5% FCS)	DMEM	500 ml
	FCS	25 ml
	Penicillin/Streptomycin (100x)	5 ml
	L-Glutamin (100x)	5 ml
	Non-essential amino acids (100x)	5 ml
	Pyruvate (100x)	5 ml
Infection medium (2% FCS)	DMEM	500 ml
	FCS	10 ml
	Penicillin/Streptomycin (100x)	5 ml
	L-Glutamin (100x)	5 ml
	Non-essential amino acids (100x)	5 ml
	Pyruvate (100x)	5 ml
Methylcellulose medium (for overlay medium)	methylcellulose	2.8 g
	dH <sub>2</sub> O	600 ml
Collagenase stock solution (20 mg/ml)	Collagenase D	20mg
	1x PBS	1 ml
DnaseI stock solution (10 mg/ml)	DnaseI	10 mg
	dH <sub>2</sub> O	1 ml
Heparin stock solution (20 U/ml)	HBSS Buffer	200 ml
	Heparin	50 ml

## 7.7 Antibodies

Antibody	Clone	Source
mAB $\alpha$ -EBOV		BNITM
mAB $\alpha$ -EBOV GP	5D2	G. Kobinger
mAB $\alpha$ -EBOV GP	5E6	G. Kobinger
<b>Anti-Mouse (<math>\alpha</math>-m)</b>		
HRP-coupled secondary $\alpha$ -m		Jackson ImmunoResearch
$\alpha$ -m CD4 (depletion)	YTS 191	BioXCell
$\alpha$ -m CD8 (depletion)	YTS 169.4	BioXCell
$\alpha$ -m Ly6G (depletion)	1A8	BioXCell
$\alpha$ -m Ly6C (depletion)	RB6-8C5	BioXCell
Isotype control	LTF-2	BioXCell
$\alpha$ -m CD103 PerCP/Cy5.5	2E7	BioLegend
$\alpha$ -m CD11b Brilliant Violet 510	M1/70	BioLegend
$\alpha$ -m CD11b PerCP/Cy5.5	M1/70	BioLegend
$\alpha$ -m I-A/I-E eFluor 450	M5/114.15.2	eBioscience
$\alpha$ -m CD11c Brilliant Violet 785	N418	BioLegend
$\alpha$ -m CD64 (Fc $\gamma$ RI) APC	X54-5/7.1	BioLegend
$\alpha$ -m Fc $\epsilon$ RI $\alpha$ PE/Cy7	MAR-1	BioLegend
$\alpha$ -m Ly-6G PE/Cy7	1A8	BioLegend
$\alpha$ -m Ly-6C APC/Cy7	HK1.4	BioLegend
$\alpha$ -m Siglec-F PE	E50-2440	BD Pharmingen
$\alpha$ -m CD45.1 A700	A20	BioLegend
$\alpha$ -m CD45.2 A700	104	BioLegend
$\alpha$ -m CD3 Brilliant Violet 785	17A2	BioLegend
$\alpha$ -m CD3 Brilliant Violet 650	17A2	BioLegend
$\alpha$ -m CD8 Pacific Blue	53-6.7	BioLegend
$\alpha$ -m CD4 APC	GK1.5	BioLegend
$\alpha$ -m B220 PE	RA3-6B2	eBioscience
$\alpha$ -m B220 Brilliant Violet 650	RA3-6B2	BioLegend
$\alpha$ -m NK1.1 Brilliant Violet 650	PK136	BioLegend
TrueStain fcX ( $\alpha$ -m CD16/32)	93	BioLegend
<b>Anti-Human (<math>\alpha</math>-h)</b>		
$\alpha$ -h HLA-DR Brilliant Violet 785	L243	BioLegend
$\alpha$ -h HLA-DR PE/Cy7	L243	BioLegend
$\alpha$ -h CD14 Brilliant Violet 510	M5E2	BioLegend
$\alpha$ -h CD14 APC	HCD14	BioLegend
$\alpha$ -h CD16 APC/Cy7	3G8	BioLegend
$\alpha$ -h CD16 PE	3G8	BioLegend
$\alpha$ -h CD11c PerCP/Cy5.5	Bu15	BioLegend
$\alpha$ -h CD11c PB	Bu15	BioLegend
$\alpha$ -h CD1c APC	L161	BioLegend
$\alpha$ -h CD141 PE/Cy7	M80	BioLegend
$\alpha$ -h CD141 PE	M80	BioLegend

α-h CD123 Brilliant Violet 650	6H6	BioLegend
α-h CD49d PE	9F10	BioLegend
α-h CD45 A700	2D1	BioLegend
α-h CD3 Pacific Blue	SK7	BioLegend
α-h CD3 PerCP/Cy5.5	SK7	BioLegend
α-h CD19 Pacific Blue	HIB19	BioLegend
α-h CD19 PerCP/Cy5.5	HIB19	BioLegend
α-h CD56 Pacific Blue	HCD56	BioLegend
α-h CD56 PerCP/Cy5.5	HCD56	BioLegend
Human TrueStain fcX		BioLegend

## 7.8 Laboratory equipment

Name	Company
BD LSRFortessa	BD
BD LSR II	BD
BD FACSCanto II	BD
Guava easyCyte 8 (3 laser)	Merck Millipore
Automated Cell Counter	Invitrogen
Scale	Kern
Thermometer for mice	Bioseb
Fast Prep homogenizer	MPbio
Reflotron	Roche
Self-shielded Cs-137 irradiator	

## 7.9 Software

Name	Manufacturer
FlowJo	FLOWJO
Inkscape	
GraphPad Prism	GraphPad Software
Microsoft Excel	Windows
Microsoft Word	Windows

## **8 Methods**

### **8.1 BSL-4 experiments**

Experiments with infectious virus were carried out in the BSL-4 laboratory at the Bernhard Nocht institute under approval IB17-42/13 issued by the Ministry of Urban Development and Environment of Hamburg. Animal experiments were conducted according to the guidelines of the German animal protection law and under approvals 104/12 and 125/12.

### **8.2 Virus amplification**

For amplification of EBOV,  $1 \times 10^6$  Vero-E6 cells were seeded in 20 ml of growth medium (DMEM with 5% FBS) in T-75 cm<sup>2</sup> flasks. Twenty-four hours later, cells were infected with an MOI (multiplicity of infection) of 0.01 in 3 ml of infection medium (DMEM with 2% FBS) and incubated for 1 hour at 37 °C and 5% CO<sub>2</sub>. Then, the inoculum was removed and 20 ml of growth medium was added to the cells. Cells were incubated for 5 days at 37 °C and 5% CO<sub>2</sub>. Supernatant was harvested and centrifuged for 5 min at 1500xg. The virus stock was aliquoted and stored at – 80 °C.

### **8.3 Focus formation assay**

Focus formation assay was utilized for quantification of viral titers in virus cultures and blood or organs of infected animals.  $1 \times 10^6$  Vero-E6 cells were seeded in a 24-well plate. Twenty-four hours later, a logarithmic dilution of the sample was prepared in infection medium in a 96 well plate. After removal of the cell culture medium sample dilutions were transferred to the cells. The 24-well plate was incubated for 1 hour at 37 °C and 5% CO<sub>2</sub>. Then, the inoculum was removed, cells were covered with overlay medium (2/3 DMEM with 10% FBS and 1/3 methylcellulose medium) and incubated for 6 days at 37 °C and 5% CO<sub>2</sub>. After 6 days, overlay medium was removed and 24 well plates were incubated with 4% formaldehyde in PBS for 30 min at room temperature (RT) for inactivation of the virus (fixation step). After fixation, plates were removed from the BSL-4 laboratory. Cells were rinsed with H<sub>2</sub>O and incubated with 0.5% Triton X-100 for 30 min at RT (permeabilization step). After permeabilization, plates were washed with H<sub>2</sub>O and blocked with 10% FBS in PBS for 1 hour at RT. Blocking was removed and cells were incubated with primary anti-

EBOV antibody (1:1000 in PBS with 10% FBS) for 1 hour at RT. After the primary antibody incubation, plates were rinsed with H<sub>2</sub>O and incubated with the HRP (horseradish peroxidase) coupled secondary anti-mouse antibody (1:1000 in PBS with 10% FBS) for 1 hour at RT. Cells were washed with H<sub>2</sub>O and incubated with TMB (3,3',5,5'-Tetramethylbenzidine) for detection of viral foci. HRP catalyzes the hydrolysis of hydrogen peroxide, the produced oxygen radicals oxidize TMB into a blue product. Blue foci were counted and taking into account the dilution factors the viral titer was determined.

#### **8.4 Isolation of murine bone marrow cells**

To obtain bone marrow (BM) cells, tibia and femur were isolated from donor animals. Then, bones were cleaned, sterilized with 70% ethanol and transferred to DMEM without FBS. Under sterile conditions, the bones were cut at their ends and BM cells were flushed out. BM cells were resuspended, filtered and centrifuged for 5 min at 1500 rpm. The pellet was resuspended in 1x Red blood cell lysis buffer to lyse erythrocytes. Lysis was stopped with PBS and cells were centrifuged for 5 min at 1500 rpm. Cells were washed with PBS and counted.

#### **8.5 Purification of human CD34<sup>+</sup> HSCs from cord blood**

Human hematopoietic stem cells (CD34<sup>+</sup>) were obtained from human cord blood via a Ficoll gradient and positive selection with an anti-CD34 antibody cocktail. Human cord blood was diluted with 2 or 3 volumes of washing buffer (PBS containing 2% FBS, 1% P/S and 2mM EDTA) in a sterile glass bottle. 35 ml of diluted cord blood was added to 15 ml of Ficoll (Biocoll) solution without disturbing the phases. For separation of white blood cells from red blood cells and serum, falcon tubes were centrifuged at 2000 rpm and 20 °C for 45 min with low acceleration and brake. The buffy coat containing white blood cells was harvested and cells were washed two times with washing buffer and then centrifuged at 1500 rpm and 20 °C for 10 min (normal brake). Cells were counted and resuspended at 2–5x10<sup>8</sup> cells in 1 ml of washing buffer and transferred to a polystyrene tube. 100 µl of CD34<sup>+</sup> positive selection cocktail was added and incubated for 15 min at RT. Then, 50 µl of magnetic nanoparticles was added and incubated for 10 min at RT. Cell suspension was filled

up to 2.5 ml with washing buffer and the tube was placed in a magnet. After 5 min incubation the supernatant was removed. CD34<sup>+</sup> cells bound to the magnetic particles will remain in the tube. The washing step was repeated five times and cells were centrifuged at 1500 rpm and 4°C for 10 min. The supernatant was removed and cells were resuspended at 1x10<sup>6</sup> CD34<sup>+</sup> cells in 1 ml of FBS containing 10% DMSO.

## 8.6 Generation of chimeras

### 8.6.1 Generation of bone marrow chimeras

Four to eight weeks old female recipient mice were lethally irradiated with 14 Gray (2x 7 Gray with 2 hours in between) in a self-shielded Cs-137 irradiator. One hour after the second irradiation, 3x10<sup>6</sup> donor bone marrow cells (in 100 µL PBS) were transplanted into recipient mice intravenously (i.v.) via the retroorbital sinus under isoflurane anesthesia. Mice were monitored closely and drinking water was supplied with antibiotics (Baytril, 0.01% (v/v) for 2 weeks post transplantation.

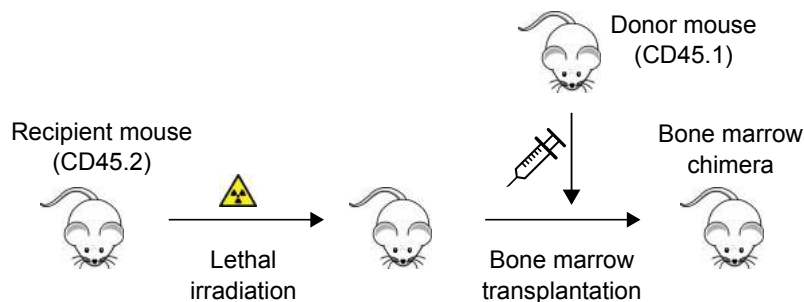


**Figure 31: Generation of bone marrow chimeric mice**

The engraftment of donor bone marrow cells in recipient mice was analyzed 4 weeks post transplantation in peripheral blood using the CD45.1 and CD45.2 alleles of the hematopoietic marker CD45. Donor mice were CD45.1, while recipient mice were CD45.2 or vice versa.

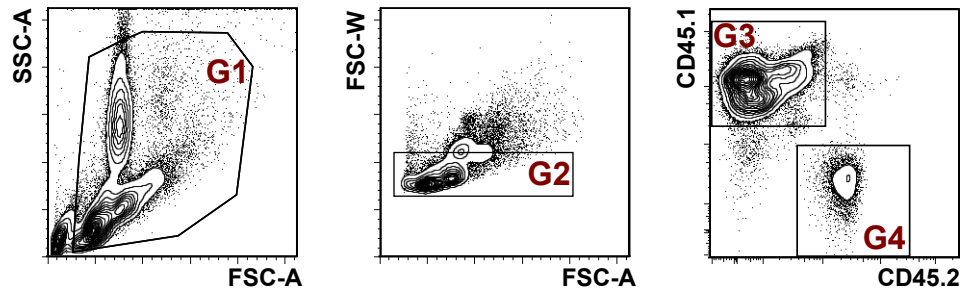


**Figure 32: Engraftment of CD45.1 donor BM cells in CD45.2 recipient mice** Cell debris was removed with gate 1 (G1) and singlet cells were gated in G2. Donor cells (G3) and recipient cells (G4) were distinguished with anti-CD45.1 and CD45.2 antibodies, respectively.

### 8.6.2 Generation of humanized NSG-A2 mice

Four to six weeks old NSG or NSG-A2 mice were sub-lethally irradiated (1.8 Gray). Four hours later,  $1 \times 10^6$  human hematopoietic stem cells were transplanted into recipient mice i.v. via the retroorbital sinus under isoflurane narcosis. Mice were monitored closely and drinking water was supplied with antibiotics (Baytril, 0.01% (v/v) for 2 weeks post transplantation.

Engraftment of human HSCs in recipient mice was analyzed 8 weeks post transplantation in peripheral blood using the human hematopoietic marker CD45.

## 8.7 Animal experiments in BSL-4

Three to five days before the experiment, mice were brought into the BSL-4 and kept in IVCs (individually ventilated cages). Cages and water bottles were changed weekly. Infected animals were monitored for signs of morbidity and weight and temperature (rectal measurement) were measured daily. Mice that lost more than 20% of their original body weight, had very low body temperature or showed other signs of morbidity, such as ruffled hair or hunched posture were sacrificed via isoflurane narcosis and cervical dislocation. Organs were harvested for determination of viral titers.

### 8.7.1 Infection

Mice were inoculated with 1000 FFU of EBOV via different routes of infection depending on the experiment. Prior to inoculation the mice were anesthetized with isoflurane.



For intranasal (i.n.) inoculation, the virus stock was diluted to  $2 \times 10^4$  FFU/ml in PBS and 50  $\mu$ l of virus dilution was applied to the nostrils of the mouse. Prior to intradermal/subcutaneous (i.d./s.c.) infection, animals were shaved at the back above their tail. For inoculation, the virus stock was diluted to  $2 \times 10^4$  FFU/ml in PBS and 50  $\mu$ l of virus dilution was administered into the skin above the tail with an insulin syringe. For intraperitoneal (i.p.) inoculation, the virus was diluted to  $10^4$  FFU/ml in PBS and 100  $\mu$ l of virus dilution was injected into the peritoneum of the animal with an insulin syringe.

### **8.7.2 Blood draw**

Blood was drawn from infected animals 2 – 3 times per week from the tail vein. Prior to the blood draw animals were kept under an infrared lamp to dilate the veins. For venipuncture, mice were restrained with a restraining device and then, a small cut with a scalpel blade was made. Three drops of whole blood were collected in 950  $\mu$ l of Heparin-HBSS buffer to viremia. Until use for titration, heparin blood was frozen at  $-80^\circ\text{C}$ . To obtain serum, whole blood was directly collected in serum tubes. After 20 – 30 minutes, serum tubes were centrifuged at  $12.000 \times g$  and stored at  $-20^\circ\text{C}$  until the analysis.

### **8.7.3 T cell depletion**

For depletion of CD4 and/or CD8 T lymphocytes in IFNAR<sup>-/-</sup> Bl6 chimeras, depletion antibodies for CD4 and CD8 were applied 3 and 1 day prior to infection (total of 300  $\mu$ g per application). An isotype control antibody was administered at the same time and dose. Depletion efficiency was analyzed 1 day before infection using flow cytometry using CD3, CD4 and CD8 antibodies. Animals depleted 98 – 100 % were used for the experiment.

### **8.7.4 Monocyte and neutrophil depletion**

Monocytes and neutrophils were depleted using an anti-Ly-6C antibody and neutrophils alone were depleted with an anti-Ly-6G antibody. Anti-Ly-6C (250  $\mu$ g per application) and Anti-Ly-6G (500  $\mu$ g per application) Antibodies were administered 3 and 5 days post-infection. An isotype control antibody was administered at the same

time and dose (250 µg per application). Depletion efficiency was analyzed at day 5 and day 7 post-infection using CD11b and Ly-6C antibodies.

### **8.8 Organ preparation**

To determine viral titers in organs, animals were sacrificed via isoflurane narcosis and cervical dislocation. Lung, spleen, liver, kidney and brain were harvested and stored at – 80°C. For organ preparation, organs were thawed, transferred to Lysing matrix D tubes and weighed. Then, 1 ml of DMEM with 2% FBS was added and organs were homogenized with a FastPrep homogenizer (3x 30 sec, level 5). To clear the supernatant, tubes were centrifuged at 5000xg and then stored at – 80°C.

### **8.9 Clinical parameters**

Levels of aspartate aminotransferase (AST) in serum were measured with a commercial kit from Roche and a Reflotron. Sera were diluted 1:10 or higher with a 0.9% saline solution.

The normal range of AST in bone marrow chimeric mice has been determined previously as 40 – 60 U/l.

### **8.10 Sample preparation for flow cytometry**

For flow cytometry analysis, blood was collected in EDTA tubes and lungs were harvested in PBS. One half of the lung was frozen at – 80°C for organ titers and the other half was processed for FACS. Lung was transferred to a 2 ml Eppendorf tube containing Collagenase D/DnaseI solution (2 mg/ml of collagenase D, 50 µg/ml of DnaseI) and cut into small pieces. The tube was incubated shaking for 25 minutes at 37°C, then vortexed and organ pieces were mashed through a cell strainer into a 50 ml falcon tube to create a single cell suspension. Cells were centrifuged and erythrocytes were lysed for 1 min with 1x Red blood cell (RBC) lysis buffer (diluted in dH<sub>2</sub>O). The lysis was stopped with PBS. The tube was centrifuged at 500xg for 5 min and the cell pellet was resuspended in PBS.

Blood was transferred from an EDTA tube to a 2 ml eppendorf tube containing 1x RBC lysis buffer. Whole blood was lysed for 10 minutes at RT and centrifuged. White blood cells were washed 1x with PBS and then resuspended in PBS.

To avoid unspecific binding fc receptors of the cells were blocked prior to the staining with FcBlock for 10 min at 4°C. For surface antibody staining, cells were resuspended in the antibody cocktail and incubated for 30 min at 4°C. Cells were centrifuged and fixed in Cytofix/Cytoperm containing 4% formaldehyde. After 30 minutes of fixation at RT, cells were removed from the BSL-4, centrifuged and resuspended in PBS for acquisition at the flow cytometer (LSRFortessa). Prior to acquisition, single colors were compensated with compensation beads.

### 8.11 Antibody panels and gating strategies for mouse experiments

Table 3: Mouse antibody panel 1 for lung myeloid cells

Laser	Color	Marker
Blue	PerCP/Cy5.5	CD103
	FITC	Anti-EBOV GP
Green	PE/Cy7	Ly6G
	PE	Siglec F
Violet	BV 785	CD11c
	BV 650	CD3 + B220
	BV 510	CD11b
	eFluor450	MHCII
Red	APC/Cy7	Ly6C
	Alexa 700	CD45.1 or CD45.2
UV	DAPI	Live/Dead Fixable Blue

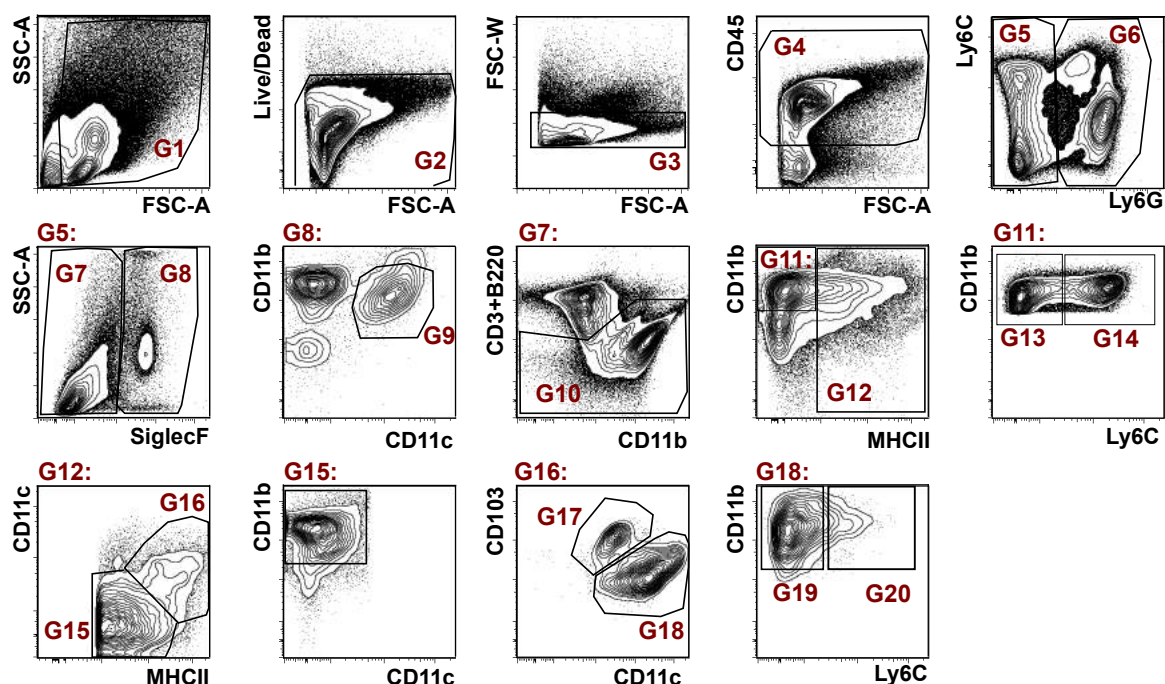


**Figure 33: Gating strategy for lung myeloid cells** Cell debris was gated out with FSC-A/SSC-A (G1), Live cells were gated as negative for Live/Dead fixable blue (G2). Singlet cells were gated with FSC-A/FSC-W (G3). Hematopoietic cells were gated as CD45 positive (G4). Neutrophils are gated as Ly6G positive (G6), Ly6G negative cells (G5) were further gated as SiglecF positive (G8) and SiglecF negative (G7). G8 defined macrophages as CD11c positive and CD11b positive (G9). In G7, lineage positive cells (T and B cells) are excluded with CD3 and B220. Lineage negative cells (G10) are further gated as CD11b positive, MHCII negative cells (G11) and MHCII intermediate – positive cells (G12). G11 defines monocytes, which can be further characterized as Ly6C high (G14) and low (G13). In G12, CD11c positive, MHCII positive staining defines dendritic cells (G16). CD11c negative, MHCII intermediate cells (G15) are CD11b positive and are probably activated monocytes. In G16, dendritic cells are further characterized as CD103 positive (G17) and CD11b positive DC subsets (G18). CD11b positive DCs are further subdivided according to their Ly6C expression: Ly6C high CD11b+ DCs (G19) and Ly6C low CD11b+ DCs (G20).

**Table 4: Mouse antibody panel for lung lymphoid cells**

Laser	Color	Marker
Violet	BV 785	B220
	BV 650	CD3
	Pacific Blue	CD8
Red	Alexa 700	CD45
	APC	CD4
UV	DAPI	Live/Dead Fixable Blue

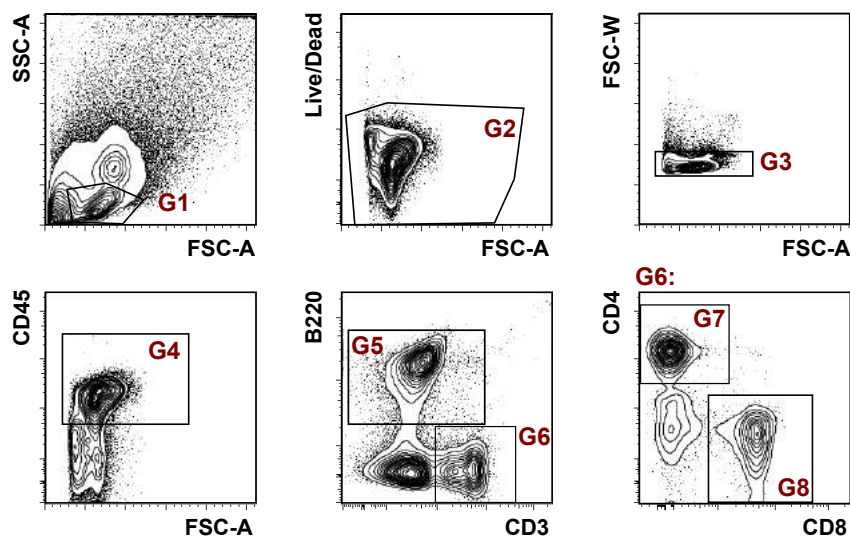


**Figure 34: Gating strategy for lung lymphoid cells** Cell debris was gated out with FSC-A/SSC-A (G1), Live cells were gated as negative for Live/Dead fixable blue (G2). Singlet cells were gated with FSC-A/FSC-W (G3). Hematopoietic cells were gated as CD45 positive (G4). B cells were characterized as B220 positive (G5) and T cells were characterized as CD3 positive (G6). Subset discrimination of T cells was achieved with anti-CD4 (G7) and anti-CD8 (G8) antibodies.

**Table 5: Mouse antibody panel 2 for lung myeloid cells**

Laser	Color	Marker
Blue	PerCP/Cy5.5	CD103
Green	FITC	Anti-EBOV GP
	PE/Cy7	MAR-1
Violet	PE	Siglec F
	BV 785	CD11c
	BV 650	CD3 + B220
	BV 510	CD11b
Red	eFluor450	MHCII
	APC/Cy7	Ly6C
	Alexa 700	CD45
	APC	CD64
UV	DAPI	Live/Dead Fixable Blue

**Table 6: Mouse antibody panel for blood**

Laser	Color	Marker
Blue	PerCP/Cy5.5	CD11b
Green	FITC	Anti-EBOV GP
	PE/Cy7	Ly6G
Violet	PE	B220
	BV 785	CD3
	Pacific Blue	CD8
Red	APC/Cy7	Ly6C
	Alexa 700	CD45.1 or CD45.2
	APC	CD4
UV	DAPI	Live/Dead Fixable Blue

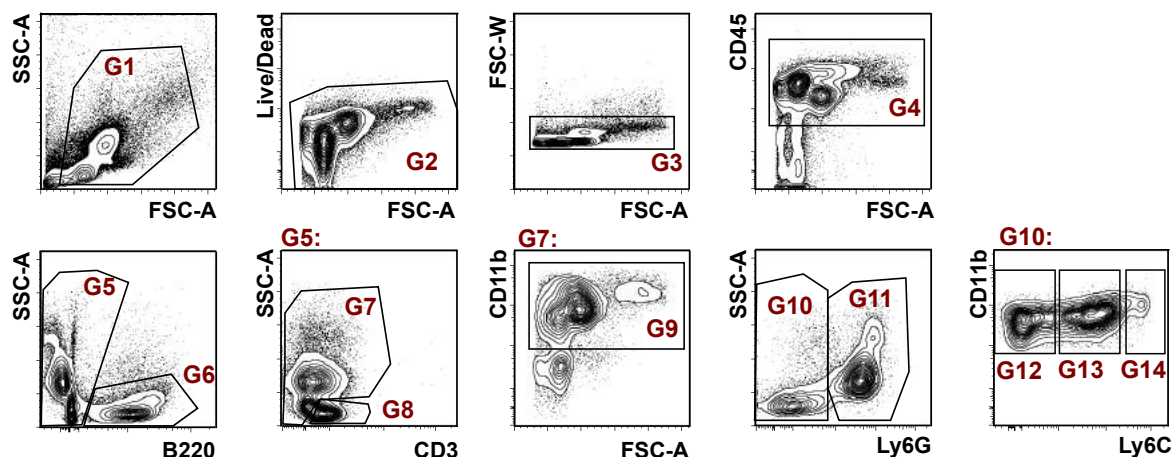


**Figure 35: Gating strategy for peripheral blood leukocytes** Cell debris was gated out with FSC-A/SSC-A (G1), Live cells were gated as negative for Live/Dead fixable blue (G2). Singlet cells were gated with FSC-A/FSC-W (G3). Hematopoietic cells were gated as CD45 positive (G4). B cells were characterized as B220 positive (G6). From B220 negative cells (G5), T cells were characterized as CD3 positive (G8). Subset discrimination was achieved with CD4 and CD8 staining (not shown). From the CD3 negative (G7) population CD11b positive cells were gated (G9) and further characterized as Ly6G positive (Neutrophils, G11) and Ly6G negative (Monocytes, G10). Monocytes were further characterized according to their Ly6C expression: Ly6C low (G12), Ly6G intermediate (G13) and Ly6G hi (G14).

**Table 7: Human antibody panel for lung myeloid cells in huNSG-A2 mice**

Laser	Color	Marker
Blue	PerCP/Cy5.5	CD11c
Green	FITC	Anti-EBOV GP
	PE/Cy7	CD141
Violet	PE	CD49d
	BV 785	HLA-DR
	BV 650	CD123
	BV 510	CD14
Red	Pacific Blue	CD3, CD19, CD56
	APC/Cy7	CD16
	Alexa 700	CD45
	APC	CD1c
UV	DAPI	Live/Dead Fixable Blue

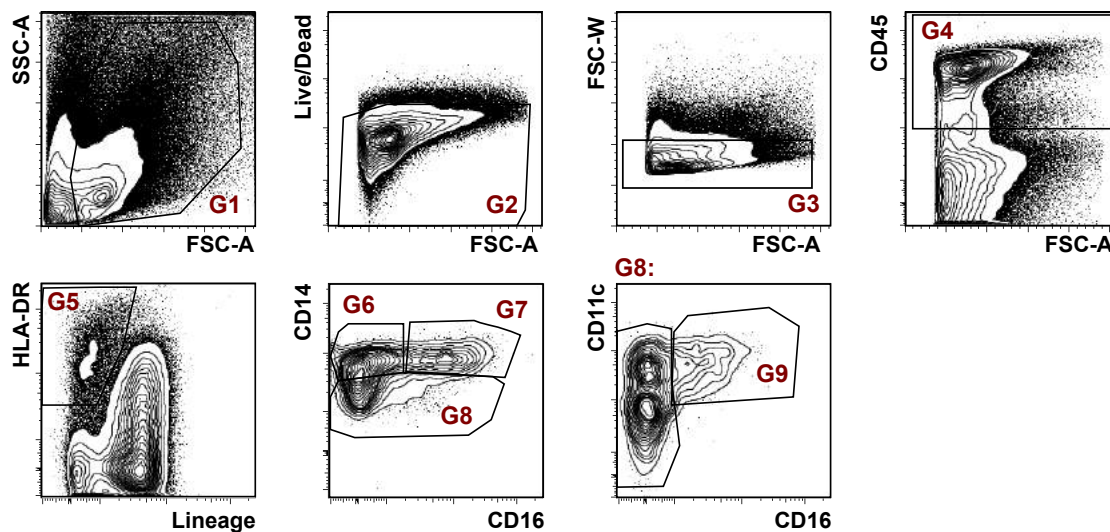


**Figure 36: Gating strategy for lung myeloid cells in humanized mice** Cell debris was removed with G1 and live cells were identified as negative for Live/Dead fixable blue (G2). Singlet cells were gated with FSC-A/FSC-W (G3) and human hematopoietic cells were gated as CD45 positive (G4). APCs were defined as HLA-DR positive and Lineage (CD3, CD19, CD56) negative (G5). APCs were further distinguished according to their CD14 and CD16 expression: CD14<sup>+</sup> myeloid cells (G6), CD14<sup>+</sup> CD16<sup>+</sup> myeloid cells (G7) and CD14 negative cells (G8). From G8, CD16<sup>+</sup> CD11c<sup>+</sup> myeloid cells were gated (G9).

## 8.12 Sample preparation of PBMCs from human EVD patients

All blood samples analyzed via flow cytometry were tested for EBOV in the European Mobile Laboratory (EML) unit in Coyah, Guinea using the RealStar Ebolavirus RT-PCR kit 1.0 (Altona Diagnostics). Blood samples were also tested for Malaria with a rapid test. Immunological studies on leftover diagnostic samples were performed at Donka Hospital in Conakry, Guinea using a Glovebox with negative pressure. Plasma was separated from blood cells via sedimentation. Then, red blood cells were lysed with 1x RBC lysis buffer (diluted in dH<sub>2</sub>O) for 10 min. Cells were washed with PBS and blocked with FcBlock for 10 min to avoid unspecific binding. For surface staining cells were resuspended in the antibody cocktail and then incubated for 30 min. After antibody incubation, cells were fixed with Cytofix/Cytoperm containing 4% formaldehyde for 30 minutes at RT. Then, samples were removed from the Glovebox, resuspended in PBS and acquired with a Guava easyCyte 8 flow cytometer.

## 8.13 Antibody panel and gating strategy for human EVD samples

Table 8: Panel for myeloid populations in peripheral blood using the 3-laser Guava

Laser	Color	Marker
Violet (405 nm)	PB	CD11c
Blue (488 nm)	BV 510	CD14
	FITC	Anti-EBOV GP
	PE	CD141
	PerCP/Cy5.5	CD3, CD19, CD56
Red (633 nm)	PE/Cy7	HLA-DR
	APC	CD1c
	APC/Cy7	CD16

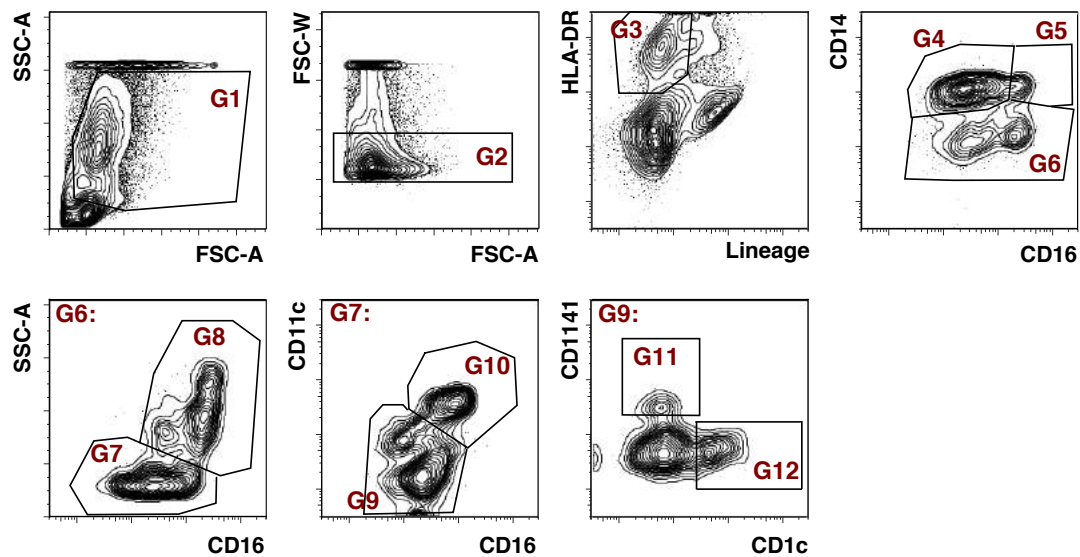


**Figure 37: Gating strategy for monocytes and DCs in peripheral blood** Cell debris and lymphocytes were removed with G1 and singlet cells were gated with FSC-A/FSC-W (G2). APCs were defined as HLA-DR positive and Lineage (CD3, CD19, CD56) negative (G3). APCs were further distinguished according to their CD14 and CD16 expression: CD14<sup>+</sup> monocytes (G4), CD14<sup>+</sup> CD16<sup>+</sup> monocytes cells (G5) and CD14 negative cells (G6). HLA-DR<sup>+</sup> Neutrophils were characterized as SSC high (G8), CD16<sup>+</sup> SSC low cells (G7) were further gated according to CD11c expression: CD11c<sup>+</sup> CD16<sup>+</sup> defines monocytes (G10), CD11c intermediate to low, CD16<sup>+</sup> cells defined the DC gate (G9). DCs were gated as CD141<sup>+</sup> DCs (G11) and CD1c<sup>+</sup> DCs (G12).



## 8.14 Statistical analysis

Statistical analyses were conducted using Graphpad Prism 5. Differences in infection rates of DC subsets over time were analyzed using a Two-Way analysis of variance (ANOVA). Evaluation of Gaussian distributions in samples was done by Kolmogorov-Smirnov tests. Paired non-parametric tests for mean comparisons were done by Mann-Whitney tests followed by Bonferroni's post-test. Multiple sample comparisons were done by Kruskal-Wallis test followed by Dunn's Multiple comparisons test. Correlation analyses were done using non-parametric Spearman correlation test. The levels of significance are depicted as follows:

ns (not significant)	$p > 0.05$
*	$p \leq 0.05$
**	$p \leq 0.01$
***	$p \leq 0.001$



## 9 References

- Aandahl EM, Michaëlsson J, Moretto WJ. Human CD4<sup>+</sup> CD25<sup>+</sup> regulatory T cells control T-cell responses to human immunodeficiency virus and cytomegalovirus antigens. *J Virol*. 2004; 78:2454–2459.
- Aldridge JR Jr, Moseley CE, Boltz DA, et al., TNF/iNOS-producing dendritic cells are necessary evil of lethal influenza virus infection. *Proc Natl Acad Sci USA*. 2009; 106:5306–5311.
- Aliberti J, Schulz O, Pennington DJ, et al., Essential role for ICSBP in the in vivo development of murine CD8 $\alpha$ <sup>+</sup> dendritic cells. *Blood*. 2003; 101:305–310.
- Asselin-Paturel C, Boonstra A, Dalod M, et al., Mouse type I IFN-producing cells are immature APCs with plasmacytoid morphology. *Nat Immunol*. 2001;2:1144–1150.
- Auffray C, Sieweke MH, Geismann F. Blood monocytes: development, heterogeneity, and relationship with dendritic cells. *Annu Rev Immunol*. 2009; 27:669–692.
- Bachem A, Güttler S, Hartung E, et al., Superior antigen- cross-presentation and XCR1 expression define human CD11c<sup>+</sup>CD141<sup>+</sup> cells as homologues of mouse CD8<sup>+</sup> dendritic cells. *J Exp Med*. 2010; 207:1273–1281.
- Baize S, Leroy EM, Georges-Courbot MC, et al., Defective humoral responses and extensive intravascular apoptosis are associated with fatal outcome in ebola virus-infected patients. *Nat Med*. 1999; 5:423–426.
- Baize S, Leroy EM, Georges AJ, et al., Inflammatory responses in ebola virus-infected patients. *Clin Exp Immunol*. 2002; 128:163–168.
- Baize S, Pannetier D, Oestereich L, et al., Emergence of Zaire Ebola virus disease in Guinea. *N Engl J Med*. 2014; 371:1418–1425.
- Ballesteros-Tato A, León B, Lund FE, et al., Temporal changes in dendritic cell subsets, cross-priming and costimulation via CD70 control CD8(+) T cell responses to influenza. *Nat Immunol*. 2010; 11:216–224.
- Baskerville A, Bowen ET, Platt GS, et al., The pathology of experimental ebola virus infection in monkeys. *J Pathol*. 1978; 125:131–138.
- Basler CF, Wang X, Mühlberger E, et al., The Ebola virus VP35 protein functions as a type I IFN antagonist. *Proc Natl Acad Sci USA*. 2000; 97:12289–12294.
- Basler CF, Mikulasova A, Martinez-Sobrido L, et al., The Ebola virus VP35 protein inhibits activation of interferon regulatory factor 3. *J Virol*. 2003; 77:7945–7956.
- Barber DL, Wherry EJ, Masopust D. Restoring function in exhausted CD8 T cells during chronic viral infection. *Nature*. 2006; 439:682–687.

Bente DA, Melkus MW, Garcia JV, et al., Dengue fever in humanized NOD/SCID mice. *J Virol*. 2005; 79:13797-13799.

Bosio CM, Aman MJ, Grogan C, et al., Ebola and Marburg viruses replicate in monocyte-derived dendritic cells without inducing the production of cytokines and full maturation. *J Infect Dis*. 2003; 188:1630–1638.

Bowen ET, Platt GS, Simpson DI, et al., Ebola haemorrhagic fever: experimental infection of monkeys. *Trans R Soc Trop Med Hyg*. 1978; 72:188–191.

Braciale TJ, Sun J, et al. Regulating the adaptive immune response to respiratory virus infection. *Nat Rev Immunol*. 2012; 12:295–305.

Bradfute SB, Warfield KL, Bavari S. Functional CD8<sup>+</sup> T cell responses in lethal ebola virus infection. *J Immunol*. 2008; 180:4058–4066.

Bradfute SB, Swanson PE, Smith MA, et al., Mechanisms and consequences of ebolavirus-induced lymphocyte apoptosis. *J Immunol*. 2010; 184: 327–335.

Brainard DM, Seung E, Frahm N, et al., Induction of robust cellular and humoral virus-specific adaptive immune responses in human immunodeficiency virus-infected humanized BLT mice. *J Virol*. 2009; 83:7305–7321.

Bray M, Davis K, Geisbert T, et al., A mouse model for evaluation of prophylaxis and therapy of ebola hemorrhagic fever. *J Infect Dis*. 1998; 179:651–661.

Bray M. The role of Type I interferon response in the resistance of mice to filovirus infection. *J Gen Virol*. 2001; 82:1365–1373.

Bray M, Geisbert TW. Ebola virus: the role of macrophages and dendritic cells in the pathogenesis of Ebola hemorrhagic fever. *Int J Biochem Cell Biol*. 2005; 37:1560–1566.

Cabrera R, Tu Z, Xu Y, et al., An immunomodulatory role of CD4(+)CD25(+) regulatory T lymphocytes in hepatitis C virus infection. *Hepatology*. 2004; 40:1062–1071.

Cao W, Taylor AK, Biber RE, et al., Rapid differentiation of monocytes into type I IFN-producing myeloid dendritic cells as an antiviral strategy against influenza virus infection. *J Immunol*. 2012; 189:2257–2265.

Carette JE, Raaben M, Wong AC, et al., Ebola virus entry requires the cholesterol transporter Niemann-Pick C1. *Nature*. 2011; 477:340–343.

Christensen JE, Thomsen AR. Co-ordinating innate and adaptive immunity to viral infection: mobility is the key. *APMIS*. 2009; 117:338–355.

Collin M, McGovern N, Haniffa M. Human dendritic cell subsets. *Immunology*. 2013; 140:22–33.

Conde P, Rodriguez M, van der Touw W, et al., DC-SIGN(+) Macrophages Control the Induction of Transplantation Tolerance. *Immunity*. 2015; 42:1143-1158.

Connolly BM, Steele KE, Davis KJ, et al., Pathogenesis of experimental ebola virus infection in guinea pigs. *J Infect Dis* 1999; 179 Suppl 1:S203–217.

Côte M, Misasi J, Ren T, et al., Small molecule inhibitors reveal Niemann-Pick C1 is essential for Ebola virus infection. *Nature*. 2011; 477:344–348.

Cox MA, Zajac AJ. Shaping successful and unsuccessful CD8 T cell responses following infection. *J Biomed Biotechnol*. 2010; 2010:159152.

Cros J, Cagnard N, Woollard K, et al., Human CD14<sup>dim</sup> monocytes patrol and sense nucleic acids and viruses via TLR7 and TLR8 receptors. *Immunity*. 2010; 33:375–386.

Crouse J, Kalinke U, Oxenius A. Regulation of antiviral T cell responses by type I interferons. *Nat Rev Immunol*. 2015; 15:231–242.

Daher KA, Selsted ME, Lehrer RI. Direct inactivation of viruses by human granulocyte defensins. *J Virol*. 1986; 60:1068–1074.

Davis KL, Anderson AO, Geisbert TW, et al., Pathology of experimental ebola virus infection in African green monkeys. Involvement of fibroblastic reticular cells. *Arch Pathol Lab Med*. 1997; 121:805–819.

Day CL, Kaufmann DE, Kiepiela P, et al., PD-1 expression on HIV-specific T cells is associated with T-cell exhaustion and disease progression. *Nature*. 2006; 443:350–354.

del Rio ML, Rodriguez-Barbosa JJ, Kremmer E, et al., CD103<sup>-</sup> and CD103<sup>+</sup> bronchial lymph node dendritic cells are specialized in presenting and cross-presenting innocuous antigen to CD4<sup>+</sup> and CD8<sup>+</sup> T cells. *J Immunol*. 2007; 178:6861–6866.

Demangel C, Palendira U, Feng CG, et al., Stimulation of dendritic cells via CD40 enhances immune responses to *Mycobacterium tuberculosis* infection. *Infect. Immun*. 2001; 69:2456–2461.

Diao H, Cui G, Wei Y, et al. Severe H7N9 infection is associated with decreased antigen-presenting capacity of CD14<sup>+</sup> cells. *PLoS One*. 2014; 9:e92823.

Diehl L, den Boer AT, Schoenberger SP, et al., CD40 activation in vivo overcomes peptide-induced peripheral cytotoxic T-lymphocyte tolerance and augments anti-tumor vaccine efficacy. *Nat Med*. 1999; 5:774–779.

Domínguez-Soto A, Sierra-Filardi E, Puig-Kröter A, et al., Dendritic cell-specific ICAM-3-grabbing nonintegrin expression on M2-polarized and tumor-associated macrophages is macrophage-CSF dependent and enhanced by tumor-derived IL-6 and IL-10. *J Immunol*. 2011; 186:2192–2200.

Dowell SF, Mukunu R, Ksiazek TG, et al., Transmission of Ebola hemorrhagic fever: a study of risk factors in family members, Kikwit Democratic Republic of the Congo, 1995. *Comission de Lutte contre les Epidemies a Kikwit. J Infect. Dis*. 1999; 179 Suppl 1:S87–91.

Dzionek A, Fuchs A, Schmidt P. et al., BDCA-2, BDCA-3 and BDCA-4: three markers for distinct subsets of dendritic cells in human peripheral blood. *J Immunol.* 2000;65:6037–6046.

Ebihara H, Takada A, Kobasa D, et al., Molecular determinants of ebola virus virulence in mice. *PLoS Pathog.* 2006; 2:e73.

Edwards AD, Diebold SS, Slack EM, et al., Toll-like receptor expression in murine DC subsets: lack of TLR7 expression by CD8 alpha+ DC correlates with unresponsiveness to imidazoquinolines. *Eur J Immunol.* 2003; 33:827–833.

Fehres CM, Bruijns SC, Sotthewes BN, et al., Phenotypic and Functional Properties of Human Steady State CD14+ and CD1a+ Antigen Presenting Cells and Epidermal Langerhans Cells. *PLoS One.* 2015; 10:e014319.

Feldmann H, Geisbert TW. Ebola haemorrhagic fever. *Lancet* 2011; 377:849–862.

Fitzpatrick G, Vogt F, Moi Gbabai OB, et al., The Contribution of Ebola Viral Load at Admission and Other Patient Characteristics to Mortality in a Médecins Sans Frontières Ebola Case Management Centre, Kailahun, Sierra Leone, June-October 2014. *J Infect Dis.* 2015; 212:1752–1758.

Franco A, Guidotti LG, Hobbs MV, et al., Pathogenetic effector function of CD4-positive T helper 1 cells in hepatitis B virus transgenic mice. *J Immunol.* 1997; 159:2001–2008.

Geijtenbeek TB, Kwon DS, Torensma R, et al., DC-SIGN, a dendritic cell-specific HIV-1-binding protein that enhances trans-infection of T cells. *Cell.* 2000; 100:587–597.

Geijtenbeek TB, Gringhuis SI. Signalling through C-type lectin receptors: shaping immune responses. *Nat Rev Immunol.* 2009; 9:465–479.

Geisbert TW, Hensley, Larsen T, et al., Pathogenesis of ebola hemorrhagic fever in cynomolgus macaques: evidence that dendritic cells are early and sustained targets of infection. *Am J Pathol.* 2003a; 163:2347–2370.

Geisbert TW, Young HA, Jahrling PB, et al., Pathogenesis of Ebola hemorrhagic fever in primate models: evidence that hemorrhage is not a direct effect of virus-induced cytolysis of endothelial cells. *Am J Pathol.* 2003b; 163:237–2382.

Geisbert TW, Young HA, Jahrling PB, et al., Mechanisms underlying coagulation abnormalities in ebola hemorrhagic fever: overexpression of tissue factor in primate monocytes/macrophages is a key event. *J Infect Dis.* 2003c; 188:1618–1629.

Geisbert TW, Jahrling PB. Exotic emerging viral diseases: progress and challenges. *Nat Med.* 2004; 10:S110–S121.

Geoffroy MC, Chelbi-Alix MK. Role of promyelocytic leukemia protein in host antiviral defense. *J Interferon Cytokine Res.* 2011; 31:145–158.

GeurtsvanKessel CH, Willart MA, van Rijt LS, et al., Clearance of influenza virus from the lung depends on migratory langerin<sup>+</sup> CD11b<sup>-</sup> but not plasmacytoid dendritic cells. *J Exp Med*. 2008; 205:1621–1634.

Gilboa E. The promise of cancer vaccines. *Nat Rev Cancer*. 2004; 4:401–411.

Guidotti LG, Ishikawa T, Hobbs MV, et al., Intracellular inactivation of the hepatitis B virus by cytotoxic T lymphocytes. *Immunity*. 1996; 4:25–36.

Gupta M, Mahanty S, Ahmed R, Rollin PE. Monocyte-derived human macrophages and peripheral blood mononuclear cells infected with ebola virus secrete MIP-1alpha and TNF-alpha and inhibit poly-IC-induced IFN-alpha in vitro. *Virology* 2001; 284:20–25.

Gupta M, Spiropoulou C, Rollin PE. Ebola virus infection of human PBMCs causes massive death of macrophages, CD4 and CD8 T cell subpopulations in vitro. *Virology* 2007; 364:45–54.

Hacker C, Kirsch RD, Ju XS, et al., Transcriptional profiling identifies Id2 function in dendritic cell development. *Nat Immunol*. 2003; 4:380–386.

Hänsel A, Günther C, Ingwersen J, et al., Human SLAN (6-sulfo LacNAc) dendritic cells are inflammatory dermal dendritic cells in psoriasis and drive strong TH17/TH1 T-cell responses. *J Allergy Clin Immunol*. 2011; 127:787–794.

Hale JS, Youngblood B, Latner DR, et al., Distinct memory CD4<sup>+</sup> T cells with commitment to T follicular helper- and T helper 1-cell lineages are generated after acute viral infection. *Immunity*. 2013; 38:805–817.

Haniffa M, Shin A, Bigley V, et al., Human tissues contain CD141<sup>hi</sup> cross-presenting dendritic cells with functional homology to mouse CD103<sup>+</sup> nonlymphoid dendritic cells. *Immunity* 2012; 37:60 – 73.

Haniffa M, Collin M, Ginhoux F. Identification of human tissue cross-presenting dendritic cells: A new target for cancer vaccines. *Oncoimmunology*. 2013; 2:e23140.

Hashimoto D, Miller J, Merad, M. Dendritic cell and macrophage heterogeneity in vivo. *Immunity*. 2011; 35:323–335.

Helft J, Manicassamy B, Guernonprez P, et al., Cross-presenting CD103<sup>+</sup> dendritic cells are protected from influenza virus infection. *J Clin Invest*. 2012; 122:4037–4047.

Henao-Restrepo AM, Longini IM, Egger M, et al., Efficacy and effectiveness of an rVSV-vectored vaccine expressing ebola surface glycoprotein: interim results from the Guinea ring vaccination cluster-randomised trial., *Lancet*. 2015; 386:857–866.

Henri S, Poulin LF, Tamoutounour S, et al., CD207<sup>+</sup> CD103<sup>+</sup> dermal dendritic cells cross-present keratinocyte-derived antigens irrespective of the presence of Langerhans cells. *J Exp Med*. 2010; 207:189–206.

Hensley L, Young HA, Jahrling PB, et al., Proinflammatory response during Ebola virus infection of primate models: possible involvement of the tumor necrosis factor receptor superfamily. *Immunol Lett.* 2002; 80:169–179.

Hildner K, Edelson BT, Purtha WE, et al., Batf3 deficiency reveals a critical role for CD8alpha+ dendritic cells in cytotoxic T cell immunity. *Science.* 2008; 322:1097–1100.

Ho AW, Prabhu N, Betts RJ, et al., Lung CD103+ dendritic cells efficiently transport influenza virus to the lymph node and load viral antigen onto MHC class I for presentation to CD8 T cells. *J Immunol.* 2011; 187:6011–6021.

Hoeffel G, Wang Y, Greter M, et al., Adult Langerhans cells derive predominantly from embryonic fetal liver monocytes with a minor contribution of yolk sac-derived macrophages. *J Exp Med.* 2012; 209:1167–1181.

Hume DA, MacDonald KP. Therapeutic applications of macrophage colony-stimulating factor-1 (CSF-1) and antagonists of CSF-1 receptor (CSF-1R) signaling. *Blood.* 2012; 119: 1810–1820.

Inaba K, Granelli-Piperno A, Steinman RM. Dendritic cells induce T lymphocytes to release B cell-stimulating factors by an interleukin 2-dependent mechanism. *J Exp Med.* 1983; 158:2040–2057.

Ivashkiv LB, Donlin LT. Regulation of type I interferon responses. *Nat Rev Immunol.* 2014; 14:36–49.

Jaiswal S, Pearson T, Fridberg H, et al., Dengue virus infection and virus-specific HLA-A2 restricted immune responses in humanized NOD-scid IL2rgammanull mice. *PLoS One.* 2009; 4:e7251.

Jaiswal S, Pazoles P, Woda M, et al., Enhanced humoral and HLA-A2-restricted dengue virus-specific T-cell responses in humanized BLT NSG mice. *Immunology.* 2012; 136:334–343.

Janeway CA Jr, Travers P, Walport M, et al. *Immunobiology: The Immune System in Health and Disease.* 5th edition. New York: Garland Science; 2001.

Joffre OP, Segura E, Savina A, et al., Cross-presentation by dendritic cells. *Nat Rev Immunol.* 2012; 12: 557-569.

Johnston LJ, Halliday GM, King NJ. Phenotypic changes in Langerhans' cells after infection with arboviruses: a role in the immune response to epidermally acquired viral infection? *J Virol.* 1996; 70:4761–4766.

Johnston LJ, Halliday GM, King NJ. Langerhans cells migrate to local lymph nodes following cutaneous infection with an arbovirus. *J Invest. Dermatol.* 2000; 114:560–568.

Kadowaki N, Antonenko S, Lau JY, et al., Natural interferon alpha/beta-producing cells link innate and adaptive immunity. *J Exp Med.* 2000; 192:219–226.



Kaplan DH, Jenison MC, Saeland S, et al., Epidermal Langerhans cell-deficient mice develop enhanced contact hypersensitivity. *Immunity*. 2005; 23:611–620.

Kelsall BL, Biron CA, Sharma O, Kaye PM. Dendritic cells at the host-pathogen interface. *Nat Immunol*. 2002; 3:699–702.

Kim TS, Braciale TJ. Respiratory dendritic cell subsets differ in their capacity to support the induction of virus-specific cytotoxic CD8<sup>+</sup> T cell responses. *PLoS One*. 2009; 4:e4204.

King NJ, Kesson AM. Interaction of flaviviruses with cells of the vertebrate host and decoy of the immune response. *Immunol Cell Biol*. 2003; 81:207–216.

Feldmann H, Klenk HD. Ebola and Marburg viruses: molecular and cellular biology. Horizon Bioscience, Wymondham, Norfolk, U.K, 2004.

Kwon DS, Gregorio G, Bitton N, et al. DC-SIGN-mediated internalization of HIV is required for trans-enhancement of T cell infection. *Immunity*. 2002; 16:135–144.

Lambrecht BN, Hammad H. Lung dendritic cells in respiratory viral infection and asthma: from protection to immunopathology. *Annu Rev Immunol*. 2012; 30:243–270.

Langlet C, Tamoutounour S, Henri S, et al., CD64 expression distinguishes monocyte-derived and conventional dendritic cells and reveals their distinct role during intramuscular immunization. *J Immunol*. 2012; 188:1751–1760.

Lanini S, Portella G, Vairo F, et al., Blood kinetics of Ebola virus in survivors and nonsurvivors. *J Clin Invest*. 2015; 125:4692–4698.

Lasala F, Arce E, Otero JR, et al., Mannosyl glycodendritic structure inhibits DC-SIGN-mediated Ebola virus infection in cis and in trans. *Antimicrob Agents Chemother*. 2003; 47:3970–3972.

Le Guenno B, Formenty P, Wyers M, et al., Isolation and partial characterization of a new strain of Ebola virus. *Lancet*. 1995; 345:1271–1274.

León B, López-Bravo M, Ardavin C. Monocyte-derived dendritic cells formed at the infection site control the induction of protective T helper 1 responses against *Leishmania*. *Immunity*. 2007; 26:519–531.

León B, Ardavin C. Monocyte-derived dendritic cells in innate and adaptive immunity. *Immunol. Cell Biol*. 2008; 86:320–324.

Leroy EM, Kumulungui B, Pourrut X, et al., Fruit bats as reservoirs of Ebola virus. *Nature*. 2005; 438:575–576.

Leroy EM, Rouquet P, Formenty P, et al., Multiple Ebola virus transmission events and rapid decline of central African wildlife. *Science*. 2004; 303:387–390.

Lever MS, Piercy TJ, Steward JA, et al., Lethality and pathogenesis of airborne infection with filoviruses in A129 alpha/beta -/- interferon receptor-deficient mice. *J Med Microbiol.* 2012; 61:8–15.

Lim JK, Obara CJ, Rivollier A, et al., Chemokine receptor Ccr2 is critical for monocyte accumulation and survival in West Nile virus encephalitis. *J Immunol.* 2011; 186:471–478.

Lin KL, Suzuki Y, Nakano H, et al., CCR2<sup>+</sup> monocyte-derived dendritic cells and exudate macrophages produce influenza-induced pulmonary immune pathology and mortality. *J Immunol.* 2008; 180:2562–2572.

Longhi MP, Trumpfheller C, Idoyaga J, et al., Dendritic cells require a systemic type I interferon response to mature and induce CD4<sup>+</sup> Th1 immunity with poly IC as adjuvant. *J Exp Med.* 2009; 206:1589-1602.

Luczkowiak J, Arribas JR, Gomez S, et al. Specific neutralizing response in plasma from convalescent patients of Ebola Virus Disease against the West Africa Makona variant of Ebola virus. *Virus Res.* 2016; 213:224–229.

Lüdtke A, Oestereich L, Ruibal P, et al. Ebola virus disease in mice with transplanted human hematopoietic stem cells. *J Virol.* 2015; 89:4700–4704.

MacDonald KP, Munster DJ, Clark GJ, et al. Characterization of human blood dendritic cell subsets. *Blood.* 2002; 100:4512–4520.

Mahanty S, Hutchinson K, Agarwal S, et al., Cutting edge: impairment of dendritic cells and adaptive immunity by ebola and lassa viruses. *J Immunol.* 2003; 170:2797–2801.

Mahanty S, Bray M. Pathogenesis of filoviral haemorrhagic fevers. *Lancet Infect Dis.* 2004; 4:487–498.

Martinez O, Johnson JC, Honko A, et al., Ebola virus exploits a monocyte differentiation program to promote its entry. *J Virol.* 2013; 87:3801–3814.

Marzi A, Feldmann F, Hanley PW, et al., Delayed Disease Progression in Cynomolgus Macaques Infected with Ebola Virus Makona Strain. *Emerg Infect Dis.* 2015; 21:1777–1783.

Martinson J, Bae J, Klingemann HG, et al., Activated platelets rapidly up-regulate CD40L expression and can effectively mature and activate autologous ex vivo differentiated DC. *Cytotherapy.* 2004; 6:487–497.

Mate SE, Kugelman JR, Nyenswah TG, et al. Molecular Evidence of Sexual Transmission of Ebola Virus. *N Engl J Med.* 2015; 373:2448–2454.

Matloubian M, Concepcion RJ, Ahmed R. CD4<sup>+</sup> T cells are required to sustain CD8<sup>+</sup> cytotoxic T-cell responses during chronic viral infection. *J Virol.* 1994; 68:8056–8063.

McElroy AK, Erickson BR, Flietstra TD, et al., Ebola hemorrhagic Fever: novel biomarker correlates of clinical outcome. *J Infect. Dis.* 2014; 210:558–566.

- McElroy AK, Akondy RS, Davis CW, et al., Human ebola virus infection results in substantial immune activation. *Proc Natl Acad Sci USA* 2015; 112: 4719–4724.
- McLachlan JB, Catron DM, Moon JJ, et al., Dendritic cell antigen presentation drives simultaneous cytokine production by effector and regulatory T cells in inflamed skin. *Immunity*. 2009; 30:277–288.
- McMichael AJ, Gotch FM, Noble GR, et al., Cytotoxic T-cell immunity to influenza. *N Engl J Med*. 1983; 309:13–17.
- Melkus MW, Estes JD, Padgett-Thomas A, et al., Humanized mice mount adaptive and innate immune responses to EBV and TSST-1. *Nat Med*. 2006; 12:1316–1322.
- Mellman I, Steinman RM. Dendritic cells: specialized and regulated antigen processing machines. *Cell*. 2001; 106:255–258.
- Merad M, Manz MG, Karsunky H, et al., Langerhans cells renew in the skin throughout life under steady-state conditions. *Nat Immunol*. 2002; 3:1135–1141.
- Merad M, Ginhoux F, Collin M. Origin, homeostasis and function of Langerhans cells and other langerin-expressing dendritic cells. *Nat Rev Immunol*. 2008; 8:935–947.
- Merad M, Sathe P, Helft J, et al., The dendritic cell lineage: ontogeny and function of dendritic cells and their subsets in the steady state and the inflamed setting. *Annu Rev Immunol*. 2013; 31:563–604.
- Mesman AW, de Vries RD, McQuaid S, et al., A prominent role for DC-SIGN<sup>+</sup> dendritic cells in initiation and dissemination of measles virus infection in non-human primates. *PLoS One*. 2012; 7:e49573.
- Morse SS. Factors in the emergence of infectious diseases. *Emerg Infect Dis*. 1995; 1:7–15.
- Mühlberger E, Weik M, Volchkov VE, Klenk HD, Becker S. Comparison of the transcription and replication strategies of Marburg and Ebola virus by using artificial replication systems. *J Virol*. 1999; 73:2333–2342.
- Müller S, Möller P, Bick MJ, et al., Inhibition of filovirus replication by the zinc finger antiviral protein. *J Virol*. 2007; 81:2391–2400.
- Muñoz-Fontela C, Pazos M, Delgado I, et al. p53 serves as a host antiviral factor that enhances innate and adaptive immune responses to influenza A virus. *J Immunol*. 2011; 187:6428–6436.
- Nakamoto N, Cho H, Shaked A, et al., Synergistic reversal of intrahepatic HCV-specific CD8 T cell exhaustion by combined PD-1/CTLA-4 blockade. *PLoS Pathog*. 2009; 5:e1000313.
- Noda T, Sagara H, Suzuki E, et al., Ebola virus VP40 drives the formation of virus-like filamentous particles along with GP. *J Virol*. 2002; 76:4855–4865.

Nordenstedt H, Bah EI, de la Vega MA, et al. Ebola Virus in Breast Milk in an Ebola Virus-Positive Mother with Twin Babies, Guinea, 2015. *Emerg Infect Dis.* 2016; 22: 759–760.

Nussenzweig MC, Steinman RM, Gutchinov B, et al., Dendritic cells are accessory cells for the development of anti-trinitrophenyl cytotoxic T lymphocytes. *J Exp Med.* 1980; 152:1070–1084.

Oestereich L, Lüdtke A, Wurr S, et al., Successful treatment of advanced ebola virus infection with T-705 (favipiravir) in a small animal model. *Antiviral Res.* 2014; 105:17–21.

Ohl L, Mohaupt M, Czeloth N, et al., CCR7 governs skin dendritic cell migration under inflammatory and steady-state conditions. *Immunity.* 2004; 21:279–288.

Perdiguerio EG, Geissmann F. The development and maintenance of resident macrophages. *Nat Immunol.* 2015; 17:2–8.

Perrone LA, Plowden JK, Garcia-Sastre A, et al., H5N1 and 1918 pandemic influenza virus infection results in early and excessive infiltration of macrophages and neutrophils in the lung of mice. *PLoS Pathog.* 2008; 4:e1000115.

Peters PJ, Borst J, Oorschot V, et al. Cytotoxic T lymphocyte granules are secretory lysosomes, containing both perforin and granzymes. *J Exp Med.* 1991; 173:1099–1109.

Plantinga M, Guillems M, Vanheerswynghe M, et al., Conventional and monocyte-derived CD11b(+) dendritic cells initiate and maintain T helper 2 cell-mediated immunity to house dust mite allergen. *Immunity.* 2013; 38:322–335.

Raymond J, Bradfute S, Bray M. Filovirus infection of STAT-1 knockout mice. *J Infect Dis.* 2011; 204:986–990.

Reid SP, Leung LW, Hartmann AL, et al., Ebola virus VP24 binds karyopherin alpha1 and blocks STAT1 nuclear accumulation. *J Virol.* 2006; 80:5156–5167.

Ridge JP, Di Rosa F, Matzinger P. A conditioned dendritic cell can be a temporal bridge between a CD4+ T-helper and a T-killer cell. *Nature.* 1998; 393:474–478.

Rosendahl Huber S, van Beek J, de Jonge J, et al., T cell responses to viral infections – opportunities for Peptide vaccination. *Front Immunol.* 2014; 5:171.

Saha P, Geissmann F. Toward a functional characterization of blood monocytes. *Immunol Cell Biol.* 2011; 89:2–4.

Samuel CE. Antiviral actions of interferons. *Clin Microbiol Rev.* 2001; 14:778–809.

Schieffelin JS, Shaffer JG, Goba A, et al., Clinical illness and outcomes in patients with Ebola in Sierra Leone. *N Engl Med.* 2014; 371:2092–2100.

Schmid MA, Harris E. Monocyte recruitment to the dermis and differentiation to dendritic cells increases the targets for dengue virus replication. *PLoS Pathog.* 2014; 10:e1004541.

- Segura E, Durand M, Amigorena S, et al., Similar antigen cross-presentation capacity and phagocytic functions in all freshly isolated human lymphoid organ-resident dendritic cells. *J Exp Med*. 2013; 210:1035–1047.
- Segura E, Touzot M, Bohineust A, et al., Human inflammatory dendritic cells induce Th17 cell differentiation. *Immunity* 2013b; 38:336–348.
- Seo SU, Kwon HJ, Ko HJ, et al., Type I interferon signaling regulates Ly6C(hi) monocytes and neutrophils during acute viral pneumonia in mice. *PLoS Pathog*. 2011; 7:e1001304.
- Serbina, NV, Salazar-Mather TP, Biron CA, et al., TNF/iNOS-producing dendritic cells mediate innate immune defense against bacterial infection. *Immunity* 2003; 19:59-70.
- Sharpe AH. Mechanisms of costimulation. *Immunol Rev*. 2009; 229:5–11.
- Shin H, Wherry EJ. CD8 T cell dysfunction during chronic viral infection. *Curr Opin Immunol*. 2007; 19:408–415.
- Shortman K, Heath WR. The CD8<sup>+</sup> dendritic cell subset. *Immunol Rev*. 2010; 234:18–31.
- Shreedhar V, Moodycliffe AM, Ullrich SE, et al., Dendritic cells require T cells for functional maturation in vivo. *Immunity*. 1999; 11:625–636.
- Shultz LD, Ishikawa F, Greiner DL. Humanized mice in translational biomedical research. *Nat Rev Immunol*. 2007; 7:118–130.
- Shultz LD, Saito Y, Nahima Y, et al., Generation of functional human T-cell subsets with HLA-restricted immune responses in HLA class I expressing NOD/SCID/IL2r gamma(null) humanized mice. *Proc Natl Acad Sci USA*. 2010; 107:13022–13027.
- Siebert R, Shu HL, Slenczka W, Peters D, Muller G. On the etiology of an unknown human infection originating from monkeys. *Dtsch Med Wochenschr*. 1967; 92:2341–2343.
- Simmons DP, Wearsch PA, Canaday DH, et al., Type I IFN drives a distinctive dendritic cell maturation phenotype that allows continued class II MHC synthesis and antigen processing. *J Immunol*. 2012; 188:3116–3126.
- Skaug B, Chen ZJ. Emerging role of ISG15 in antiviral immunity. *Cell*. 2010; 143:187–190.
- Soilleux EJ, Morris LS, Leslie G, et al., Constitutive and induced expression of DC-SIGN on dendritic cell and macrophage subpopulations in situ and in vitro. *J Leukoc Biol*. 2002; 71:445–457.
- Steinman RM, Cohn ZA. Identification of a novel cell type in peripheral lymphoid organs in mice. I Morphology, quantitation, tissue distribution. *J Exp Med*. 1973; 137:1142–1162.
- Steinman RM, Witmer MD. Lymphoid dendritic cells are potent stimulators of the primary mixed leukocyte reaction in mice. *Proc Natl Acad Sci USA*. 1978; 75:5132–5136.

Steinman RM, Kaplan G, Witmer MD, et al., Identification of a novel cell type in peripheral lymphoid organs in mice. V. Purification of spleen dendritic cells, new surface markers, and maintenance in vitro. *J Exp Med*. 1979; 149:1–16.

Sullivan NJ, Hensley L, Asiedu C, et al., CD8<sup>+</sup> cellular immunity mediates rAd5 vaccine protection against ebola virus infection of nonhuman primates. *Nat Med*. 2011; 17:1128–1131.

Takada A, Ebihara H, Jones S, et al., Protective efficacy of neutralizing antibodies against Ebola virus infection. *Vaccine*. 2007; 25:993–999.

Takeuchi O, Akira S. Pattern recognition receptors and inflammation. *Cell*. 2010; 140:805–820.

Tapia MD, Sow SO, Lyke KE, et al., Use of ChAd3-EBO-Z ebola virus vaccine in Malian and US adults, and boosting of Malian adults with MVA-BN-Filo: a phase 1, single-blind, randomized trial, a phase 1b, open-label and double-blind, dose-escalation trial, and a nested, randomized, double-blind, placebo-controlled trial., *Lancet Infect Dis*. 2016; 16:31–42.

Tassaneetrithep B, Burgess TH, Granelli-Piperno A, et al., DC-SIGN (CD209) mediates dengue virus infection of human dendritic cells. *J Exp. Med*. 2003; 197:823–829.

Towner JS, Amman BR, Sealy TK, et al., Isolation of genetically diverse Marburg viruses from Egyptian fruit bats. *PLoS Pathog*, 2009; 5 e1000536.

van der Groen G, Jacob W, Pattyn SR. Ebola virus virulence for newborn mice. *J Med Virol*. 1979; 4:239–240.

van Griensven J, Edwards T, de Lamballerie X, et al., Evaluation of Convalescent Plasma for Ebola Virus Disease in Guinea. *N Engl Med*. 2016; 374:33–42.

van Mierlo GJ, den Boer AT, Medema JP, et al., CD40 stimulation leads to effective therapy of CD40(-) tumors through induction of strong systemic cytotoxic T lymphocyte immunity. *Proc Natl Acad Sci USA*. 2002; 99:5561–5566.

Villinger F, Rollin PE, Brar SS, et al., Markedly elevated levels of interferon (IFN)-gamma, IFN-alpha, interleukin (IL)-2, IL-10, and tumor necrosis factor-alpha associated with fatal ebola virus infection. *J Infect Dis*. 1999; 179 Suppl 1:S188–191.

Volchkov VE, Becker S, Volchkova VA, et al., GP mRNA of Ebola virus is edited by the Ebola virus polymerase and by T7 and vaccinia virus polymerases. *Virology*, 1995; 214:421–430.

Warfield KL, Olinger G, Deal EM, et al., Induction of humoral and CD8<sup>+</sup> T cell responses are required for protection against lethal ebola virus infection. *J Immunol*. 2005; 175:1184–1191.

Wauquier N, Becquart P, Padilla C, et al., Human fatal zaire ebola virus infection is associated with an aberrant innate immunity and with massive lymphocyte apoptosis. *PLoS Negl Trop Dis*. 2010; 4:e837.

Wherry EJ, Ahmed R. Memory CD8 T-cell differentiation during viral infection. *J Virol*. 2004; 78:5535–5545.

WHO. Ebola haemorrhagic fever in Sudan, 1976. *Bull World Health Organ*. 1978; 56:247–270.

WHO. Ebola haemorrhagic fever in Zaire, 1976. *Bull World Health Organ*. 1978; 56:271–293.

Wing K, Sakaguchi S. Regulatory T cells exert checks and balances on self tolerance and autoimmunity. *Nat Immunol*. 2010; 11:7–13.

Yen B, Mulder LC, Martinez O, et al., Molecular basis for ebolavirus VP35 suppression of human dendritic cell maturation. *J Virol*. 2014; 88:12500–12510.

Yewdell JW, Hill AB. Viral interference with antigen presentation. *Nat Immunol*. 2002; 3:1019–1025.

Zajac AJ, Blattman JN, Murali-Krishna K, et al., Viral immune evasion due to persistence of activated T cells without effector function. *J Exp Med*. 1998; 188:2205–2213.

Zaki SR, Shieh WJ, Greer PW, et al., A novel immunohistochemical assay for the detection of Ebola virus in skin: implications for diagnosis, spread, and surveillance of Ebola haemorrhagic fever. *Commission de Lutte contre les Epidemies a Kikwit. J Infect Dis*. 1999; 179(suppl 1):S36–S47.

Zickovich JM, Meyer SI, Yagita H, et al., Agonistic anti-CD40 enhances the CD8<sup>+</sup> T cell response during vesicular stomatitis virus infection. *PLoS One*. 2014; 9:e106060.












## 10 Appendix

### 10.1 Publication list

1. **Lüdtke A\***, Ruibal P\*, Becker-Ziaja B\*, Rottstegge M, Wozniak DM, Cabeza-Cabrerizo M, Thorenz A, Weller R, Kerber R, Idoyaga J, Magassouba N, Gabriel M, Günther S, Oestereich L, Muñoz-Fontela C. (2016). *Ebola virus disease is characterized by poor activation and reduced levels of circulating CD16+ monocytes*. J Infect Dis, in press.
2. Oestereich L, **Lüdtke A**, Ruibal P, Pallasch E, Kerber R, Rieger T, Wurr S, Bockholt S, Pérez-Girón JV, Krasemann S, Günther S, Muñoz-Fontela C. (2016). *Chimeric mice with competent hematopoietic immunity reproduce key features of severe Lassa fever*. Plos Pathogens. 12, e1005656.
3. Ruibal P\*, Oestereich L\*, **Lüdtke A\***, Becker-Ziaja B\*, [...], Magassouba N, Carroll MW, Günther S, Muñoz-Fontela C. (2016). *Unique human immune signature of Ebola virus disease in Guinea*. Nature. 533, 100-104.
4. Oestereich L, Rieger T, **Lüdtke A**, Ruibal P, Wurr S, Pallasch E, Bockholt S, Kraseman S, Muñoz-Fontela C, Günther S. (2016). *Efficacy of favipiravir alone and in combination with ribavirin in a lethal, immunocompetent mouse model of Lassa fever*. J Infect Dis. 213, 934-938.
5. Pérez-Girón JV, Gómez-Medina S, **Lüdtke A**, Muñoz-Fontela C. (2015). *Intranasal administration of recombinant influenza vaccines in chimeric mouse models to study mucosal immunity*. J. Vis. Exp. 25, 100.
6. Carroll MW, [...], **Lüdtke A**, Maes P, McCowen J, Mély S, Mertens M, Meschi S, Meyer B, Michel J, Molkenhuth P, Muñoz-Fontela C, Muth D, Newman EN, Ngabo D, Oestereich L, [...], Wölfel R, Formenty P, Günther S. (2015). *Temporal and spatial analysis of the 2014-2015 Ebola virus outbreak in West Africa*. Nature. 524, 97-101.
7. **Lüdtke A\***, Oestereich L\*, Ruibal P, Wurr S, Pallasch E, Bockholt S, Ip WH, Rieger T, Gomez-Medina S, Stocking C, Rodriguez E, Günther S, Muñoz-Fontela C. (2015). *Ebola virus disease in mice with transplanted human hematopoietic stem cells*. J. Virol. 89, 4700-4704.
8. Perez-Giron JV, Belicha-Villanueva A, Hassan E, Gomez-Medina S, Cruz JLG, **Lüdtke A**, Ruibal P, Albrecht RA, Garcia-Sastre A, Muñoz-Fontela C. (2014). *Mucosal polyinosinic-polycytidylic acid improves protection elicited by replicating influenza vaccines via enhanced dendritic cell function and T cell immunity*. J Immunol. 193, 1324-1332.
9. Oestereich L, **Lüdtke A**, Wurr S, Rieger T, Muñoz-Fontela C, Günther S. (2013). *Successful treatment of advanced Ebola virus infection with T-705 (favipiravir) in a small animal model*. Antiviral Res. 105, 17-21.

\* Equal contribution

## 10.2 Toxicity of chemicals

Substance	GHS symbol	Hazard statements	Precautionary statements
EDTA		H332, H373	P260
Ethanol		H225, H319	P210, P233 P305+P351+P338
Formaldehyde		H301+H311+H331 H314, H317, H341, H350, H370-H335	P281 P303+P361+P353 P304+P340 P305+P351+P338 P308+P310
Peracetic acid		H242, H314 H335-H336	P280, P261 P301+P312 P304+P340 P330 P302+P352
Sodium Hypochlorite		H290, H314, H400	P280 P303+P361+P353 P305+P351+P338 P301+P330+P331 P310
Triton X-100		H302, H318	P280 P301+P312 P305+P351+P338
Trizol		H330, H301, H311, H314, H341, H373, H412	P260, P280, P284 P301+P330+P331 P304+P340 P305+P351+P338 P303+P361+P353 P309+P311

### 10.3 Acknowledgments

There is a lot to say and I would like to start by saying that I am very happy to be part of your lab, César. I am grateful for this very exciting project, everything that I learned from you and all the new experiences, like setting up a lab in Africa. I want to thank you for your crazy ideas and your trust. I really appreciate your patience and the long and endless discussions. Thank you, César, for the awesome time in your lab. Hopefully in the future we continue our great teamwork!

Vielen Dank, Stephan, für das spannende Forschungsthema und für die Betreuung und Unterstützung während der gesamten Zeit meiner Doktorarbeit. Danke, dass ich ein Teil deiner Arbeitsgruppe sein durfte.

Ich möchte mich bei Herrn Prof. Dr. Chris Meier für die Zweitbetreuung und die Übernahme des Zweitgutachtens bedanken.

Mein Dank gilt auch Herrn Prof. Dr. Wolfgang Maison und Herrn Prof. Hans-Willi Mittrücker für die Begutachtung der Disputation.

I want to thank Juliana for the great time during my stay in Mt. Sinai, New York and her intense teaching of steady state immunology.

I want to thank my super amazing lab members. Thank you, Sergio, for always helping me and for your friendship. Thank you, Paula, for your help, for the time we spend in Guinea, your positive energy and your friendship. Thank you, Vicente, for teaching me a lot with all your corners in your manner. Thank you, Jazmina, for teaching me so many things and being my friend. Thank you, Monika, for being the best crazy Master student ever and thank you, Fani, for always having time for me. Thank you all for the great time!

Besonders möchte ich mich auch bei dem tollen S4 Labor Team bedanken. Danke, Lisa, für alles was du mir beigebracht hast, für die vielen gemeinsamen Experimente, Diskussionen und viele, viele S4 Labor Stunden und deine Freundschaft. Danke, Elli, für deine Hilfe und Freundschaft. Ich danke auch Sabrina, David und Steffi für ihre Hilfe. Vielen Dank, dass ich mit euch diese Zeit verbringen durfte!

Außerdem danke ich allen anderen Mitgliedern der Virologie Arbeitsgruppe Maria, Sophia, Toni, Romy, Tobias, Dominik, Carola, Petra, Martin G., Beate und Maike für ihre Unterstützung.

Meinen Freunden Rami, Bernadette, Franzi, Sandra, Steffi und Leonie danke ich für ihre Unterstützung und tolle Freundschaft.

Ich möchte meiner besten Freundin Vici für alles danken. Danke, dass du immer für mich da bist!

Besonders danke ich meiner ganzen Familie. Danke, dass ihr immer für mich da seid! Worte reichen nicht aus zu beschreiben wie wichtig ihr für mich seid.

Danke, Benny, dafür, dass du immer an meiner Seite bist. Ich bin froh, dass du in meinem Leben bist!

#### **10.4 Eidesstattliche Versicherung**

Hiermit erkläre ich an Eides statt, dass ich die vorliegende Dissertationsschrift selbst verfasst und keine anderen als die angegebenen Quellen und Hilfsmittel benutzt habe. Ich versichere, dass diese Dissertation nicht in einem früheren Promotionsverfahren eingereicht wurde.

Hamburg, den 23.03.2016

Anja Lüdtkke